Centennial to multidecadal timeseries of North Atlantic climatology during the last two glacial-interglacial transitions and marine-terrestrial teleconnections

Tesis doctoral realizada por:
PATRICIA JIMÉNEZ AMAT

Bajo la dirección del Doctor Rainer Zahn en el Instituto de Ciencia y Tecnología Ambiental (ICTA), de acuerdo con los requerimientos del programa de doctorado en Ciencia y Tecnología Ambientales de la Universidad Autónoma de Barcelona (UAB) para la obtención del título de **Doctor en Ciencia y Tecnología Ambientales**.

Bellaterra (Barcelona), Octubre de 2013

---------- ----------

El doctorando

El director de tesis

UAB Universitat Autònoma de Barcelona

icta

"*Fer ciència no és més que aprofundir en l'actitud d'observar, de contemplar. Les preguntes i les respostes neixen de la contemplació. Com un pingüí enfilat a un baobab, veus moltes coses però no tens ni idea de què volen dir. I, tanmateix, ja mai més no vols deixar d'enfilar-te." Rafel Simó.*

"Si trabajas en lo que está delante de ti, siguiendo con serenidad, energía y calma la razón correcta sin permitir que nada te distraiga, salvo mantener en estado puro tu parte divina, como si debieras devolverla de inmediato; si haces esto, sin esperar nada más que la satisfacción de vivir de acuerdo con la naturaleza, pronunciando verdades heroicas en cada palabra, vivirás feliz. Y no habrá hombre capaz de evitarlo." Marco Aurelio.

Contents

Acknowledgments/Agradecimientos

Barcelona, domingo 27 de octubre, 18h en punto… y punto final de la tesis…

… y en este estado de euforia y agotamiento hecho la vista atrás para agradecer todo el apoyo, fuerza y cariño recibido durante esta aventura… So, thanks…

In first place, I want to thank my mentor Rainer… I want to sincerely thank you this unique opportunity you gave me to do this PhD… it has been a real pleasure to learn so much from you and work with you… thank you very much for all your knowledge and enthusiasm, your guidance and support, thank you for your always constructive and positive supervision of my work… you have taught me vital tools for life… I wish you all my best…

Thanks to all my colleagues and friends in the group, Graham and Patrizia, Mika merci beaucoup pour tout mon cher ami!! Anaid, Angelita, Marari, Kelsey, Giangi, Sonia, Poppis y Annita, gracias por todo, por vuestras risas diarias, y vuestro ánimo y cariño siempre; Lukas y Laura, gracias por todo, por vuestra ayuda, compañía y comprensión, por todo lo que me habéis enseñado de este mundillo, por vuestra amistad y por vuestra paciencia…gracias!! Gracias a Nuria y Gemma por esas horas interminables de laboratorio con vosotras, siempre dispuestas a echar un cable y siempre con esa sonrisa enorme en la cara….Carme, gracias por nuestras risas y por todo tu ánimo y ayuda estos últimos meses sobre todo!! Gracias a Miguel, Sara, Rafa y Jordina, gracias por vuestra ayuda siempre tan eficaz… El SAQ…que sería de esta tesis sin Ignasi y Conchi? Gracias por estos datos tan maravillosos, por esas horas de análisis a vuestro lado pues son geniales, así que gracias por vuestra paciencia con nuestros foraminíferos, por vuestro trabajo y esfuerzo y por todos los buenos ratos pasados…

Y de la UAB vuelvo al ICM… porque esta tesis no hubiese sido posible sin mi paso por ahí… del ICM me llevé unos años inolvidables de trabajo, de motivación, de amistad, de experiencias inolvidables y de sueños cumplidos… gracias a ***todos*** *vosotros por haber hecho de esos años una etapa única e inolvidable en mi vida…*

Lo que tengo claro a estas alturas, es que además de haber realizado una tesis doctoral, he cursado un doctorado en conocimiento y gestión de mí misma… estos últimos años han sido una etapa crucial en mi vida, única e inolvidable… Gracias a mis ***amigos****, que sabéis quienes sois, un pilar básico para mí, gracias por existir… gracias por vuestro apoyo y vuestro cariño en todo momento, por acompañarme de esta manera estos años, por vuestra amistad, que es de verdad un tesoro… Gracias a la extensa banda sonora que ha acompañado esta tesis… en especial a jota y floren… jjeje… y gracias a mis carreritas por Collserola por devolverme la serenidad en los momentos complicaditos…*

Gracias a mi familia, siempre atentos, siempre interesados por mi tesis, siempre animándome, gracias por vuestro apoyo, entusiasmo y ánimo incondicional… en especial a mi pilar vital, mis hermanos y mis padres,… gracias por ese núcleo de amor incondicional, me habéis enseñado el

valor del trabajo y el esfuerzo, que para conseguir tus sueños hay que luchar por ellos, gracias por confiar en mí y apoyarme siempre…

Gracias alex, gracias por creer en mí, por tu ánimo, apoyo y amor incondicional… gracias por ser un motor y un pilar para mí, gracias por haberme hecho recordar que lo más importante era volver a disfrutar de la gran broma final…

Y como no, esto ha sido posible gracias a los cuartos que han permitido pagar todo este trabajo, asi que:

I acknowledge the Past4Future project for funding this PhD thesis. The research leading to these results has received funding from the European Union's Seventh Framework programme (FP7/2007-2013) under grant agreement n^{o} 243908, "Past4Future. Climate change-Learning from the past climate."

Abstract

In order to identify and understand the timing of events and mechanisms involved in glacial-interglacial transitions and the establishment of interglacial periods it is essential to learn about the climate variability and ocean sensitivity of key areas such as the North Atlantic at high resolution time scales. This region is highly sensitive to the changes of climatic conditions during glacial terminations because of its proximity to the Northern Hemisphere ice sheets. Moreover, the North Atlantic is a prime location where surface-to-deep-ocean coupling occurs that is critically involved with setting the mode of the Atlantic Meridional Overturning Circulation. Hence any perturbations in this region likely are of global consequence. North Atlantic climate reconstructions of the last interglacial period (Marine Isotope Stage, MIS 5e) show many features that model projections predict for the 21st century under continuing human influence and increasing greenhouse gas forcing. Hence, the MIS5e period is considered a good analogue for future climate warming.

This thesis contributes to this theme with high resolution records that depict the variability of North Atlantic surface ocean climatology during the present (Holocene) and last (MIS5e) interglacial periods and the preceding deglaciations: the MIS6-T2-MIS5e (150-105 ky) and MIS2-T1-Holocene (25-0 ky) sequences. The data are generated for ODP Site 976 in the Alboran Sea, westernmost Mediterranean, which receives North Atlantic climate signals through the atmosphere and the advection of Atlantic inflow waters entering the Mediterranean Sea. Time series are presented of planktonic (*Globigerina bulloides*) Mg/Ca derived sea surface temperature ($SST_{Mg/Ca}$) and $\delta^{18}O$ that both in combination are used to indicate sea surface salinity variability ($\delta^{18}O_{sw}$). High rates of sediment deposition at the site, in the order of 23 cm/ky (Bernasconi et al., 1999), allow us to resolve variability at centennial to multi-decadal timescales.

In order to assess the extent to which the ODP976 data profiles indeed represent the marine climatology in the area they are compared with similar profiles from other sites in the Alboran Sea, ODP 977 (Martrat et al., 2004) and MD95-2043 (Cacho et al., 1999, 2002); at the western Iberian margin, MD95-2042 (Shackleton et al., 2000, 2004), MD95-2040 (Schönfeld et al., 2003), MD99-2339 (Voelker et al., 2006) and MD99-2334 (Skinner et al., 2003), and with Greenland ice core $\delta^{18}O$ records NGRIP (NGRIP members, 2004), NEEM (NEEM community members, 2013) and the synthetic record of Greenland climate variability (Barker et al., 2011). During the MIS2-T1-Holocene sequence the data profiles are tightly correlated while ODP976 consistently displays highest temporal resolution hence confirming the quality of this site as representing the North Atlantic climate evolution. Multiple-step features connected with the incursion of accelerated ice-sheet disintegration are captured by the ODP 976 palaeo-climatic records across the MIS6-T2-MIS5e and MIS2-T1-Holocene sequences reflecting periodic ice-sheet break down albeit at different magnitudes and relative timing. The most prevalent feature of both glacial terminations is the accelerated warming by 5-6°C immediately after the major deglacial meltwater surges

associated with Heinrich events H1 and H11. During T1 this occurs at ~15 ky i.e., during the Bolling/Allerod episode, when ODP976 registers a warming of $SST_{Mg/Ca}$ to full-interglacial levels of 20°C. At 12.5 ky, $SST_{Mg/Ca}$ decreases by ~4-4.5°C into the Younger Dryas cold phase that is documented in the ODP 976 records as a two-phase event with an initial dry and cold period at 12.5-12 ky followed by a more humid interval at 12-11.5 ky. Holocene $SST_{Mg/Ca}$ stabilizes around 17.5°C closely matching today's Alboran Sea region modern spring SST (MEDATLAS II, Medar Group, 2002). T2 by comparison was almost entirely controlled by a single massive meltwater surge that was coincident with H11 or that embedded the main H11 event in it. This event clearly stands out in the $SST_{Mg/Ca}$ profile and the computed $\delta^{18}O_{sw}$ data depicting salinity changes. The scenario of a single massive meltwater surge is supported by North Atlantic benthic $\delta^{13}C$ records (MD95-2042, U1308) revealing low North Atlantic Deep Water (NADW) formation and weak overturning circulation at this time. Once H11 ends, an abrupt and uninterrupted $SST_{Mg/Ca}$ increase of ~5°C occurs within 1 ky, reaching full interglacial SST levels (~20°C) at 129 ky. This $SST_{Mg/Ca}$ shift is accompanied by the rapid establishment of interglacial flora evidenced by an abrupt expansion of temperate and Mediterranean forest pollen taxa in ODP 976 (Combourieu-Nebout, unpublished) and the Iberian margin (Sánchez Goñi et al., 2012; Shackleton et al., 2003; Tzedakis, pers. comm.), which suggests an in-phase onset of the interglacial period in the regional terrestrial and marine environments.

In order to overcome the difficulties of obtaining precise dating of the MIS6-T2-MIS5e sequence this thesis attempts generating an alternative age model for ODP976 that exploits the tight correlation of North Atlantic and Mediterranean temperature with the variability of the Asian monsoon and Mediterranean rainfall. Those environmental variables are depicted in speleothem records and hence the ODP 976 $SST_{Mg/Ca}$ record is correlated with the speleothem profiles of Antro del Corchia in Italy (Drysdale et al., 2004, 2009), BD-La Chaise in France (Couchoud et al., 2009) and Dongge Cave in China (Kelly et al., 2006). Transferring the uranium-series dated chronologies of those speleothems to the ODP976 data profiles provides a new chronology that aids an improved correlation of continental, marine and ice core records. A major uncertainty derives from the offset structure of T2 in the Corchia and La Chaise profiles from that of the ODP976 $SST_{Mg/Ca}$ profile which possibly reflects shifted atmospheric trajectories during H11 of moist air masses reaching the Mediterranean.

References:

Barker, S., G. Knorr et al. (2011). "800,000 years of abrupt climate variability." Science 334(6054):347.

Cacho, I. (1999)."Dansgaard-Oeschger and Heinrich event imprints in the Alboran Sea paleotemperatures." Paleoceanography 14:698.

Cacho, I., J. O. Grimalt, et al. (2002). "Response of the Western Mediterranean Sea to rapid Climatic variability during the last 50,000 years: a molecular biomarker approach." Journal of Marine Systems 33-34(0):253.

Couchoud, I., Genty, D., Hoffmann, D., Drysdale, R. N. and Blamart, D. (2009) "Millennial-scale climate variability during the Last Interglacial recorded in a speleothem from south-western France." Quaternary Science Reviews 28:3263-3274.

Drysdale, R. N., G. Zanchetta, et al., (2004) "Palaeoclimatic implications of the growth history and stable isotope (d18O and d13C) geochemistry of a middle to late Pleistocene stalagmite from central-western Italy." Earth and Planetary Science Letters 227(3-4):215.

Drysdale, R. N., J. C. Hellstrom, et al., (2009) "Evidence for obliquity forcing of Glacial Termination II." Science 325 (5947):1527.

Kelly, M. J., Lawrence Edwards, R., Cheng, H., Yuan, D., Cai, Y., Zhang, M., Lin, Y. and An, Z. "High resolution characterization of the Asian Monsoon between 146,000 and 99,000 years B.P. from Dongge Cave, China and global correlation of events surrounding Termination II." Paleaeogeography, Palaeoclimatology, Palaeoecology 236:20-38.

Martrat, B., J. O. Grimalt, et al. (2004). "Abrupt Temperature Changes in the Western Mediterranean over the past 250,000 years." Science 306 (5702):1762.

NEEM community members (2013) Eemian interglacial reconstructed from a Greenland folded ice core. Nature, vol. 493:489-494, doi:10.1038/nature11789.

North Greenland Ice Core Project (2004). Nature 431(7005):147-151.

Sánchez Goñi, M. F., Bakker, P., Desprat, S., Carlson, A. E., van Meerbeeck, C. J., Peyron, O., Naughton, F., Fletcher, W. J., Eynaud, F., Rossignol, L. and Renssen, H. (2012) European climate optimum and enhanced Greenland melt during the Last Interglacial. Geology, vol. 40(7):627-630.

Shackleton, N. J. and Hall, M. A., Vincent, E. (2000) "Phase relationships between millennial-scale events 64,000-24,000 years ago. Paleoceanography, vol. 15(6):565-569.

Shackleton, N. J., Sánchez Goñi, M. F., Pailler, D. and Lancelot, Y. (2003) "Marine Isotope Substage 5e and the Eemian Interglacial." Global and Planetary Change (36):151-155.

Shackleton, N. J., Fairbanks, R. G., Chiu, T. and Parrenin, F. (2004) "Absolute calibration of the Greenland time scale: implications for Antarctic time scales and for Δ^{14}C." Quaternary Science Reviews 23:1513-1522.

Schönfeld, J., Zahn, R. and Abreu, L. (2003) "Surface and deep water response to rapid climate changes at the Western Iberian Margin." Global and Planetary Change 36(4):237-264.

Voelker, A. H. L., Lebreiro, S. M., Schönfeld, J., Cacho, I., Erlenkeuser, H. and Abrantes, F. (2006) "Mediterranean outflow strengthening during northern hemisphere coolings: A salt source fr the glacial Atlantic?." Earth and Planetary Science Letters 245:39-55.

Skinner, L. (2003) "Millennial climate change in the northeast Atlantic: The role of surface and deep hydrographic change determined by stable isotope geochemistry and Mg/Ca palaeothermometry." Doctoral Thesis, University of Cambridge, 142pp.

Introduction.

Surface ocean circulation and the ensuing distribution of marine heat play a crucial role in driving and amplifying climate variability. The North Atlantic advects surface waters from tropical-subtropical latitudes and with it heat is transported to high latitudes where it affects the atmosphere's heat budget. The sinking of cold and dense waters in the Greenland and Labrador Seas, contributes to the deep water current flowing southwards to the South Atlantic and on into the Southern Ocean, where wind-driven upwelling draws deep waters back to the surface, completing the overturning loop of the Atlantic Meridional Overturning Circulation (AMOC). Since the 1980s, the deep-water formation regions in the North Atlantic have been a major hotspot of palaeoceanographic studies, as the consensus was that this is one of the key regions driving and modulating the AMOC by way of changing the mode of deep-water formation. The AMOC sensitive to buoyancy changes (Kuhlbrodt, 2007) and past changes in the surface density near the centres of convection were of consequence in shifting the AMOC to different states with onward consequences for the state of climate (Broecker et al., 1990; Carlson et al., 2008; McManus et al., 2004).

The AMOC influences climate in the North Atlantic and Europe and is hypothesized to be an important mechanism for driving climate changes on decadal to millennial timescales. Long-term projections of the AMOC that are presented in the Assessment Reports of the Intergovernmental Panel on Climate Change (IPCC, 2007, 2013) predict anything from virtually no change to a 50% decrease of the AMOC (Schmittner et al., 2005; Weber et al., 2007). IPCC (2007, 2013) further states that the climate trajectory of the coming centuries can be decomposed into natural and anthropogenically induced trends but neither the natural long-term variability nor its interaction with human-induced impacts are currently well constrained (e.g., Polyakov et al., 2010). Much of the debate in observational oceanography today focuses on the understanding of the magnitude of Atlantic climate variability at multidecadal time-scales, and implications for the ventilation of the northern North Atlantic deep waters that occurs on similar time scales (Talley et al., 2011). North Atlantic climate variability at 50-80yr timescales is observed in multi-proxy and instrumental records (Delworth and Mann, 2000; Gray et al., 2004; Wyatt et al., 2012) and modeling studies suggest that variability in the AMOC is a feasible explanation for part of the multi-decadal variability in the Northern Hemisphere mean temperature record (Czaja and

Marshall, 2001; Zhang et al., 2007). The Atlantic Multidecadal Oscillation (AMO) operates on a timescale of 50-80 years (Polyakov et al., 2005; Talley et al., 2011) and is a natural mode of the AMOC associated with surface temperatures throughout the Atlantic (Talley et al., 2011), significantly impacting climate in North America and Europe. Moreover, the North Atlantic Oscillation (NAO) multidecadal scale variability (Visbeck, 2003) is of prominent interest for studies of present and past North Atlantic climate variability and dynamics, specially due to its influence on storm tracks and precipitation across Western and Mediterranean Europe (Meyers and Pagani, 2006). Freshwater perturbation by ice melting, enhanced precipitation and continental runoff is predicted in ocean projections to cause a progressive slowing of the AMOC over the coming decades (Cunningham et al., 2010; Curry and Mauritzen, 2005). Salinity changes at decadal time-scales known as Great Salinity Anomalies (GSAs) are thought to be associated with the NAO and associated changes in freshwater inputs (ice melting, ocean circulation, river discharges) (Bersch, 2002; Dickson et al., 1988, 2007).

The short instrumental record of direct observations together with the high variability of the North Atlantic region did not allow yet to establish evidence confirming an ongoing change in AMOC strength that is predicted with ocean model simulations (IPCC, 2007). Palaeoceanographic proxy records go back in time far enough to depict ocean variables and the AMOC under climatic forcing changes far larger than expected to incur in the near future. This enables to test the sensitivity of the AMOC to changing boundary conditions and to provide a data base to test the capacity of climate models to adequately simulate ocean changes under different forcing scenarios. Hence, reconstructing past North Atlantic climate variability at high resolution, centennial to multi-decadal timescales, is a key objective. High-resolution palaeo-records from North Atlantic sediment cores indeed depict a direct correlation of the regional ocean climatology and terrestrial environments with the millennial to centennial changes of atmospheric temperature recorded in Greenland ice cores (Cacho et al., 1999, 2002; Combourieu-Nebout et al., 1998, 2002, 2009; Eynaud et al., 2009; Martrat et al., 2004, 2007; Sánchez-Goñi et al., 1999; Schönfeld et al., 2002; Shackleton et al., 2000, 2003, 2004; Skinner et al., 2003, 2006, 2013). The last glacial-interglacial transition (Termination 1, T1) in several of these records displays in a sequence of high-amplitude events further corroborating a tight ocean-atmosphere coupling: the Heinrich event 1 (H1; 17 to 14.8 ky; Heinrich, 1988; Hemming, 2004) freshwater perturbation and ensuing AMOC collapse, the subsequent abrupt strengthening of the AMOC and ensuing warming

during the Bølling/Allerød (B/A; 14.8 to 12.9 ky) period (Weaver et al., 2003; Gherardi et al., 2009), and the Younger Dryas (YD; 12.9 to 11.5 ky; Walker et al., 2009) cold spell with a reduced AMOC. This sequence of events underscores the sensitivity of the AMOC to external forcing and the particular role of freshwater perturbation as a transient that shifts the AMOC to different states.

The penultimate termination (T2, 135 ky) likewise resulted in a large-scale redistribution of freshwater stored in the circum-North Atlantic ice sheets to the ocean but far less is known about this climatic transition. The fact that this time period was beyond the reach of radiocarbon dating made it less attractive for palaeoceanographic research. The Greenland ice core records that serve as a prime reference of atmospheric temperature variability in the North Atlantic region do not go beyond 129 ky (NEEM community members, 2013), which further contributed to the only limited interest in high-resolution palaeoceanographic research of this period. Interest in the penultimate glacial-interglacial transition and notably, the subsequent interglacial period (Marine Isotope Stage, MIS5e; 123-116.2kyrs) increased over the last decade because it became apparent that the shifted configuration of Earth's orbital parameters during this period caused an approximately 3% higher radiative forcing driving climate to warmer-than-present conditions (CAPE-Last Interglacial Project Members, 2006); the Greenland Ice Sheet (GIS) was shown to have been smaller than present (Hillaire-Marcel et al., 2001; Otto-Bliesner et al., 2006; Carlson et al., 2008; Colville et al., 2011) and global sea level was 4-6m higher than present (Overpeck et al., 2006; Rohling et al., 2008); above all, polar temperatures were modelled at levels comparable to those expected by 2100 (Otto-Bliesner et al., 2006; Jouzel et al., 2007). Today, MIS5e is considered a plausible analogue scenario for the impending global warming under continued greenhouse gasses forcing of the next century. This stimulated renewed interest in reconstructing the North Atlantic surface hydrology and climate during MIS5e with a particular focus on millennial-to-centennial timescales (Bauch et al., 2012; Bauch and Kandiano, 2007; Cortijo et al., 1999; Fronval and Jansen, 1996, 1997; Martrat et al., 2007; Oppo et al., 2006; Sanchez Goñi et al., 2012; Winsor et al., 2012; Irvali et al., 2012; Hodell et al., 2009).

High sedimentation rates in the Alboran Sea, and the close link with the North Atlantic climate variability (Cacho et al., 1999, 2002; Combourieu-Nebout et al., 2002, 2009; Martrat et al., 2004, 2013, submitted) make the area a key location for conducting similar research with the possibility of achieving still higher temporal resolution. Such reconstructions can contribute to a fuller documentation of the sequence of events during glacial terminations and notably, their impact on

the climate of the subsequent interglacials (Piotrowski et al., 2005; Cheng et al., 2006; Sidall et al., 2006). Improving our knowledge on the sequence, timing and magnitude of the events and their connection with the dynamical AMOC hence is key to assess the sensitivity of the interconnected ocean-climate system to different boundary conditions and forcing scenarios. Comparing the developments during the transition from the penultimate full-glacial to the penultimate full-interglacial, the MIS6-T2-LIG sequence, with the transition from the last glacial to the current interglacial, the MIS2-T1-Holocene sequence, is expected to be particularly instructive as both time periods were exposed to different solar radiation levels and rates of changes (Berger and Loutre, 1999; Berger, 2007; Yin and Berger, 2011).

The main object of this thesis is to reconstruct at high resolution the North Atlantic Ocean surface hydrology and climate variability during the last two glacial-interglacial transitions and the following interglacial periods. Placing the reconstructions into a framework of other palaeoceanographic records that reflect AMOC and atmospheric processes seeks to assess the linking between North Atlantic variability, its linking with the AMOC and teleconnections with far-field climate systems such as the Asian monsoon.

References:

Bauch, H. A., and E. S. Kandiano (2007), Evidence for early warming and cooling in North Atlantic surface waters during the last interglacial, Paleoceanography, 22, PA1201, doi:10.1029/2005PA001252.

Bauch, H. A., Kandiano, E. S. and Helmke, J. P. (2012) "Contrasting ocean changes between the subpolar and polar North Atlantic during the past 135 ka." Geophysical Research Letters 39.

Berger, A. Li, X. S. and Loutre, M. F. (1999) "Modelling northern hemisphere ice volume over the last 3Ma." Quaternary Science Reviews 18(1):1-11.

Berger, A., Loutre, M. F., Kaspar, F., and Lorenz, S. J. (2007). 2. Insolation during interglacial. *Developments in Quaternary Sciences*, *7*, 13-27.

Bersch, M. (2002) "North Atlantic Oscillation-induced changes of the upper layer circulation in the northern North Atlantic Ocean." Journal of Geopgysical Research: Oceans 107(C10):1-11.

Broecker, W. S., Bond, G., Klas, M., Bonani, G. and Wolfli, W. (1990) "A salt oscillator in the glacial Atlantic? Paleoceanography 5(4):469-477.

Cacho, I. (1999)."Dansgaard-Oeschger and Heinrich event imprints in the Alboran Sea paleotemperatures." Paleoceanography 14:698.

Cacho, I., J. O. Grimalt, et al. (2002). "Response of the Western Mediterranean Sea to rapid Climatic variability during the last 50,000 years: a molecular biomarker approach." Journal of Marine Systems 33-34(0):253.

CAPE Last Interglacial Project Members (2006) "Last interglacial arctic warmth confirms polar amplification of climate change" Quaternary Science Reviews 25:1383-1400.

Carslon, A. E., Stoner, J. S., Donnelly, J. P. and Hillaire-Marcel, C. (2008) "Response of the southern Greenland Ice Sheet during the last two deglaciations." Geology 36(5):359-362.

Cheng, H., Lawrence Edwards, R., Wang, Y., King, X., Ming, Y., Kelly, M. J., Wang, X. and gallup, C. D. (2006) "A penultimate glacial monsoon record from Hulu cave and two-phase glacial terminations." Geology 34(3):217-220.

Colville, E. J., Carlson, A. E., Beard, B. L., Hatfield, R. G., Stoner, J. S., Reyes, A. V. and Ullman, D. J. (2011) "Sr-Nd-Pb Isotope evidence for ice-sheet presence on southern Greenland during the Last Interglacial." Science 333(6042):620-623.

Combourieu-Nebout, N., Paterne, M., Turon, J. L. and Siani, G. (1998) "A high-resolution record of the last deglaciation in the central Mediterranean Sea: palaeovegetation and palaeohydrological evolution." Quaternary Science Reviews 17(4-5):303-317.

Combourieu-Nebout, N., Turon, J. L., Zahn, R., Capotondi, L., Londeix, L. and Pahnke, K. (2002) "Enhanced aridity and atmospheric high-pressure stability over the western Mediterranean during the North Atlantic cold events of the past 50 k.y." Geology 30(10):863-866.

Combourieu-Nebout, N., O. Peyron, et al. (2009) "Rapid climatic variability in the west Mediterranean during the last 25,000 years from high resolution pollen data." Climate of the Past 5(3):503.

Cortijo, E., Lehman, S., Keigwin, L., Chapman, M., Paillard, D. and Labeyrie, L. (1999) "Changes in meridional temperature and salinity gradients in the North Atlantic Ocean (30°-72°N) during the Lat Interglacial Period." Paleoceanography 14(1).

Cunningham, S. A. and Marsh, R. (2010) "Observing and modeling changes in the Atlantic MOC." Wiley Interdisciplinary Reviews: Climate Change 1(2):180-191.

Curry, R. and Mauritzen, C. (2005) "Dilution and Northern North Atlantic Ocean in recent decades." Science 308(5729):1772-1774.

Czaja, A. and Marshall, J. (2001) "Observations of atmosphere-ocean coupling in the North Atlantic." Quaterly Journal of the Royal Meteorological Society 127(576):1893-1916.

Delworth, T. L. and Mann, M. E. "Observed and simulated multidecadal variability." Climate Dynamics 16:661-676.

Dickson, R. R., Meincke, J., Malmberg, A. A. and Lee, A. J. (1988) "The great salinity anomaly in the Northern North Atlantic in 1968-1982." Progress in Oceanography 20(2):103-151.

Dickson, R., Rudels, B., Dye, S., Karcher, M., Meincke, J. and Yashayaev, I. (2007) "Current estimates of freshwater flux through Arctic and subarctic seas." Progress in Oceanography 37(3-4):210-230.

Eynaud, F., de Abreu, L., Voelker, A., Schönfeld, J., Salgueiro, E., Turon, J. L. Penaud, A., Toucanne, S, Naughton, F. (2009) "Position of the polar front along the western Iberian marign during key cold episodes of the last 45 ky." Geochemistry, Geophysics, Geosystems 10(7):1525-2027.

Gherardi, J. M., Labeyrie, L., Nave, S., francois, R., McManus, J. F. and Cortijo, E. (2009) "Glacial-interglacial circulation changes inferred from 231Pa/230Th sedimentary record in the North Atlantic región." Paleoceanography 24(2).

Gray ST, Graumlich LJ, Betancourt JL, Pederson GT (2004) A treering based reconstruction of the Atlantic Multidecadal scillation since 1567 A.D. Geophys Res Lett 31:L12205. doi: 10.1029/2004GL019932.

Fronval, T. and Jansen, E. (1996) "Rapid changes in ocean circulation and heat flux in the Nordic seas during the last interglacial period." Nature 383:806-810.

Fronval, T. and Jansen, E. (1997) "Rapid changes in ocean circulation and heat flux in the Nordic seas during the last interglacial period." Oceanographic Literature Review 44(4):328.

Heinrich, H. (1988) "Origin and consequences of cyclic ice rafting in the Northeast Atlantic Ocean during the past 130,000 years." Quaternary Research 29:142-152.

Hemming, S. R. (2004) "Heinrich events: Massive late Pleistocene detritus layers of the North Atlantic and their global climate imprint." Reviews of Geophyisics 42(1).

Hillaire‐Marcel, C., De Vernal, A., Candon, L., Bilodeau, G., and Stoner, J. (2001) "Changes of potential density gradients in the northwestern North Atlantic during the last climatic cycle based on a multiproxy approach." *The Oceans and Rapid Climate Change*, 83-100.

Hodell, D. A., Minth, E. K., Curtis, J. H., McCave, N., Hall, I. R., Channell, J. E. T. and Xuan, C. (2009) "Surface and deep-water hydrography on Gardar Drift (Iceland Basin) during the last interglacial period." Earth and Planetary Science Letters 288:10-19.

IPCC, Climate Change 2007: The Physical Science Basis. Contribution of Working Group I to the Fourth Assessment Report of the Intergovernmental Panel on Climate Change. S. Solomon et al., Eds. (Cambridge University Press, Cambridge, 2007), pp. 996.

Irvali, N., Ninnemann, U. S., Galaasen, E. V., Rosenthal, Y., Kroon, D., Oppo, D. W., Kleiven, H. F., Darling, K. F. and Kissel, C. (2012) "Rapid switches in subpolar North Atlantic hydrography and climate during the Last Interglacial (MIS5e)." Paleoceanography 27.

Jouzel, J., Masson-Delmotte, V., Cattani, O., Dreyfus, G., Falourd, S., Hoffmann, G., Minster, B., Nouet, J., Barnola, J. M., Chappellaz, J., Fischer, H., Gallet, J. C., Johnsen, S., Leuenberger, M., Loulergue, L., Luethi, D., Oerter, H., Parrenin, F., Raisbeck, G., Raynaud, D., Schilt, A., Schwander, J., Selmo, E., Schouez, R., Spahni, R., Stauffer, B., Steffenesen, J. P., Stenni, B., Stocker, T. F., Tison, J. L., Werner, M. and Wolff, E. E. (2007) "Orbital and millennial Antarctic climate variability over the past 800,000 years." Science 317(5839):793-796.

Kuhlbrodt, T., Griesel, A., Montoya, M., Levermann, A., Hofmann, M. and Rahmstorf, S. (2007) "On the driving processes of the Atlantic meridional overturning circulation." Review of Geophysics 45(2) doi: 10.1029/2004RG000166.

Martrat, B., J. O. Grimalt, et al. (2004). "Abrupt Temperature Changes in the Western Mediterranean over the past 250,000 years." Science 306 (5702):1762.

Martrat, B., Grimalt, J. O., Shackleton, N. J., de Abreu, L., Hutterli, M. A. and Stocker, T. F. (2007) Four climate cycles of recurring deep and surface water destabilizations on the Iberian Margin. Science, vol. 317 (502), doi: 10.1126/science.1139994.

McManus, J. F. (2004) "A great grand-daddy of ice cores." Nature 429:611612.

Meyers, S. R., and Pagani, M. (2006). "Quasi-periodic climate teleconnections between northern and southern Europe during the 17th–20th centuries." *Global and Planetary Change*, *54*(3), 291-301.

Otto-Bliesner, B. L., Marshall, S. J., Overpeck, J. T., Miller, G. H., Hu, A. and CAPE Last Interglacial Project members (2006) "Simulating Arctic climate warmth and icefield retreat in the Last Interglaciation." Science 311(5768):1751-1753.

Overpeck; J. T., Otto-Bliesner, B. L., Miller, G. H., Muhs, D. R., Alley, R. B. and Kiehl, J. T. (2006) "Paleoclimatic evidence for future ice-sheet instability and rapid sea-level rise." Science 311(5768):1747-1750.

Piotrowski, A., Hemming, S. R., and Goldstein, S. L. (2005). Northern vs Southern Hemispheric Controls on Ocean Circulation from Authigenic Nd isotopes in Atlantic Sediments. In *AGU Spring Meeting Abstracts* (Vol. 1, p. 01).

Polyakov IV et al (2005) Multidecadal variability of North Atlantic temperature and salinity during the 20th century. J Clim 18(21):4562–4581

Polyakov, I. V., Alexeev, V. A., Bhatt, U. S., Polyakova. E. I. and Zhang, X. (2010) North Atlantic warming: patterns of long-term and multidecadal variability. Climate Dynamics, vol. 34:439-457, doi:10.1007/s00382-0522-3.

Rohling, E. J., Grant, K., Hemleben, C., Kucera, M., Roberts, A. P., Schmeltzer, I., Schulz, H., Siccha, M., Sidall, M. and Trommer, G. (2008) "New constraints on the timing of sea level fluctuations during early to middle marine isotope stage 3." Paleoceanography 23(3).

Sánchez Goñi, M. F., Eynaud, F., Turon, J. L. and Shackleton, N. J. (1999) "High resolution palynological record off the Iberian margin: direct land-sea correlation for the Last Interglacial complex." Earth and Planetary Science Letters 171:123-137.

Sánchez Goñi, M. F., Bakker, P., Desprat, S., Carlson, A. E., van Meerbeeck, C. J., Peyron, O., Naughton, F., Fletcher, W. J., Eynaud, F., Rossignol, L. and Renssen, H. (2012) European climate optimum and enhanced Greenland melt during the Last Interglacial. Geology, vol. 40(7):627-630.

Shackleton, N. J. and Hall, M. A., Vincent, E. (2000) "Phase relationships between millennial-scale events 64,000-24,000 years ago. Paleoceanography, vol. 15(6):565-569.

Shackleton, N. J., Sánchez Goñi, M. F., Pailler, D. and Lancelot, Y. (2003) "Marine Isotope Substage 5e and the Eemian Interglacial." Global and Planetary Change (36):151-155.

Shackleton, N. J., Fairbanks, R. G., Chiu, T. and Parrenin, F. (2004) "Absolute calibration of the Greenland time scale: implications for Antarctic time scales and for $\Delta^{14}C$." Quaternary Science Reviews 23:1513-1522.

Schönfeld, J., Zahn, R. and Abreu, L. (2003) "Surface and deep water response to rapid climate changes at the Western Iberian Margin." Global and Planetary Change 36(4):237-264.

Sidall, M., bard, E., Rohling, E. J. and Hemleben, C. (2006) "Sea-level reversal during Temrination II." Geology 34(10):817-820.

Skinner, L. C. (2003) “Millennial climate change in the northeast Atlantic: The role of surface and deep hydrographic change determined by stable isotope geochemistry and Mg/Ca palaeothermometry.” Doctoral Thesis, University of Cambridge, 142pp.

Skinner, L. C. and Shackleton, N. J. (2006) “Deconstructing Terminations I and II: revisiting the glacioeustatic paradigm based on deep-water temperature estimates.” Quaternary Science Reviews 25:3312-3321.

Skinner, L., C., Scrivner, A. E., Vance, D., Barker, S., Fallon, S. and Waelbroeck, C. (2013) “North Atlantic versus Southern Ocean contributions to a deglacial surge in deep ocean ventilation.” Geology 41(6):667-670.

Talley, L. D., Pickard, G. L., Emery, W. J., & Swift, J. H. (2011). *Descriptive physical oceanography: an introduction*. Access Online via Elsevier.

Visbeck, M., Chassignet, E. P., Curry, R. G., Delworth, T. L., Dickson, R. R., & Krahmann, G. (2003). The ocean's response to North Atlantic Oscillation variability. *The North Atlantic Oscillation: climatic significance and environmental impact*, 113-145.

Walker, M. *et al.* Formal definition and dating of the GSSP (Global Stratotype Section and Point) for the base of the Holocene using the Greenland NGRIP ice core, and selected auxiliary records. *Journal of Quaternary Science* **24**, 3-17, doi:10.1002/jqs.1227 (2009).

Weaver, A. J., Saenko, O. A., Clark, P. and Mitrovica, J. X. (2003) “Meltwater Pulse 1A from Antarctica as a trigger of the Bølling-Allerød warm interval.” Science 299:1709-1713.

Winsor, K., Carlson, A. E., Klinkhammer, G. P., Stoner, J. S. and Hatfield, R. G. (2012) “Evolution of the northeast Labrador Sea during the last interglaciation.” Geochemistry, Geophysics, Geosystems 13(11).

Wyatt, M. G., Kravstov, S. and Tsonis, A. A. (2012) “Atlantic Multidecadal Oscillation and Northern Hemisphere’s climate variability.” Climate Dynamics 38:929-949.

Yin, Q. Z. and Berger, A. (2011) Individual contribution of insolation and CO_2 to the interglacial climates of the past 800,000 years. Climate Dynamics, vol. 38(3-4) :709-724

Zhang, R., Delworth, T. L. and Held, I. M. (2007) “Can the Atlantic Ocean drive the observed multidecadal variability in the Northern Hemisphere mean temperature?” Geophysical Research Letters 34(2).

Regional setting.

Ocean Drilling Program Site 976 (36^{o} 12'N, 4^{o} 18'W, 1108 m water depth) is located in the Alboran Sea, westernmost Mediterranean Sea, approximately 100 km east of the Strait of Gibraltar and 60 km south of the southern Spanish continental margin (Fig. 1). The site was drilled in 1995 during ODP Leg 161 as part of a trans-Mediterranean transect of drill sites that aimed at reconstructing the Plio-Pleistocene palaeoceanography of the Mediterranean Sea (Comas, Zahn et al., 1997). Initial stratigraphic and palaeoceanographic work demonstrated the continuity of cores retrieved and the high sedimentation rates at Site 976 of >20 cm/ky (von Grafenstein et al., 1999; Combourieu-Nebout et al., 1999; Linares et al., 1999; de Kaene et al., 1999; Serrano et al., 1999).

Figure 1. Location of the multi-core drilled Site ODP 976 (insert map, blue dot) used in this study. Atlantic Ocean satellite image of public domain:
http://commons.wikimedia.org/wiki/File:Atlantic_Ocean_satellite_image_location_map.jpg

a. The Alboran Sea: Oceanography

The Alboran Sea constitutes the gateway for Atlantic waters entering the Mediterranean as a surface inflow; at depth Mediterranean Outflow Water (MOW) exits the Mediterranean through the Alboran Sea and transports salt to the upper North Atlantic (Rohling et al., 2009).

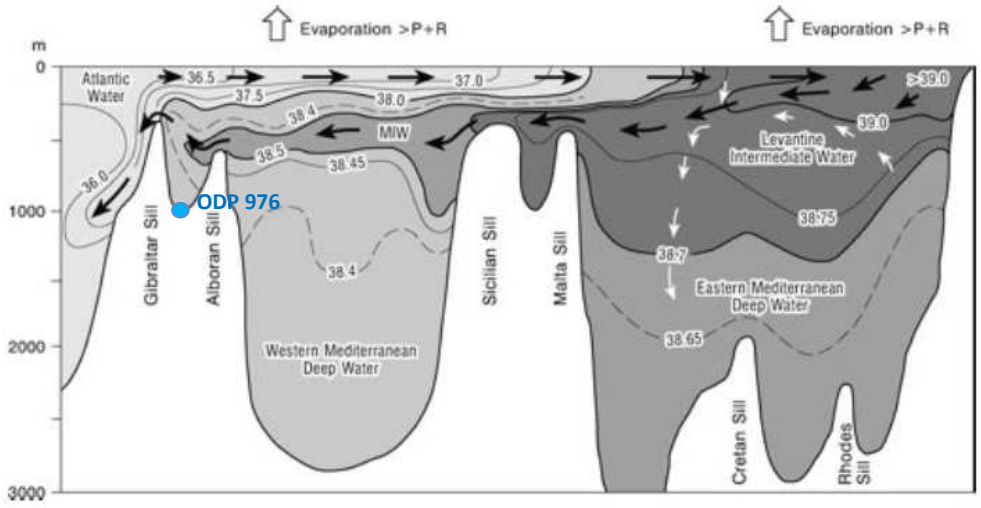

Figure 2. Longitudinal cross-section showing water mass circulation in the Mediterranean Sea today. Isolines indicate salinity values (psu, practical salinity units) and arrows indicate the direction of water flow. Modified from Rohling et al., 2009.

Atlantic Surface Waters (ASW) coming from the North Atlantic Ocean enter the Mediterranean Sea through the shallowest point in the Strait of Gibraltar, the Camarinal Sill (280m water depth). The 200-300m-thick Atlantic inflow enters the western Alboran Sea with a temperature around 15°C and salinity around 36.1-36.2 psu (Malanotte-Rizzoli, Robinson et al. 1994); Bethoux, 1980; Rohling et al., 2009). The surface waters maintain their "Atlanticity" as evaporation is low and the original hydrography of those waters remain largely unaltered.

In-situ instrumental hydrographic data from the MEDAR Group/MEDATLAS database (2002) display an average annual surface salinity in the Alboran Sea of 36.5 psu and an average annual sea surface temperature (SST) of 18°C. The full temperature range over the whole year is minimum SST of 15°C in February to maximum SST of 23°C in August; average Fall and Spring SST is 18°C and 17°C (Fig. 3).

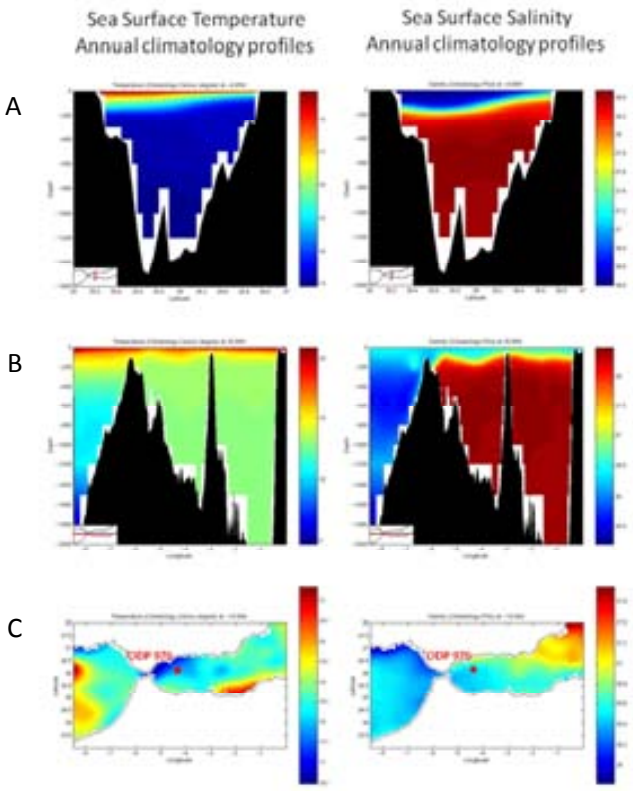

Figure 3. Sea Surface Temperature (SST, given in °C) and salinity (SSS, given in psu) annual averages in the western Alboran Sea. (A) Data are displayed along a north-south transect at 4.05°W. (B) Same as in A but along a west-east transect at 35.95°N. (C) Surface hydrography at 10m water depth. Source: MEDATLAS II, MEDAR Group (2002).
SST climatology: http://modb.oce.ulg.ac.be/backup/medar/medar_alboran_temp_clim.html
SSS climatology: http://modb.oce.ulg.ac.be/backup/medar/medar_alboran_psal_clim.html

The regional surface circulation pattern is subject to strong seasonal variations and controlled by both climate and the water exchange through the Strait of Gibraltar, where the entrance of the Atlantic inflow generates two semi-permanent anticyclonic gyres that are centred in the Western Alboran (WAG) and Eastern Alboran (EAG) Sea (Fig. 4).

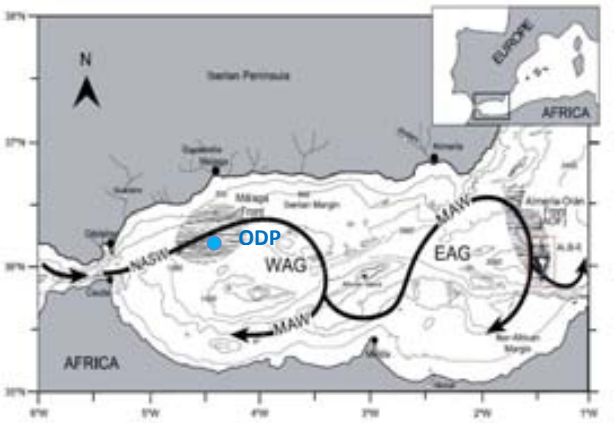

Figure 4. Schematic representation of the Alboran Sea surface circulation. Arrows indicate the mean trajectories of water masses and shaded areas indicate high productivity zones at the northern limb of the Western Alboran Gyre (WAG) and the eastern limb of the Eastern Alboran Gyre (EAG). Blue dot marks ODP Site 976. Modified from Bárcena et al., 2004.

Two systems of high biological productivity exist in the Alboran basin that are associated with the WAG and EAG and stimulated by westerly winds over this area. Two types of upwelling events take place in this region (Garcia-Gorriz and Carr 2001): wind-induced upwelling, especially along the northern limb of the WAG off the southern Spanish coast, in the vicinity of ODP Site 976, and gyre-induced upwelling along the periphery of these features. Primary production in the upper 100m in the Modified Atlantic Water (MAW) and the Alboran gyres is higher than in the surrounding oligotrophic Mediterranean waters (Pujol and Grazzini 1995) (Fig. 5).

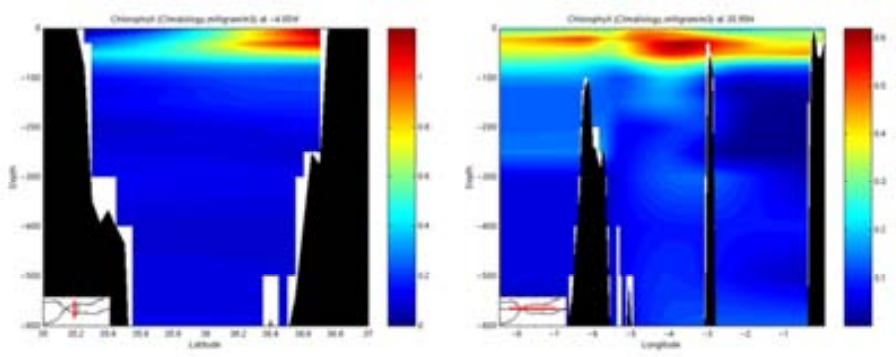

Figure 5. Chlorophyll-A (mg/m^3) concentrations in the Alboran Sea. Left panel: data from a vertical South-North section at 4.05°W. Right panel: data from a West-East section at 35.95°N. Source: MEDATLAS II, MEDAR Group (2002).
http://modb.oce.ulg.ac.be/backup/medar/medar_alboran_cphl_clim.html

The ensuing hydrographic and environmental conditions determine the assemblage and relative abundances of the different planktic communities, which are sensitive indicators of surface water conditions and therefore considered important tracers of oceanographic changes. This bears relevance for this study that uses planktic foraminifera as carriers of palaeoceanographic signals. In order to correctly interpret past hydrographic reconstructions based on these planktic organisms is vital to understand their modern ecology and depth habitats and the environmental factors controlling both spatial and temporal distribution of foraminifers. Several studies have contributed to improve the interpretation of palaeoceanographic records in this regard, focusing on determining the influence of seasonal oceanographic changes in the seasonal variability and evolution of particles and planktic foraminiferal assemblages fluxes in this area and the integrated signal left in the bottom sediments combining sediment trap and surface sediment analyses: geochemical, micropalaeontological analyses, planktic faunal assemblages and particle fluxes (Bárcena et al., 2004; Hernández-Almeida et al., 2011; Rigual-Hernández et al.,

2012). García-Gorriz and Carr (2001) distinguish four productivity regimes in the Alboran Sea: an autumn-to-winter bloom regime from November to March, a non-bloom regime from May to September, a Spring-time transitional regime in April-May that develops with the onset of thermal stratification of the water column, and another transitional regime in Fall, October-November, coinciding with maximum wind stress and vigorous vertical mixing breaking up the stratification within the basin. These regimes impact the regional SST as was demonstrated with temperature time series studies (Fig. 6) (García-Gorriz and Carr, 2001).

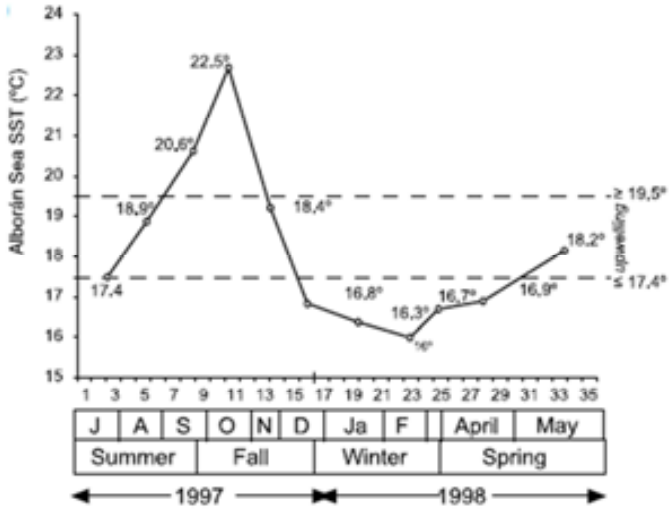

Figure 6. Temporal evolution of surface temperature in the WAG region (García-Gorriz and Carr, 2001), figure extracted from Hernández Almeida et al., 2011.

Sediment trap studies in the Western Mediterranean show that planktic foraminifera are present throughout the entire year and their production displays a prominent seasonal pattern (Bárcena et al., 2004; Hernández Almeida et al., 2011; Rigual-Hernández et al., 2012). In the Alboran Sea the seasonal evolution of planktic foraminifera directly follows the seasonal evolution of the regional oceanography, showing an annual maximum abundance during the spring plankton bloom that produces a most pronounced proliferation of *Globigerina bulloides* that constitutes the main faunal component of the planktic foraminiferal assemblage in the Alboran Sea (Bárcena et al., 2004). This species' abundance distribution thus presents a seasonal trend that is very similar to the total planktonic foraminiferal abundance distribution (left panel in Fig. 7, Bárcena et al., 2004). *Globigerinoides ruber* and *Globorotalia inflata* are the only two other species of significant abundance and together with *G. bulloides*, they account for more than 90% of the foraminiferal assemblage in the Alboran Sea.

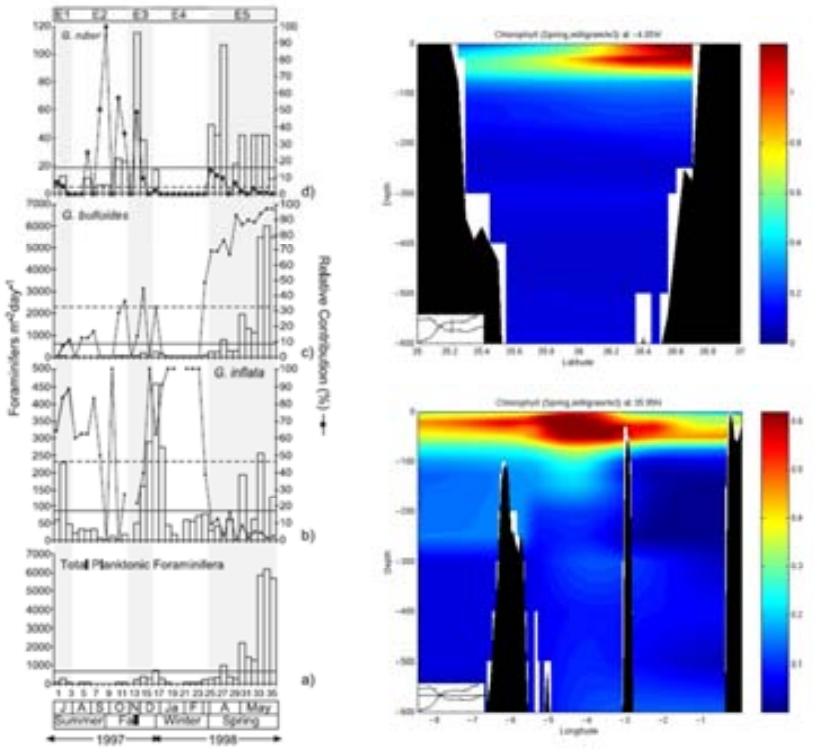

Figure 7. Left panel: Seasonal pattern of flux (bars) and relative abundance (solid lines) of the three most significant species of the planktonic foraminifera assemblage in the Alboran Sea. (a) total foraminifera, (b) *Globorotalia inflata* (c) *Globigerina bulloides* (d) *Globigerinoides ruber*. From Bárcena et al., 2004. Right panel: Chlorophyll-A (mg/m^3) spring average in the Alboran Sea, from a vertical South-North transect at 4.05°W (top) and from a West-East transect at 35.95°N (bottom). Source: MEDATLAS II, MEDAR Group (2002). http://modb.oce.ulg.ac.be/backup/medar/medar_alboran_cphl_spring.html

G. inflata is a deep-dwelling (50-300m) planktonic foraminifera (Hemleben et al., 1989) generally found along the gyre-margin region of the North Atlantic, in the transitional zone between the subpolar and subtropical Atlantic regions. In the Western Mediterranean, it is present throughout the year and is considered the dominant species during winter, in association with *G. bulloides* (Pujol and Vergnau-Grazzini, 1995; Bárcena et al. 2004). According to Rigual-Hernández et al. (2012) the highest contribution of *G. inflata* regarding its distribution in surface sediments is in the Alboran Sea following the path of the Modified Atlantic Waters (MAW).

G. ruber alba (white) is a shallow dwelling species, preferring well stratified waters. It is the most widely distributed in the tropical and subtropical Atlantic (Bé, 1977). In the Alboran Sea it is the main contributor to the foraminiferal assemblage at the end of summer and therefore, considered a summer species (Pujol and Vergnaud-Grazzini, 1995; Bárcena et al., 2004).

The direct linking of the seasonal hydrography in the Alboran Sea on the planktonic foraminiferal assemblage (Bárcena et al., 2004; Pujol and Vergnaud Grazzini, 1989, 1995) confirms the value of planktonic foraminifera and the chemical proxy-signals extracted from them as tools for reliably reconstructing the palaeoceanography of the Alboran Sea as has been demonstrated in numerous studies (Pujol and Vergnaud-Grazzini, 1995, Bárcena et al., 2004; Hernández-Almeida et al., 2011; Rigual-Hernández et al., 2012; Cacho et al., 1999, 2000). At the same time, the Alboran Sea and ODP Site 976 receive surface waters directly derived from the North Atlantic and hence they are at a watchdog position to monitor the hydrographic variability of North Atlantic inflow waters and by extension, of North Atlantic surface ocean climatology.

b. Alboran Sea climatology and Atlantic climatic connections

The Mediterranean climate is characterized by mild wet winters and dry warm summers, largely as a result of its latitudinal position in the transitional zone between the mid-latitude temperate westerlies system and the subtropical high pressure belt over North Africa. During northern hemisphere summer, the Intertropical Convergence Zone (ITCZ) moves north and the Mediterranean region comes under the influence of North Africa's arid climatic belt, causing warm and dry summers. During northern hemisphere winter, when the ITCZ is displaced south, the Mediterranean climate is more closely connected with the temperate and humid conditions of central and northern Europe that are driven by the westerly wind system and the marine air masses they carry with them. Because of this transitional character, the Mediterranean region is particularly sensitive to changes in atmospheric circulation and it indeed is identified as a hotspot for future climate change projections (Giorgi 2006); (Giorgi and Lionello 2008)).

Western Mediterranean climate is influenced by atmospheric teleconnections connecting it with the African and Asian monsoon systems in summer (Alpert, Baldi et al. 2006) and the North Atlantic Oscillation (NAO) in winter (Hurrell, 1995; Trigo et al., 2002; Krichak and Alpert, 2005; Giorgi and Lionello, 2008) (Fig. 8). The NAO constitutes one of the lead climate oscillators in the North Atlantic region and is driven by variations in the atmospheric pressure gradient between the subtropical high pressure anticyclone near the Azores and the subpolar low pressure system near Iceland. It influences storm track trajectories and creates a dipole pattern of precipitation between

northern and southern Europe (Meyers and Pagani 2006). An important consequence of NAO variability is its impact on the climate and freshwater balance of the Mediterranean Sea. A positive NAO phase, defined as a stronger than normal gradient between the subtropical high and subpolar low pressure centres, results in stronger westerlies and a more northerly directed trajectory of the North Atlantic low pressure systems causing wetter than normal conditions over Europe and drier than normal conditions in the Mediterranean region (Krichak and Alpert, 2005). A negative NAO phase, defined as a reduced meridional pressure gradient results in weaker westerlies and a more zonal trajectory of low pressure systems bringing the Mediterranean region under the influence of moist air masses arriving from the Atlantic and causing above-normal humid conditions. A substantial drying and warming signal over the Mediterranean region, present in most global (Gibelin and Déqué 2003); (Ulbrich, May et al. 2006) and regional (Dequé et al., 2007) model projections, is associated with a northward shift of the mid-latitude North Atlantic storm track, which is consistent with an anthropogenic forcing in modeling studies suggesting increasing intensity and frequency of positive NAO conditions in future climate simulations (Terray, Demory et al. 2004); Giorgi and Lionello, 2008).

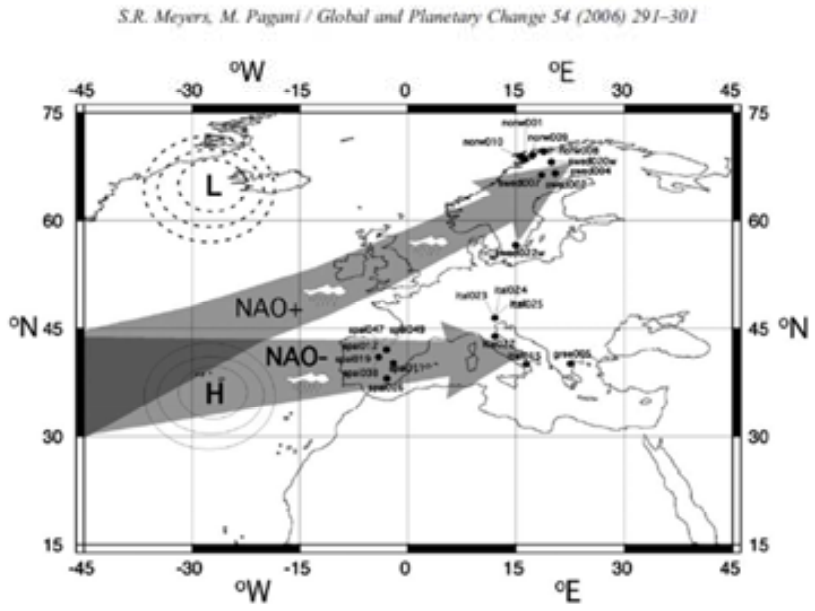

Figure 8. Positive and negative NAO phases affecting precipitation over the Mediterranean region. Grey arrows indicate Atlantic low pressure trajectories associated with NAO+ and NAO- phases. From Meyers and Pagani (2006).

Beyond impacting weather patterns, the NAO has also been linked with marine ecosystem changes. Strong diatom blooms have been attributed to negative NAO phases, and viceversa (Gómez and Gorsky, 2003). Planktonic foraminiferal fluxes, on the other hand, did not display a connection with the NAO and (Rigual-Hernández et al., 2010, 2012). But an impact of atmospheric circulation has been demonstrated in several palaeoceanographic studies in the Mediterranean, demonstrating that the teleconnections between high and mid latitudes that define the regional climate today also operated in the past (Cacho et al., 1999; Frigola et al., 2007; Gonzalez-Mora et al., 2008).

Several studies reported on possible links between El Niño-Southern Oscillation (ENSO) event and the climatology of the Alboran Sea through remote teleconnections (Alpert et al., 2006; Giorgi and Lionello, 2008), preventing the development of winter upwelling and eventually collapsing the local gyre circulation (Hernandez Almeida et al., 2011) with consequences for planktonic assemblages and biological productivity levels (Bárcena et al., 2004; Rigual-Hernández et al., 2010).

c. ODP976 as a palaeo-monitoring station of North Atlantic Ocean climatology and climate variability.

Climate variations and variability that prominently impacted the North Atlantic region on orbital and suborbital time scales in the past has also been observed at core sites in the Alboran Sea and has been used to confirm the influence of migrating North Atlantic pressure systems on the western Mediterranean, much like the patterns driven by the NAO today (Cacho et al., 1999; Combourieu Nebout et al., 2002; (Moreno, Cacho et al. 2005). Moreover, the Alboran Sea is particularly suitable for palaeoceanographic studies, because sedimentation rates are high enabling fine-scale palaeo-records to be established for testing the ocean-atmosphere connections under the varying boundary conditions of past climatic states (Rohling 1998), Cacho et al., 1999, Cacho et al., 2000, Combourieu Nebout et al., 2002, Combourieu-Nebout et al., 2009; Martrat et al., 2004). Terrestrial records from Iberian lake sequences suggest that the impacts stimulated by these connections also extended to the terrestrial environment, including the

hydrologic cycle and vegetation turnover (González-Sampériz, Valero-GarcÃ©s et al. 2006), Moreno et al., in press; and references therein).

References:

Alpert, P., M. Baldi, et al. (2006). Chapter 2 Relations between climate variability in the Mediterranean region and the tropics: ENSO, South Asian and African monsoons, hurricanes and Saharan dust. Developments in Earth and Environmental Sciences, Elsevier. **Volume 4:** 149-177.

Bé, A. H. W., An ecological, zoogeographic and taxonomic review of recent planktonic Foraminifera, in Oceanic Micropaleontology 1, edited by A. T. S. Ramsay, pp. 1– 100, Academic, San Diego, Calif., 1977.

Bethoux, J.P. (1980) "Mean water fluxes across sections in the mediterranean-sea, evaluated on the basis of water and salt budgets and of observed salinities. Oceanologica Acta 3(1):79-88.

Cacho, I. (1999)."Dansgaard-Oeschger and Heinrich event imprints in the Alboran Sea paleotemperatures." Paleoceanography 14:698.

Cacho, I., J. O. Grimalt, et al. (2001) "Variability of the western Mediterranean Sea surface temeprature during the last 25,000 years and its connection with the Northern Hemisphere Climatic changes." Paleoceanography 16(1):40.

Comas, M.C., Zahn, R., and Klaus, A., et al., 1996. *Proc. ODP, Init. Repts.*, 161: College Station, TX (Ocean Drilling Program). doi:10.2973/odp.proc.ir.161.1996

Combourieu Nebout, N., Londeix, L., Baudin, F., Turon, J.-L., von Grafenstein, R., and Zahn, R., 1999. Quaternary marine and continental paleoenvironments in the western Mediterranean (Site 976, Alboran Sea): palynological evidence. *In* Zahn, R., Comas, M.C., and Klaus, A. (Eds.), *Proc. ODP, Sci. Results*, 161: College Station, TX (Ocean Drilling Program), 457–468. doi:10.2973/odp.proc.sr.161.238.1999

Combourieu-Nebout, N., Turon, J. L., Zahn, R., Capotondi, L., Londeix, L. and Pahnke, K. (2002) "Enhanced aridity and atmospheric high-pressure stability over the western Mediterranean during the North Atlantic cold events of the past 50 k.y." Geology 30(10):863-866.

Combourieu-Nebout, N., O. Peyron, et al. (2009) "Rapid climatic variability in the west Mediterranean during the last 25,000 years from high resolution pollen data." Climate of the Past 5(3):503.

de Kaenel, E., Siesser, W.G., and Murat, A., 1999. Pleistocene calcareous nannofossil biostratigraphy and the western Mediterranean sapropels, Sites 974 to 977 and 979. *In* Zahn, R., Comas, M.C., and Klaus, A. (Eds.), *Proc. ODP, Sci. Results*, 161: College Station, TX (Ocean Drilling Program), 159–183. doi:10.2973/odp.proc.sr.161.250.1999

Hemleben, Ch., M. Spindler, and O. R. Anderson, Modern Planktonic Foraminifera, p. 363, Springer-Verlag, New York, 1989.

Frigola, J., Moreno, A., Cacho, I., Canals, M., Sierro, F. J., Flores, J. A., Grimalt, J. O., Hodell, D. A., and Curtis, J. H. (2007) "Holocene climate variability in the Western Mediterranean region from a deepwater sediment record." Paleooceanography, 22 .

Garcia-Gorriz, E. and M.-E. Carr (2001). "Physical control of phytoplankton distributions in the Alboran Sea: A numerical and satellite approach." Journal of Geophysical Research: Oceans **106**(C8): 16795-16805.

Gibelin, A. L. and M. Déqué (2003). "Anthropogenic climate change over the Mediterranean region simulated by a global variable resolution model." Climate Dynamics **20**(4): 327-339.

Giorgi, F. (2006). "Climate change hot-spots." Geophysical Research Letters **33**(8): L08707.

Giorgi, F. and P. Lionello (2008). "Climate change projections for the Mediterranean region." Global and Planetary Change **63**(2â€“3): 90-104.

González-Mora, B., Sierro, F. J., Schönfeld, J. (2008) "Temperature and stable isotope variations in different wáter masses from the Alboran Sea (Western Mediterranean) between 250 and 150 ka." Geochemistry, Geophysics, Geosystems 9(10):1525-2027.

González-Sampériz, P., B. L. Valero-GarcÃ©s, et al. (2006). "Climate variability in the Spanish Pyrenees during the last 30,000 yr revealed by the El Portalet sequence." Quaternary Research **66**(1): 38-52.

Hurrell, J. W. (1995). NAO index data provided by the climate analysis section.*NCAR, Boulder, USA*.

Krichak, S., Alpert, P., Bassat, K., & Dayan, M. An RCM Evaluation of Climate Change Trends and Uncertainties over the Eastern Mediterranean Region for GLOWA Jordan River Project.

Linares, D., González-Donoso, J.M., and Serrano, F., 1999. Paleoceanographic conditions during the Quaternary at Sites 976 (Alboran Sea) and 975 (Menorca Rise) inferred from the planktonic foraminiferal assemblages: basis for a biostratigraphy. *In* Zahn, R., Comas, M.C., and Klaus, A. (Eds.), *Proc. ODP, Sci. Results*, 161: College Station, TX (Ocean Drilling Program), 441–455. doi:10.2973/odp.proc.sr.161.240.1999

Malanotte-Rizzoli, P., A. Robinson, et al. (1994). The Mediterranean Sea, a Test Area for Marine and Climatic Interactions. Ocean Processes in Climate Dynamics: Global and Mediterranean Examples, Springer Netherlands. **419:** 239-254.

Martrat, B., J. O. Grimalt, et al. (2004). "Abrupt Temperature Changes in the Western Mediterranean over the past 250,000 years." Science 306 (5702):1762.

Meyers, S. R. and M. Pagani (2006). "Quasi-periodic climate teleconnections between northern and southern Europe during the 17thâ€"20th centuries." Global and Planetary Change **54**(3â€"4): 291-301.

Moreno, A., I. Cacho, et al. (2005). "Links between marine and atmospheric processes oscillating on a millennial time-scale. A multi-proxy study of the last 50,000 yr from the Alboran Sea (Western Mediterranean Sea)." Quaternary Science Reviews **24**(14-15): 1623.

Pujol, C. and C. V. Grazzini (1995). "Distribution patterns of live planktic foraminifers as related to regional hydrography and productive systems of the Mediterranean Sea." Marine Micropaleontology **25**(2â€"3): 187-217.

Rohling, E. J. (1998). "Magnitude of sea-level lowstands of the past 500,000 years." Nature **394**: 162.

Rohling, E. J., Abu-Zied, R. H., Casford, J. S. L., Hayes, A., and Hoogakker, B. A. A. (2009), The marine environment: present and past, in J. C.Woodward (ed.), *The Physical Geography of theMediterranean*. Oxford University Press, Oxford, 33–67.

Serrano, F., González-Donoso, J.M., and Linares, D., 1999. Biostratigraphy and paleoceanography of the Pliocene at Sites 975 (Menorca Rise) and 976 (Alboran Sea) from a quantitative analysis of the planktonic foraminiferal assemblages. *In* Zahn, R., Comas, M.C., and Klaus, A. (Eds.), *Proc. ODP, Sci. Results*, 161: College Station, TX (Ocean Drilling Program), 185–195. doi:10.2973/odp.proc.sr.161.239.1999

Terray, L., M.-E. Demory, et al. (2004). "Simulation of Late-Twenty-First-Century Changes in Wintertime Atmospheric Circulation over Europe Due to Anthropogenic Causes." Journal of Climate **17**(24): 4630-4635.

Trigo, R. M., Osborn, T. J., & Corte-Real, J. M. (2002). The North Atlantic Oscillation influence on Europe: climate impacts and associated physical mechanisms. *Climate Research*, *20*(1), 9-17.

Ulbrich, U., W. May, et al. (2006). Chapter 8 The Mediterranean climate change under global warming. Developments in Earth and Environmental Sciences, Elsevier. **Volume 4:** 399-415.

von Grafenstein, R., Zahn, R., Tiedemann, R., and Murat, A., 1999. Planktonic $\delta^{18}O$ records at Sites 976 and 977, Alboran Sea: stratigraphy, forcing, and paleoceanographic implications. *In* Zahn, R., Comas, M.C., and Klaus, A. (Eds.), *Proc. ODP, Sci. Results*, 161: College Station, TX (Ocean Drilling Program), 469–479.doi:10.2973/odp.proc.sr.161.233.1999

Methodology

a. Core sampling

A composite depth section was generated from Holes B, C and D for the upper 350 meters at Site 976 by matching GRAPE density, magnetic susceptibility, natural gamma radiation and 550-nm-wavelenthg color reflectance records of the three holes. This resulted in a common depth scale, the Meters Composite Depth (mcd) scale. In this thesis the splice table listing the common depth for the various Holes and Sections was used when preparing the sample request that was sent to the ODP/IODP Core Repository at the University of Bremen, Germany. Once approved, the sampling party took place in May 2010, and with the technical assistance of the curating personnel over 18m of core sections were sampled at the ODP Repository in Bremen (Germany): from Holes A and D from 0.07 to 9.11 mbsf (meters below sea floor) and from Hole C from 36.01 to 44.48 mbsf at 2 cm intervals; these sections correspond to the MIS2-T2-Holocene and MIS6-T2-MIS5e that are targeted in this thesis. An offset correction was applied to convert the mbsf of individual samples to the continuous mcd scale. A total of 943 samples containing 15 cm^3 of sediment were taken at ~2cm intervals: 486 samples spanning the MIS2-T1-PIG sequence and 457 samples spanning the MIS6-T2-MIS5e sequence. The 15 cm^3 samples were divided into three subsamples of 5 cm^3each in order to accommodate the needs of two scientific groups collaborating on the Site 976 palaeo-reconstruction. Drs. Belen Martrat and Joan O. Grimalt, at the Institute of Environmental Assessment and Water Research (IDAEA), of the Spanish Council for Scientific Research (CSIC), conducted organic geochemical analyses to reconstruct the SST from alkenones ($U^{k'}_{37}$) (Martrat et al., 2013, submitted) and to assess marine palaeoproductivity changes and the level of oxygenation at the seafloor sediment-water interface by using n-nonacosane and n-hexacosan-1-ol compounds (C_{26}-OH and C_{29}). Drs. Nathalie Combourieu Nebout at the Comissariat à l'Energie Atomique, and Frédérique Eynaud at the Laboratoire Environnements et Paléoenvironnements Océaniques (EPOC, Université de Bordeaux) in France were generating palynological records to reconstruct the terrestrial palaeoclimatology on the land surrounding ODP Site 976, and to estimate SST from planktonic foraminiferal census counts.

b. Sample preparation

All samples were freeze-dried in order to aid disaggregation and subsequently washed through a 63µm mesh; the fine fraction <63 µm was kept for geochemical and coccolithophore studies in a separate project (MEDSEA, Ziveri et al., unpublished data). A recent study (Friedrich et al., 2012) reveals an overall decrease in Mg/Ca ratios with increasing test size for non-symbiotic species as *G. bulloides*, suggesting the use of very narrow size fraction windows (if possible as narrow as 50µm), especially for surface-dwellers, such as in our case. Therefore, in this thesis, *Globigerina bulloides* specimens were picked from the 250-315µm size fraction. Ideally, 30-40 specimens were sufficient for both paired stable isotope and Mg/Ca measurements but 65% of all samples did not yield this number of specimens and additional samples were requested from the collaborating partners to enable extracting more specimens. In case this procedure did still not yield enough specimens consecutive samples were joined together or the samples were used for either trace element or oxygen isotope analysis. Across the MIS2-T1-Holocene sequence, 55% of the samples were either joined or used for one of the two analyses. In the case of the MIS6-T2-MIS5e sequence, this was applied to 34% of the samples. A consequent decrease in temporal resolution resulted in these cases. Overall a total of 1563 foraminiferal samples were extracted. Prior to analysis the foraminiferal samples were carefully cleaned; this involved gently crushing the shells between methanol-cleaned glass slides to break open individual chambers in order to release possible sediment filling and support an efficient cleaning of the samples. From the crushed material, approximately ¼ of the sample was used for stable isotope measurements and the rest for trace element analyses.

Globigerina bulloides is a spinose and non-symbiotic planktonic foraminifera species (Fig. 9) that can be found in subpolar to tropical regions in the open ocean but it is predominantly considered a subpolar species (Bé and Tolderlund, 1971). It is a surface-dweller with a depth habitat of 50-100 m water depth (Elderfield and Ganssen, 2000), although some authors (Pujol and Vergnaud-Grazzini, 1995) describe the occurrence of this at variable depths and below the thermocline which is ascribed to the feeding opportunistic behaviour of this species (Schiebel et al., 1997; Schiebel and Hemleben, 2005). Hence, its distribution principally responds to high food availability conditions, mainly associated to upwelling events (Bé and Hutson, 1977; Pujol and Vergnaud-Grazzini, 1995; Schiebel and Hemleben, 2000; Bárcena et al., 2004; Hernández-Almeida

et al., 2011). *G. bulloides* is present at considerable abundances in surface sediments of the Western Mediterranean especially in high primary productivity areas (Bárcena et al., 2004; Hernández-Almeida et al., 2011). Trace elements and stable isotopes measured in *G. bulloides* in the Alboran Sea should record surface conditions in spring, because this is the season with the highest fluxes of this surface-dweller foraminiferal species (Bárcena et al., 2004; Hernández Almeida, 2011; Rigual-Hernández et al., 2012).

Therefore, in this thesis preference is given to *G. bulloides* as a surface-dweller for stable isotope and trace element analyses in order to confidently record the palaeo-signals that were connected with Atlantic surface waters entering the Alboran Sea.

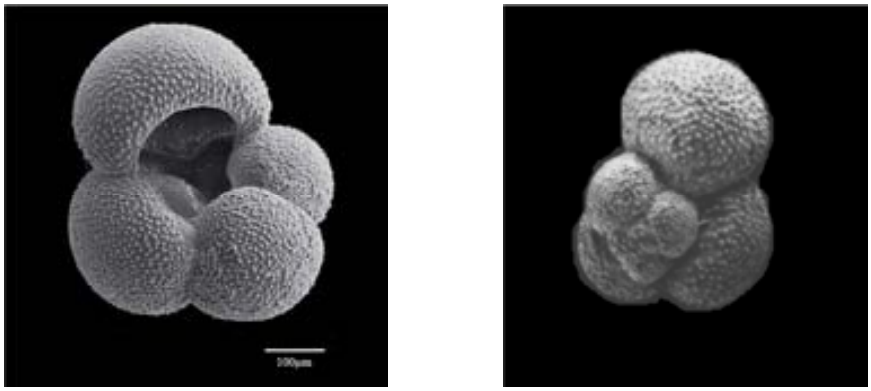

***Globigerina bulloides* d'Orbigny, 1826.**
Class: *Rotalia*
Subclass: *Globigerinana*
Order: *Globigerinida*
Family: *Globigerinidae*

Figure 9. SEM-image of a specimen of *Globigerina bulloides* by Lúcia de Abreu. Source: Foraminifera EU Project Team. http://foraminifera.eu/singleopo.php?no=1005678&aktion=suche

c. Age model development

The age model for the MIS2-T2-Holocene sequence is based on 13 accelerator mass spectrometry (AMS) radiocarbon data determined for the upper 15.9 mcd of ODP 976 Holes C and D (Fig. 10) (Combourieu-Nebout et al., 2002). The data were measured on monospecific samples of >125µm *Globigerina bulloides* and *Neogloboquadrina pachyderma (s)*. They were corrected for reservoir fractionation by 400 yr (Bard, 1988; Siani et al., 2000) and converted to calendar years using Intcal09 (Heaton et al., 2009, Reimer et al., 2009). The age model published by Combourieu-Nebout et al. (2002) was shown to yield close correlation of the ODP976 palaeoclimatic records with the Greenland Ice Sheet Project 2 (GISP2) ice core $\delta^{18}O$ record (Grootes et al., 1993).

TABLE 1. RADIOCARBON DATES AND ISOTOPIC EVENT USED FOR AGE MODEL OF OCEAN DRILLING PROGRAM SITE 976

Core, Hole, section, interval (cm)	Sample type	Depth (mcd**)	^{14}C age (yr B.P.)	Error	Calendar age (yr B.P.)
C 1H 1 60–62	*G. bulloides*	0.61	1710	± 40	1620§
C 1H 1 102–104	*G. bulloides*	1.03	3235	± 30	3460§
C 1H 2 53–55	*G. bulloides*	2.14	7010	± 50	7820§
C 1H 2 132–134	*G. bulloides*	2.83	8730	± 60	9700§
C 1H 3 60–62	*N. pachyderma*	3.61	10075	± 50	11 682§
C 1H 4 10–12	*G. bulloides*	4.61	9630	± 60	11 090†
C 1H 4 50–52	*G. bulloides*	5.01	11960	± 80	13 988§
D 2H 3 100–102	*G. bulloides*	5.51	12720	± 80	14 911§
D 2H 4 37–39	*N. pachyderma*	6.38	14330	± 90	16 856§
D 2H 5 2–4	*G. bulloides*	7.53	17220	± 120	20 309§
C 2H 3 55–57	*G. bulloides*	9.78	22420	−310 + 320	26 394§
C 2H 4 47–49	*N. pachyderma*	11.21	27140	−450 + 470	31 776#
C 2H 5 45–47	*N. pachyderma*	12.69	29930	−640 + 700	34 894#
C 2H 6 61–63	*G. bulloides*	14.35	33750	−610 + 660	39 087#
C 2H 6 75–77	*N. pachyderma*	14.49	34230	−1050 +1210	39 609#
D 3H 3 120–122	*G. bulloides*	15.40	35700	−750 + 820	41 194#
D 3H 4 18–20	*G. bulloides*	15.88	32270	−760 + 700	37 473†
Isotope stages	OIS ½ transition	23.00			58 960*

Note: Accelerator mass spectrometry ^{14}C dates are corrected of the constant water reservoir age of 400 yr.
§ Converted to calendar years after Stuiver et al. (1998) and Bard et al. (1998).
# Converted to calendar years after Bard (1998) and Bard et al. (1998).
* Age after Martinson et al. (1987).
† Dates rejected as abnormally young.
**Meters composite depth.

Figure 10. Radiocarbon dates and isotopic events used for establishing the age model of ODP Site 976. Extracted from Combourieu-Nebout et al., 2002)

For the MIS6-T2-MIS5e sequence, the age model was established by Martrat et al. (2013, submitted) and is based on a slightly modified version of the synthetic record of Greenland temperature published by Barker et al. (2011). The synthetic profile mainly uses the Antarctic EDC3 isotopic signal as a reference (EPICA Community members, 2006; Masson-Delmotte et al., 2011) and is further contrasted and improved using stalagmites and developed ice core chronologies (Bazin et al., 2013; Veres et al., 2013).

Based on the age models established for the two time periods, the time step achieved between samples is on average multi-decadal (60-90 yr) for the stable isotope profiles and centennial (110-150yr) for the trace element measurements.

d. Stable isotope analysis

For the stable isotope analyses in our study, around 30 μg of crushed homogenized calcite for each sample was cleaned by means of consecutive methanol rinses and brief sonication to remove clays and other possible sedimentary components from the sample. Measurements were conducted in a Thermo Scientific MAT253 Isotope Ratio Mass Spectrometer (IR-MS) coupled to a Kiel IV sample gas preparation device installed at the Universitat Autònoma de Barcelona. To monitor data quality and possible instrument drift, the IAEA-CO-1 carbonate standard provided by the International Atomic Energy Agency (IAEA) was measured regularly, typically every 10th sample, which amounted to 10 analyses of carbonate standard per batch of 36 samples. The IAEA certifies the $\delta^{13}C$ value of its CO-1 standard to +2.492±0.03‰ on the VPDB scale and recommends a $\delta^{18}O$ value of -2.4±0.1‰ VPDB (Stichler, 1995; Copen et al., 2006). Based on 349 analyses of this carbonate standard, external reproducibility was better than 0.08 for $\delta^{18}O$ and better than 0.04 for $\delta^{13}C$.

For this thesis a total of 794 stable isotope measurements were carried out (including 184 replicates, which were possible when enough sample abundance was available), 329 analyses covering the MIS2-T1-Holocene section and another 371 for the MIS6-T2-MIS5e sequence.

e. Trace element analysis

To include or not the reductive step in the cleaning procedure in order to remove a variety of contaminant phases such as Mn-Fe-oxide commonly associated to the foraminiferal tests is a key step among paleothermometry (Pena et al., 2005). Therefore, as a previous step and in order to define the cleaning procedure to follow, we selected 10 samples with sufficient abundance of *G. bulloides* (60 specimens, 30 per cleaning protocol) along the MIS2-T1-Holocene sequence (0.07-

9.11mcd) representing glacial, deglacial and interglacial intervals. Reductive and oxidative cleaning procedures were applied to each subsample of 30 specimens. Very similar Mg/Ca ratios were obtained from the different cleaning methods, but Mn/Ca ratios were always higher with the oxidative cleaning. Hence, in order to avoid potential Mg/Ca bias from Mn-oxide coatings to our Mg/Ca results, we included the reductive step in the cleaning procedure (Barker et al., 2003).

First, foraminiferal samples underwent repeated ultra-purified water (milli-Q) and methanol rinses combined with sonication episodes in order to remove clay minerals. Next, the mentioned reductive step consisted on the action of a reductive reagent (hydrous hydrazine in a citric acid/ammonia buffer) in a 30 minute-boiling water bath sonicating of samples for several seconds every 2 minutes. Next, to remove organic matter, samples were cleaned with an oxidative reagent: 100 µL of hydrogen peroxide (H_2O_2 30%) and 10 mL NaOH 0.1M, for 10 minutes in a 70^{o}C bath, sonicating samples every 2 and 5 minutes. Weak acid (0.001M HNO_3) leaching was used as a final cleaning step to remove adsorbed contaminants before dissolving the foraminiferal calcite in 400µL of 1% HNO_3. Preliminary calcium [Ca^{2+}] determination was provided by analyzing an aliquot of the samples (20µL in 980 µL ultrapured 1% HNO_3) using an Inductively Coupled Plasma Mass Spectrometer (ICP-MS, Agilent model 7500ce) at the SAQ department at the UAB (*Servei d'Anàlisi Química*, Chemical Analyses Service). The remaining solutions were diluted to 40ppm [Ca^{2+}] and injected into the ICP-MS. A total of 514 Mg/Ca ratios were measured, 232 for the MIS2-T2-Holocene sequence and 282 for the MIS6-T2-MIS5e sequence. No duplicates were possible as the abundance of *G. bulloides* was a limiting factor (as already mentioned in section (b) "*Sample preparation*"). Besides calcium [Ca^{2+}] and magnesium [Mg^{2+}], other trace elements concentrations (Yu et al., 2005; de Villiers et al., 2002) were measured, such as aluminum [Al^{3+}], manganese [Mn^{2+}] and iron [Fe^{3+}], as indicators of possible silicate and clay minerals contamination and Fe-Mn oxide coatings (Boyle, 1983; Barker and Elderfield, 2001; Barker et al., 2003; Skinner and Elderfield, 2005; Pena et al., 2005). No correlation was found between Al/Ca, Fe/Ca, Mn/Ca and Mg/Ca ratios (Al/Ca vs Mg/Ca, r^2= 0.01; Mn/Ca vs Mg/Ca, r^2 =0.03; Fe/Ca, r^2= 0.04). Therefore, the possibility of potential biases of the foraminiferal Mg/Ca ratios from contamination by silicates, clays or Fe-Mn-oxide coatings (Barker et al., 2003; Pena et al., 2005; Ferguson et al., 2008) can be considered unlikely. However, in order to be fully consistent with commonly accepted procedures, Mg/Ca ratios from samples with Al/Ca >400µmol/mol (Boyle, 1983) and/or Mn/Ca >100µmol/mol

(Wit, 2010) were eliminated from the data set as these values used commonly as an indication of potential contamination.

Analytical precision was monitored calculating the relative standard deviation (rsd) of two in-house standard solutions, CS2 (Mg/Ca=2.571±0.003) and CS4 (Mg/Ca=7.713±0.009 mmol mol^{-1}) analyzed every 5 and 10 samples, respectively, with an average rsd of 1.69% (n=65). Additionally, another limestone standard (ECRM752-1) with a specified Mg/Ca of 3.75 mmol mol^{-1} was also measured (Greaves et al., 2008) with a result obtained of 3.77±0.09 mmol mol^{-1}. A potential partial dissolution biasing the Mg/Ca is discarded as a result of the lack of correlation between the Mg/Ca and the Sr/Ca (Dekens et al., 2002; Skinner and Elderfield, 2005).

For this thesis, a total of 514 trace elements analyses were performed, 232 for the MIS2-T1-Holocene and 282 for the MIS-T2-MIS5e sequence.

Regarding temperature calibration, Mg/Ca ratios were converted into sea surface temperature (SST) estimates using the specific calibration equation for *G. bulloides* by Elderfield and Ganssen (2000):

$$Mg/Ca=0.56*exp(0.1*T)$$

Using Elderfield and Ganssen (2000) calibration, the most recent Holocene Mg/Ca derived SSTs in our study closely match to modern spring SST observations in the region (17-18°C, MEDATLAS II, Medar Group, 2002), supporting the use of this equation in this study. Due to the close link between North Atlantic surface waters and the Alboran basin throughout the late Pleistocene, Elderfield and Ganssen (2000) calibration has also been considered by previous studies (Gonzalez-Mora et al., 2008) as an adequate option for the calculation of the Mg/Ca derived SST in the Alboran Sea.

Local core top calibrations are ideal for a more robust interpretation of Mg/Ca derived SST records in this region (Jonkers et al., 2013). Mg/Ca ratios from previous core top studies have been made available for this purpose (Masqué et al., 2003; Cacho, pers. comm.). Core top locations Alb-1, Alb-2 and T-1 are close to ODP Site 976 (Fig. 11, left panel). SSTs derived from *G. bulloides* Mg/Ca measured in core tops Alb-1 (~17.4°C) and T-1 (~18.1°C) closely match modern annual SST

(MEDATLAS II, Medar Group, 2002), but Alb-2 shows a much higher SST than annual SST (~21°C), close to summer values in the region. In a following step, based on both *in situ* measurements from MEDATLAS II, Medar Group, 2002 and the World Ocean Atlas WOA09 (Locarnini et al., 2010; Antonov et al., 2010) together with satellite observations from the Aqua MODIS NASA database (Feldman and McClain, 2013) a present-day Alboran Sea spring average SST of 17.5°C and spring average sea surface salinity (SSS) of 36.5psu was calculated. We used a linear equation to convert SSS to seawater $\delta^{18}O$ ($\delta^{18}O_{sw}$) and converted it to the VPDB (Vienna Pee Dee Belemnite) scale by subtracting 0.27‰ (Hut, 1987). Later, Bemis et al. (1998) palaeotemperature equation for *G. bulloides* was used to calculate temperatures which were then plotted against Mg/Ca ratios from the core tops (Alb-1 and T-1) in to Elderfield and Ganssen (2000) calibration (Fig. 11, right panel) to further confirm the suitability of this calibration equation for ODP 976 *G. bulloides* Mg/Ca derived SST record.

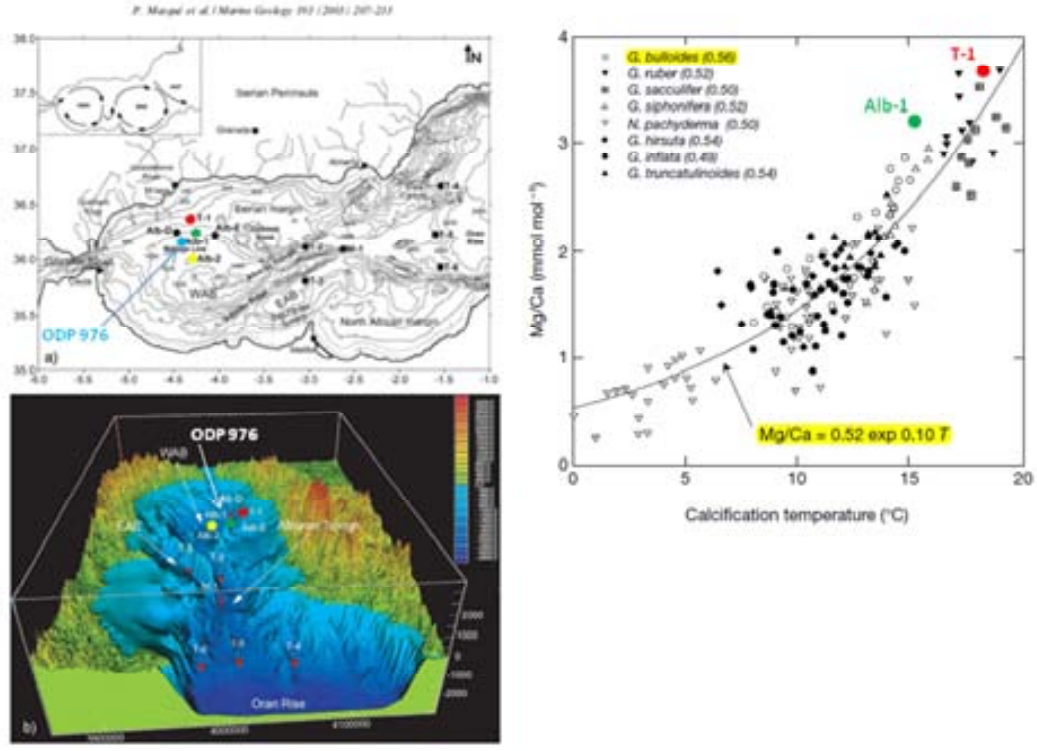

Figure 11. Left panel: Map of the Alboran Sea indicating the main physiographic features and the location of the core tops considered for our calibration: Alb-1 (green dot), Alb-2 (yellow dot) and T-1 (red dot). ODP Site 976 is indicated by the blue circle. Abbreviations: WAG, Western Alboran Gyre; EAG, Eastern Alboran Gyre; AOF, Almeria-Oran Front; WAB, Western Alboran Basin; EAB, Eastern Alboran Basin. Below, the 3-D view of the Alboran Basin is courtesy of J.L. Casamor. (Modified from Masqué et al., 2003, Fig. 1). Right panel: Mg/Ca versus calcification temperature calibration curve for eight species. The curve shows the best fit for all data by Elderfield and Ganssen (2000) and the numbers in the figure legend are the pre-exponential constants (m) derived from best-fit curves for individual species of the form: Mg/Ca (mmol/mol)= *m* exp 0.10*T*, where T is temperature in °C. The mean for all species gives the equation highlighted in yellow. Inserted into the calibration are the $\delta^{18}O$ derived temperature versus Mg/Ca ratios from Alb-1 and T-1 Alboran Sea core tops (Masqué et al., 2003; Cacho, pers. comm., 2013). (Modified from Elderfield and Ganssen, 2000, Fig. 2.

f. $\delta^{18}O$ seawater computation

The oxygen isotope composition of calcite from planktonic foraminifera ($\delta^{18}O$) reflects sea surface temperature (SST) and seawater $\delta^{18}O$ ($\delta^{18}O_{sw}$). If the independent Mg/Ca derived SST proxy is measured in the same signal carrier, the temperature signal from the $\delta^{18}O$ can be removed and we can extract the $\delta^{18}O_{sw}$, which is considered an indicator of seawater salinity, once corrected for the global ice volume signal (Shackleton, 1974; Elderfield and Ganssen, 2000; Waelbroeck et al., 2002). Samples for which paired analyses of $\delta^{18}O$ and Mg/Ca derived temperature were available were used to calculate the $\delta^{18}O$ of ambient seawater ($\delta^{18}O_{sw}$). First the ice-volume contribution to planktonic $\delta^{18}O$ was eliminated by subtracting the global mean-ocean $\delta^{18}O_{sw}$ change of 1.0 ‰ for ~120m of sela level change (Schrag et al., 1996). For the MIS2-T1-Holocene sequence, a composite sea level change record was used, including: U/Th dated coral records (Peltier and Fairbanks, 2006; Bard et al., 2010), a radiocarbon and paleomagnetically dated Red Sea sea-level record extracted from the temperature-corrected benthic stable oxygen isotopes using coral-based sea-level data as constraints for the sea-level/oxygen isotope relationship (Arz et al., 2007) and an independently dated high resolution Red Sea sea-level record based on Soreq cave speleothem age model (Grant et al., 2012). This latter was used for the MIS6-T2-MIS5e sequence. Subtracting the mean ocean $\delta^{18}O_{sw}$ record from the *G. bulloides* $\delta^{18}O$ data yielded an ice-volume corrected profile ($\delta^{18}O_{ivc}$) that was then used as input to the *G. bulloides* specific palaeotemperature equation of Bemis et al. (1998):

$$T(°C) = 13.2(\pm0.3) - 4.89(\pm0.21)*(\delta_c - \delta_w) \quad r^2 = 0.99$$

where *T* corresponds to the Mg/Ca derived SST calculated using Elderfield and Ganssen (2000) calibration equation, and δ_c is the $\delta^{18}O$ measured in *G. bulloides*. Moreover, modern Alboran Sea SSS data was used to test the positive suitability of this equation. In order to indicatively assess the magnitude of salinity changes expressed in the computed $\delta^{18}O_{sw}$ record a relation between $\delta^{18}O_{sw}$ and salinity was established using hydrocast data of Pierre (1999) from samples retrieved at eight stations in the Alboran Sea (Stations 4, 5, 7, 11, 15, 17, 19b, 25; Pierre, 1999). Using only data of the upper 100 m water column resulted in the $\delta^{18}O_{sw}$:salinity relation:

$$\delta^{18}O_{sw} = 0.26*S - 8.50 \ (n=38; r^2=0.89)$$

, with a specific slope of 0.26, which is an intermediate slope value in the range between the characterisitc 0.45 slope of northeast Atlantic surface waters from tropical to mid latitudes and the 0.1 slope of equatorial Atlantic surface waters (Craig and Gordon, 1965). This low slope appears to be specific for this region, imprinted by the climatic regime, characterized by an excesss of evaporation over freshwater input, which differs significantly from the climate of the open Atlantic Ocean (Pierre, 1999).

References:

Antonov, J. I., D. Seidov, T. P. Boyer, R. A. Locarnini, A. V. Mishonov, H. E. Garcia, O. K. Baranova, M. M. Zweng, and Johnson, D. R. (2010) "World Ocean Atlas 2009" Volume 2: Salinity. S. Levitus, Ed. NOAA Atlas NESDIS 69, U.S. Government Printing Office, Washington, D.C., 184 pp.

Arz, H. W., Lamy, F., Ganopolski, A., Nowaczyk, N., and Pätzold, J. (2007)"Dominant Northern Hemisphere climate control over millennial-scale glacial sea-level variability." Quaternary Science Reviews, 26(3), 312-321.

Bárcena, M. A., Flores, J. A., Sierro, F. J., Pérez-Folgado, M., Fabres, J., Calafat, A. and Canals, M. (2004) "Planktonic response to main ocenaographic changes in the Alboran Sea (Western Mediterranean) as documented in sediment traps and surface sediments." Marine Micropaleontology 53:423-445.

Bard, E., Arnold, M., Fairbanks, R. G., and Hamelin, B. (1993) "^{230}Th-^{234}U and ^{14}C Ages Obtained by Mass Spectrometry on Corals." Radiocarbon,35(1), 191-199.

Barker, S. and Elderfield, H. (2001, December) "Core-top calibrations of foraminiferal Mg/Ca from a North Atlantic transect: Refining Mg/Ca paleothermometry." In AGU Fall Meeting Abstracts (Vol. 1, p. 0468).

Barker, S., Greaves, M. and Elderfield, H. (2003) "A study of cleaning procedures used for foraminiferal Mg/Ca paleothermometry." Geochemistry, Geophysics, Geosystems. 4, 8407. doi:10.1029/2003GC000559.

Barker, S., G. Knorr et al. (2011). "800,000 years of abrupt climate variability." Science 334(6054):347.

Bazin, L., Landais, A., Lemieux-Dudon, B., Toy«e Mahamadou Kele, H., Veres, D., Parrenin, F., Martinerie, P., Ritz, C., Capron, E., Lipenkov, V., Loutre, M.-F., Raynaud, D., Vinther, B., Svensson, A., Rasmussen, S., Severi, M., Blunier, T., Leuenberger, M., Fischer, H., Masson-Delmotte, V., Chappellaz, J., and Wolff, E. (2013) "An optimized multi-proxies, multi-site Antarctic ice and gas orbital chronology (AICC2012): 120-800 ka." Climate of the Past 9(4):1715-1731.

Bé, A. W. H., and Tolderlund, D. S. (1971) "Distribution and ecology of living planktonic foraminifera in surface waters of the Atlantic and Indian Oceans." The micropaleontology of oceans, 105-149.

Bé, A. W., and Hutson, W. H. (1977) "Ecology of planktonic foraminifera and biogeographic patterns of life and fossil assemblages in the Indian Ocean." Micropaleontology, 23(4), 369-414.

Boyle, E. A. (1983) "Manganese carbonate overgrowths on foraminifera tests." Geochimica et Cosmochimica Acta 47(19):1815-1819.

Combourieu-Nebout, N., Turon, J. L., Zahn, R., Capotondi, L., Londeix, L. and Pahnke, K. (2002) "Enhanced aridity and atmospheric high-pressure stability over the western Mediterranean during the North Atlantic cold events of the past 50 k.y." Geology 30(10):863-866.

Coplen, T. B., Brand, W. A., Gehre, M., Gröning, M., Meijer, H. A., Toman, B., and Verkouteren, R. M. (2006) "New guidelines for d^{13}C measurements." Analytical Chemistry, 78(7), 2439-2441.

Craig, H., and Gordon, L. I. (1965) "Deuterium and oxygen 18 variations in the ocean and the marine atmosphere." Consiglio nazionale delle richerche, Laboratorio de geologia nucleare.

de Villiers, S., Greaves, M. and Elderfield, H. (2002) "An intensity ratio calibration method for the accurate determination of Mg/Ca and Sr/Ca of marine carbonates by ICP-AES." Geochemistry, Geophysics, Geosystems. 3, 1001.

Dekens, P. S., Lea, D. W., Pak, D. K., and Spero, H. J. (2002) "Core top calibration of Mg/Ca in tropical foraminifera: Refining paleotemperature estimation." Geochemistry Geophysics Geosystems, 3(4), 1022.

Elderfield, H. and Ganssen, G., 2000. Past temperature and 18O of surface ocean waters inferred from foraminiferal Mg/Ca ratios. Nature. 405, 442-445.

EPICA community members: Barbante, C., Barnola, J. M., Becagli, S., Beer, J., Bigler, M., Boutron, C. ... and Maggi, V. (2006) "One-to-one coupling of glacial climate variability in Greenland and Antarctica." Nature, 444(7116), 195-198.

Feldman, G. C., McClain, C. R., Ocean Color Web, MODIS Reprocessing L·, NASA Goddard Space Flight Center. Eds. Kuring, N., Bailey, S. W. hhtp://oceancolor.gsfc.nasa.gov.

Ferguson, J.E., Henderson, G.M., Kucera, M. and Rickaby, R.E.M., (2008) "Systematic change of foraminiferal Mg/Ca ratios across a strong salinity gradient." Earth and Planetary Science Letters 265, 153–166,

González-Mora, B., Sierro, F. J., Schönfeld, J. (2008) "Temperature and stable isotope variations in different wáter masses from the Alboran Sea (Western Mediterranean) between 250 and 150 ka." Geochemistry, Geophysics, Geosystems 9(10):1525-2027.

Grant, K. M., Rohling, E. J., Bar-Matthews, M., Ayalon, A., Medina-Elizalde, M., Ramsey, C. B. and Roberts, A. P. (2012) "Rapid coupling between ice volume and polar temperature over the past 150,000 [thinsp] years." Nature,491(7426), 744-747.

Greaves, M., Caillon, N., Rebaubier, H., Bartoli, G., Bohaty, S., Cacho, I., and Wilson, P. A. (2008) "Interlaboratory comparison study of calibration standards for foraminiferal Mg/Ca thermometry." Geochemistry, Geophysics, Geosystems,9(8).Locarnini, R. A., A. V. Mishonov, J. I. Antonov, T. P. Boyer, H. E. Garcia, O. K. Baranova, M. M. Zweng, and Johnson, D. R. (2010) "World Ocean Atlas 2009", Volume 1: Temperature. S. Levitus, Ed. NOAA Atlas NESDIS 68, U.S. Government Printing Office, Washington, D.C., 184 pp.

Grootes, P.M., Stuiver, M., White, J.W.C., Johnsen, S., and Jouzel, J. (1993) "Comparison of oxygen isotope records from the GISP 2 and GRIP Greenland ice cores." Nature, v. 366, p. 552–554.

Hernández-Almeida, I., Bárcena, M. A., Flores, J. A., Sierro, F. J., Sanchez-Vidal, A. and Calafat, A. (2011) "Microplankton response to environmental conditions in the Alboran Sea (Western Mediterranean): one year sediment trap record." Marine Micropaleontology 78:14-24.

Heaton T. J., Blackwell P. G. and Buck C. E. (2009) "A Bayesian approach to the estimation of radiocarbon calibration curves: the IntCal09 methodology." Radiocarbon 51(4):1151–64.

Masque, P., Fabres, J., Canals, M., Sanchez-Cabeza, J. A., Sanchez-Vidal, A., Cacho, I.,and Bruach, J. M. (2003) "Accumulation rates of major constituents of hemipelagic sediments in the deep Alboran Sea: a centennial perspective of sedimentary dynamics." Marine Geology, 193(3), 207-233.

Masson-Delmotte, V., Buiron, D., Ekaykin, A., Frezzotti, M., Gallée, H., Jouzel, J., ... and Vimeux, F. (2011) "A comparison of the present and last interglacial periods in six Antarctic ice cores." Climate of the Past, 7(2), 397-423.

Peltier, W. R., and Fairbanks, R. G. (2006) "Global glacial ice volume and Last Glacial Maximum duration from an extended Barbados sea level record." Quaternary Science Reviews, 25(23), 3322-3337.

Pena, L. D., Calvo, E., Cacho, I., Eggins, S., andPelejero, C. (2005) "Identification and removal of Mn‐Mg‐rich contaminant phases on foraminiferal tests: Implications for Mg/Ca past temperature reconstructions." Geochemistry, Geophysics, Geosystems, 6(9).

Pierre, C. (1999) "The oxygen and carbon isotope distribution in the Mediterranean water masses." Marine Geology, 153(1), 41-55.

Pujol, C. and C. V. Grazzini (1995). "Distribution patterns of live planktic foraminifers as related to regional hydrography and productive systems of the Mediterranean Sea." Marine Micropaleontology 25(2-3): 187-217.

Reimer P.J., Baillie M. G. L., Bard E., Bayliss A., Beck J. W., Blackwell P. G., Bronk, Ramsey C., Buck C. E., Burr G. S., Edwards R. L., Friedrich M., Grootes P. M., Guilderson T. P., Hajdas I., Heaton T. J., Hogg A. G., Hughen K. A., Kaiser K. F., Kromer B., McCormac F. G., Manning S. W., Reimer R. W., Richards D.A., Southon J.R., Talamo S., Turney C. S. M., van der Plicht J. and Weyhenmeyer C. E. (2009) "IntCal09 and Marine09 radiocarbon age calibration curves, 0–50,000 years cal BP." Radiocarbon 51(4):1111–50.

Rigual-Hernández, A. S., Sierro, F. J., Bárcena, M. A., Flores, J. A. and Heussner, S. (2012) "Seasonal and interannual changes of planktic foraminiferal fluxes in the Gulf of Lions (NW Mediterranean) and their implications for paleoceanographic studies: two 12-year sediment trap records." Deep-Sea Research 66:26-40.

Schiebel, R., Bijma, J., and Hemleben, C. (1997) "Population dynamics of the planktic foraminifer Globigerina bulloides from the eastern North Atlantic." Deep Sea Research Part I: Oceanographic Research Papers, 44(9), 1701-1713.

Schiebel, R., and Hemleben, C. (2000) "Interannual variability of planktic foraminiferal populations and test flux in the eastern North Atlantic Ocean (JGOFS)." Deep Sea Research Part II: Topical Studies in Oceanography, 47(9), 1809-1852.

Schiebel, R., and Hemleben, C. (2005) "Modern planktic foraminifera." Paläontologische Zeitschrift, 79(1), 135-148.

Schrag, D. P., Hampt, G., and Murray, D. W. (1996) "Pore fluid constraints on the temperature and oxygen isotopic composition of the glacial ocean." Science,272(5270), 1930-1932.

Shackleton, N. J. (1974) "Attainment of isotopic equilibrium between ocean water and the benthonic foraminifera genus Uvigerina: Isotopic changes in the ocean during the last glacial." Colloques Internationaux du CNRS.

Siani, G., Paterne, M., Michel, E., Sulpizio, R., Sbrana, A., Arnold, M., and Haddad, G. (2001) "Mediterranean sea surface radiocarbon reservoir age changes since the Last Glacial Maximum." Science, 294(5548), 1917-1920.

Skinner, L. C., and Elderfield, H. (2005) "Constraining ecological and biological bias in planktonic foraminiferal Mg/Ca and $d^{18}O_{cc}$: a multispecies approach to proxy calibration testing." Paleoceanography, 20(1).

Stichler, W. (1995) "Interlaboratory comparison of new materials for carbon and oxygen isotope ratio measurements." Reference and Intercomparison Materials for Stable Isotopes of Light Elements, IAEA TECDOC-825, 67-74.

Veres, D., Bazin, L., Landais, A., Lemieux-Dudon, B., Parrenin, F., Martinerie, P., Toy«e Mahamadou Kele, H., Capron, E., Chappellaz, J., Rasmussen, S., Severi, M., Svensson, A., Vinther, B., and Wolff, E. "The Antarctic ice core chronology (AICC2012): an optimized multi-parameter and multi-site dating approach for the last 120 thousand years." Climate of the Past.9(4).

Waelbroeck, C., Labeyrie, L., Michel, E., Duplessy, J. C., McManus, J. F., Lambeck, K., and Labracherie, M. (2002) "Sea-level and deep water temperature changes derived from benthic foraminifera isotopic records." Quaternary Science Reviews, 21(1), 295-305.

Wit, J. C., Reichart, G. J.,, Jung, S. J. A. and Kroon, D. (2010) "Approaches to unravels seasonality in sea surface temperatures using paired single-specimen foraminiferal $d^{18}O$ and Mg/Ca analyses." Paleoceanography 25(4).

Yu, J., Day, J., Greaves, M. and Elderfield, H. (2005) "Determination of multiple element/calcium ratios in foraminiferal calcite by quadrupole ICP-MS." Geochemistry, Geophysics, Geosystems. 6, Q08P01.

Results.

a. Planktonic foraminiferal oxygen isotope records

The oxygen isotope record of the MIS2-T1-Holocene sequence (Fig. 12) shows a multiple-step transition from mean glacial values of 3.15±0.32‰ (n=78) to mean interglacial values of 0.47±0.18‰ (n=134). The record displays abundant high-frequency variability including several rapid steps during T1 (Fig.12, red arrows) that are constrained by several data points.

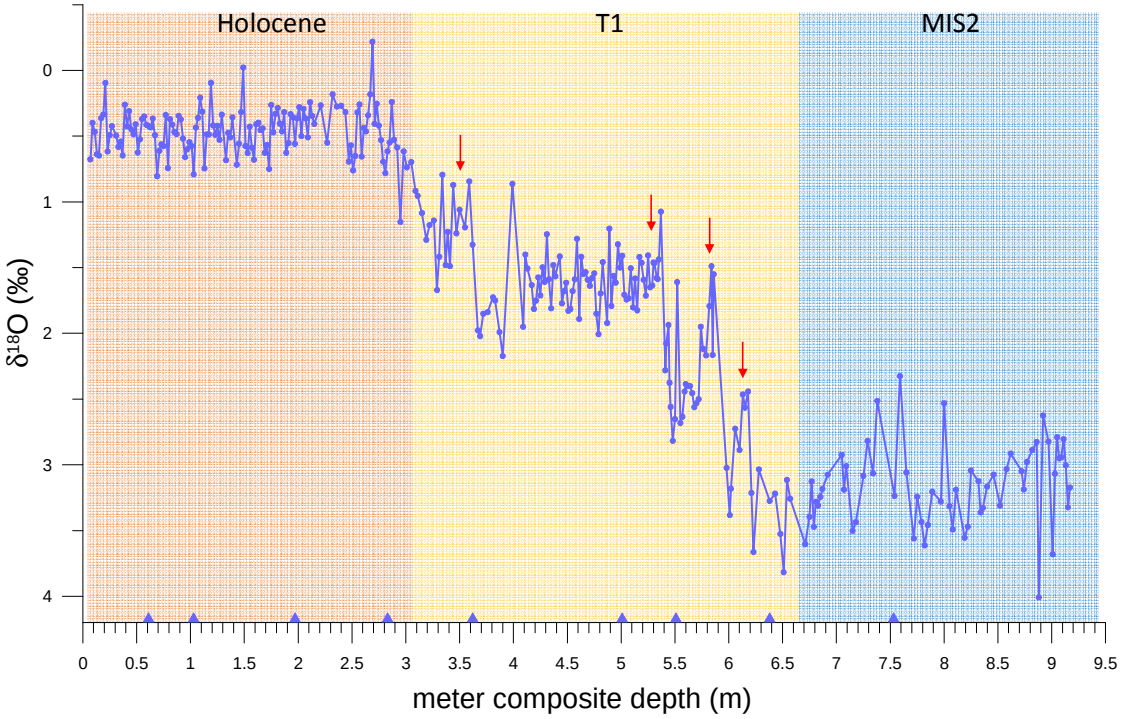

Figure 12: Planktonic $\delta^{18}O$ record of *G. bulloides* at ODP 976 on a meters-composite-depth (mcd) scale. Red arrows indicate abrupt steps to lighter $\delta^{18}O$ values. Blue, yellow and orange shading marks Marine Isotope Stage 2 (MIS2), Glacial Termination 1 (T1) and the Holocene. Blue diamonds along the mcd axis indicate position of samples for accelerator radiocarbon dating (Combourieu-Nebout et al., 2002).

The second core section examined at ODP976 spans from 35.91 to 45.11 mcd and comprises the section of MIS6-T2-MIS5e (Fig. 13). It likewise reveals a multiple-step glacial-interglacial transition (Glacial Termination 2, T2) from mean MIS6 $\delta^{18}O$ values of 2.45±0.46‰ (n=104) to mean MIS5e values of 0.20±0.23‰ (n=96). In comparison to the MIS2-T1-Holocene profile, this section overall reveals isotope values lighter by 0.70‰ in the glacial section and by 0.26‰ in the

interglacial section. In its upper part the $\delta^{18}O$ record displays an increase by 1.5 ‰ reflecting the transition to MIS 5d (Fig. 13, green shading). The structure of T2 in the $\delta^{18}O$ record closely resembles that displayed during T1 in that multiple rapid steps are developed to lighter $\delta^{18}O$ values.

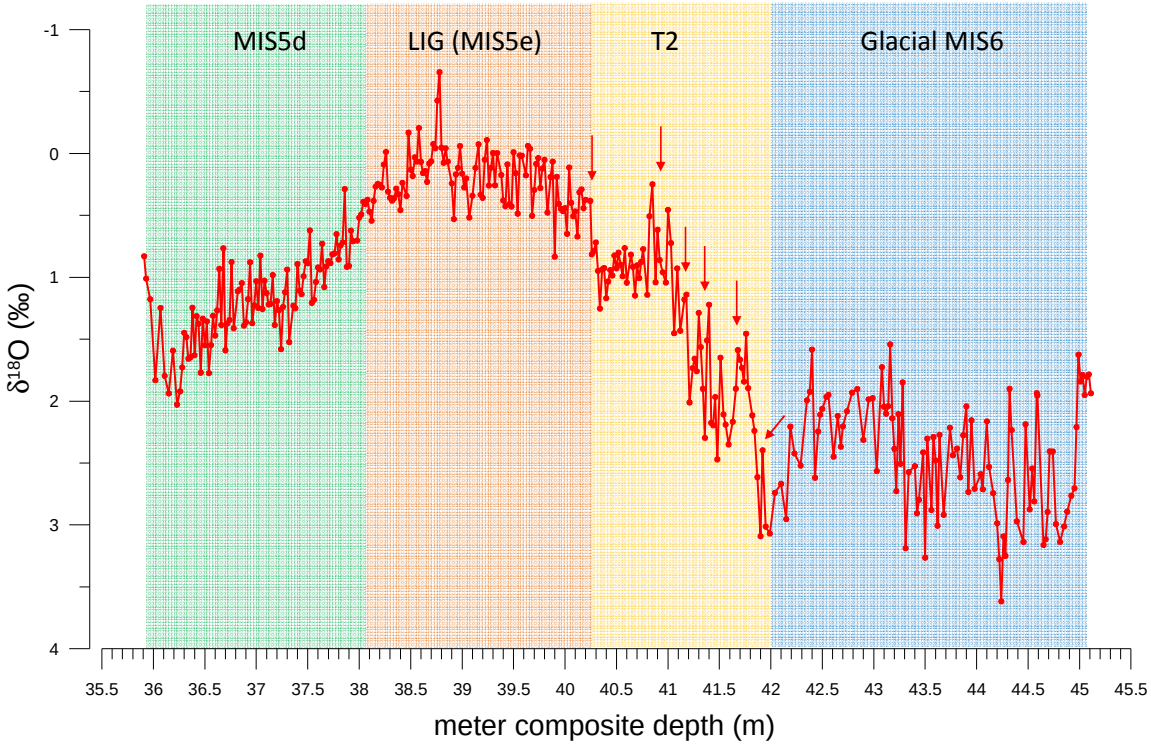

Figure 13: Planktonic $\delta^{18}O$ record of *G. bulloides* at ODP 976 on a meters-composite-depth (mcd) scale. Red arrows indicate abrupt steps to lighter $\delta^{18}O$ values. Blue, yellow and orange shading marks Marine Isotope Stage 6 (MIS6), Glacial Termination 2 (T2) and the last interglacial period (MIS5e).

To place the isotope profiles of both stratigraphic sequences into a perspective of global ice volume changes we subtract the mean-ocean $\delta^{18}O$ signal to derive the ice-volume corrected $\delta^{18}O_{ivc}$ (for procedures see Chapter *"Methodology, section (f) $\delta^{18}O$ seawater computation""*). The resultant profile displays glacial-interglacial amplitudes of 2.0-2.3‰ that are not supported by ice volume and therefore reflect the combined influence of ambient seawater temperature (i.e., SST) and seawater oxygen isotope variation ($\delta^{18}O_{sw}$) that is connected with seawater salinity. The $\delta^{18}O_{sw\text{-}ivc}$ profile hence will be used later in conjunction with SST estimates derived from *G.*

bulloides Mg/Ca to infer $\delta^{18}O_{sw}$ variations and, by extension, variations of surface salinity in the vicinity of ODP Site 976 (see Discussion Chapter 1 "*ODP 976 and Alboran Sea palaeoclimatology during the last two deglaciations*").

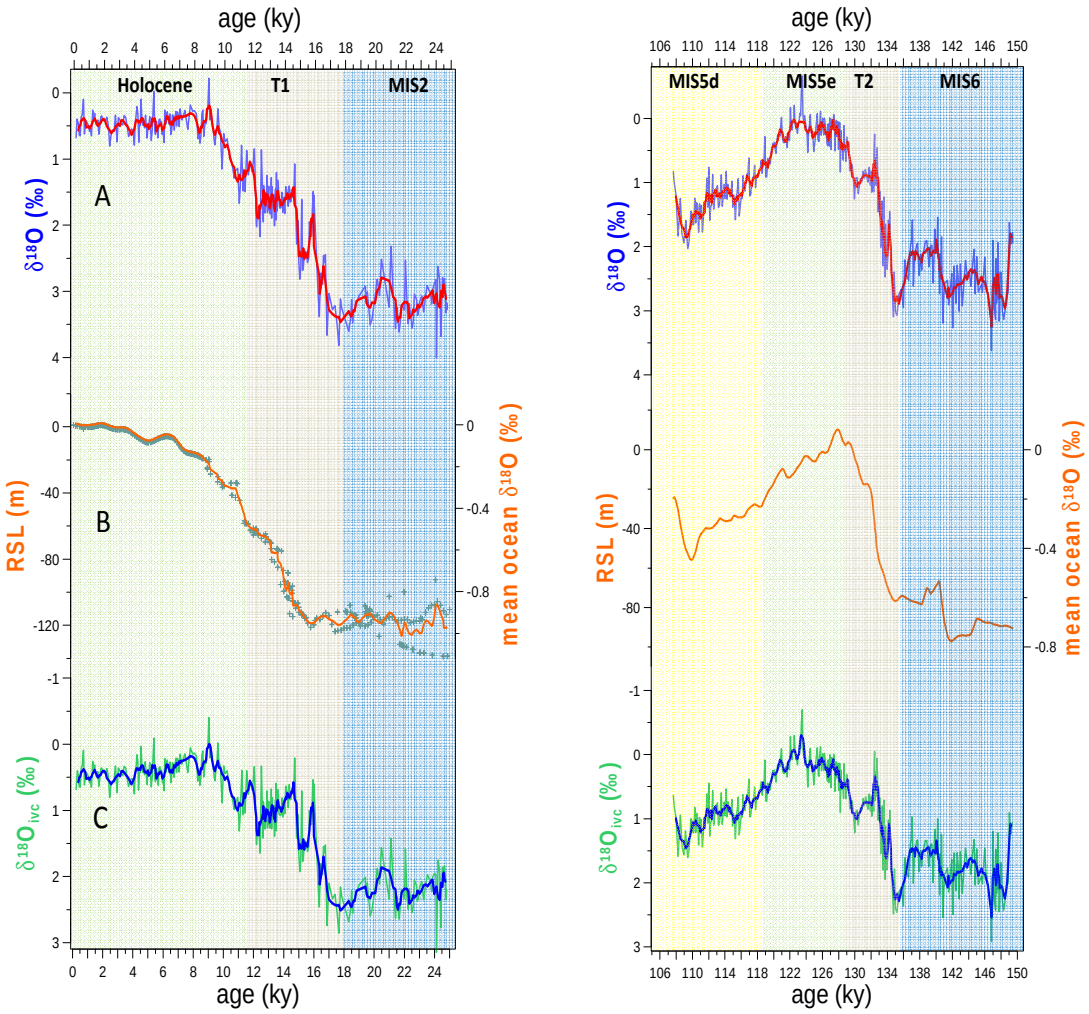

Figure 14: Ice volume correction of the ODP 976 oxygen isotope records. Left panel, MIS2-T1-Holocene section; right panel, MIS6-T2-MIS5e section. For both panels: (A) $\delta^{18}O$ measured in *G. bulloides* in blue and smoothed record in red. (B) Relative sea level change (RSL, in m, left Y-axis and per mil, right Y-axis). MIS2-T1-Holocene RSL data compilation from Bard et al. (1996, 2010), Peltier and Fairbanks (2006), Grant et al. (2012) and Arz et al. (2012). MIS6-T2-MIS5e RSL from Grant et al. (2012). (C) Ice volume corrected $\delta^{18}O$ ($\delta^{18}O_{ivc}$) in green and smoothed record in dark blue. Blue, grey and green shadings envelop the glacial MIS2 and MIS6, glacial terminations T1 and T2, and interglacial periods (Holocene and MIS5e) of each stratigraphic section. Yellow shading in right panel marks the transition into MIS5d.

b. Planktonic foraminiferal Mg/Ca and derived SST records

The Mg/Ca derived SST record of the MIS2-T1-Holocene sequence shows mean glacial values of 14.6±1.51°C (n=72). In this sequence, T1 is represented by the first SST increase into the Bolling/Allerod interval (4.15-5.42 mcd) with mean SST values of 18.8±2.1°C (n=35), a following decrease in SST during the YD cold episode reaching minimum SST values of 15.8°C and a final transition into interglacial levels with mean values of 17.5±1.4°C (n=99). The Mg/Ca derived SST record of the MIS6-T2-MIS5e sequence reveals mean glacial values of 16.4±0.95°C (n=133) and an abrupt an uninterrupted SST increase with mean SST values of 20.25±1.75°C (n=13), reaching maximum values of 21.9°C at around 40 mcd. A following decrease precedes a SST stabilization during the MIS5e at mean interglacial values of 18.21±1.1°C (n=50). Not only the last interglacial period, MIS5e, shows warmer-than-Holocene SST values, but also the preceding glacial period, MIS6 is warmer than MIS2 and the abrupt warming episode during T2 reaches higher SST levels than the B/A warm interval during T1.

The Mg/Ca derived SST records along both sequences are highly variable, displaying frequent single-point excursions to lower and higher SST values (Fig. 15A). In order to study the reasons behind this variability different considerations were made. According to the ratios of potential contamination indicators, no correlation was found between Al/Ca, Fe/Ca, Mn/Ca and Mg/Ca ratios (Al/Ca vs Mg/Ca, r^2= 0.01; Mn/Ca vs Mg/Ca, r^2 =0.03; Fe/Ca, r^2= 0.04) so, in principle, contamination due to this elements was ruled out as a source of the scatter in the records. However, maximum threshold values established as potential contamination indications for Al/Ca and Mn/Ca (Boyle et al., 1983; Wit et al., 2010) were taken into account in order to consider possible individual sample contamination and therefore, contribute to reducing this variability throughout the record.

G. bulloides present highest fluxes in spring (Bárcena et al., 2004; Hernández Almeida, 2011; Rigual-Hernández et al., 2012), hence, Mg/Ca derived SST measured in this species should record spring SST. Using Elderfield and Ganssen (2000) calibration, not only the Holocene mean SST is of 17.5 °C, but also the most recent samples of the record reflect SST values of 17.6°C, which strongly agrees with modern spring surface SST observations in the Alboran Sea (17-18°C, MEDATLAS II, Medar Group, 2002). Modern observations (for details, see Fig. 4 in Chapter "*Regional setting,*

section (a) The Alboran basin: Oceanography") yield SSTs in the Alboran basin between 15°C in winter and 23°C in summer. Moreover, paleotemperature studies in the Alboran basin (Cacho et al., 1999; Martrat et al., 2004, Martrat et al., 2013, submitted) report maximum SSTs during MIS5e of ~23°C. From these studies, it seems that 23°C is within the upper range of SST to be expected in the Alboran Sea, corresponding to Mg/Ca ratios in the range of 6 mmol/mol. As a conservative approach to reducing the scatter of the data profiles, this ratio was used as a first cut-off level and all data points above Mg/Ca of 6mmol/mol that coincided with Al/Ca and Mn/Ca ratios above 400µmol/mol and 100µmol/mol were eliminated as potentially being contaminated (Boyle et al., 1983; Wit, 2010) (Fig. 15B). In a next step, the Al/Ca and/or Mn/Ca cut-off levels of 400 µmol/mol and 100 µmol/mol cut-off levels were applied to all data independently of the Mg/Ca ratio and computed SST (Fig. 15C). Finally, the 5pt running weighted average was computed of the resultant record and all SST values that exceeded the average by equal or more than two times the propagated analytical and calibration error (equivalent 3°C) were eliminated (Fig. 15D). Comparing of the different records shows that the progressive "cleaning" of the records on occasion slightly modifies the fine-structure and amplitude of changes, while the overall character of the profiles remains unchanged.

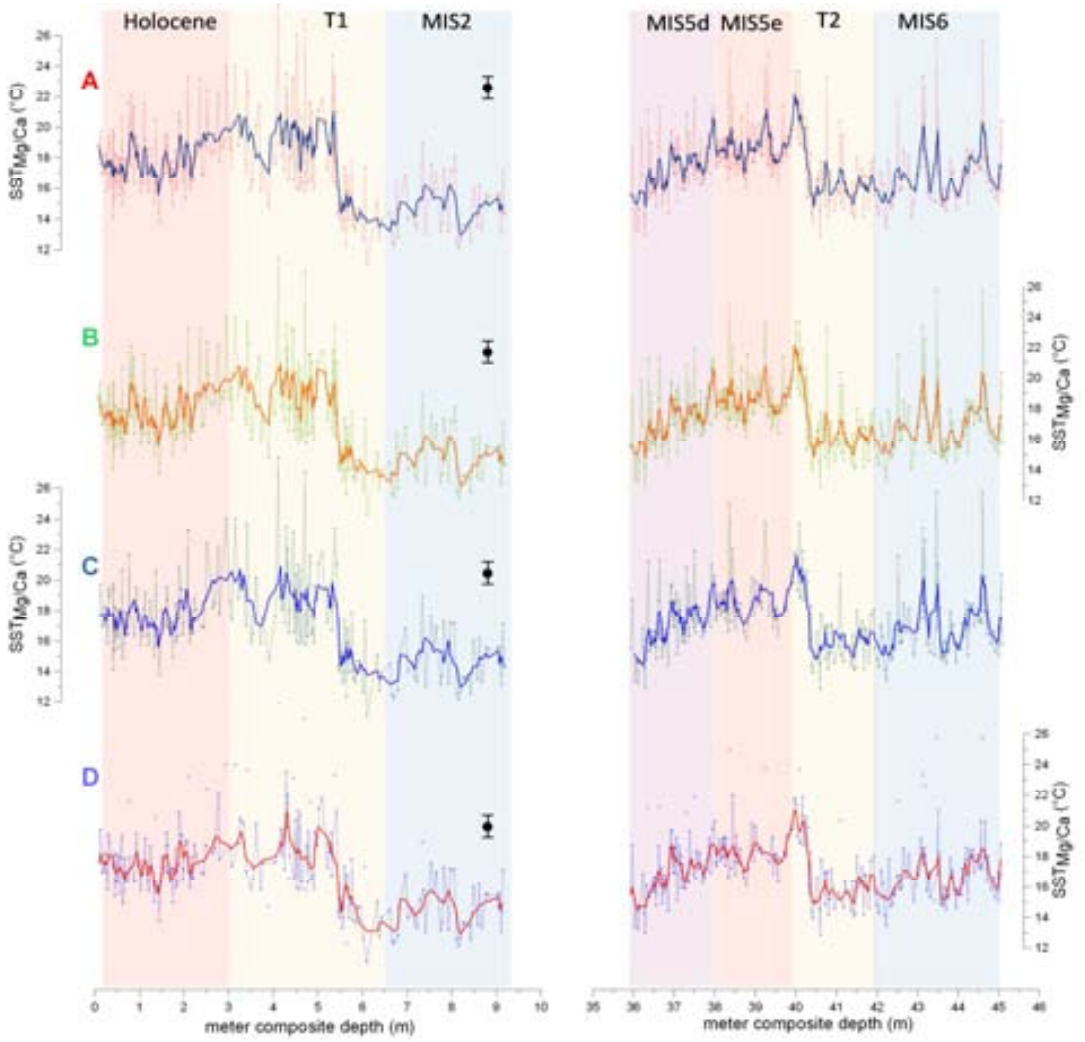

Figure 15. Cleaning of the Mg/Ca derived SST data set. (A) Raw $SST_{Mg/Ca}$ record in red, together with a 5pt running weighted average smoothed record in dark blue. (B) $SST_{Mg/Ca}$ record with Mg/Ca > 6 mmol/mol removed if Al/Ca and/or Mn/Ca ratios exceeded thresholds of 400µmol/mol (Boyle et al., 1983) and 100µmol/mol (Wit, 2010). (C) $SST_{Mg/Ca}$ record with all Mg/Ca data removed if Al/Ca and/or Mn/Ca were above thresholds. (D) Same as (C) but disregarding SST values that exceeded the 5pt running weighted average smoothed record (red curve) by equal or more than 3°C which is equivalent 2 times the propagated analytical and calibration error. SST values exceeding the threshold are plotted along the record as isolated data points while are not used in the later discussion of SST developments during both stratigraphic sequences.

Applying the age modeling described in Chapter "*Methodology, Section (c) Age model development*" for the MIS2-T1-Holocene and the MIS6-T2-MIS5e sections, the planktonic $\delta^{18}O$ and Mg/Ca-derived SST profiles were placed into the time domain and combined with other palaeoceanographic profiles from the same region to assess the robustness of the ODP976 data records (Figures 16, 17). This included an SST record at Site 976 based on alkenones ($SST_{Uk'37}$, Martrat et al., 2013, submitted) that plausibly depicts mean annual SST (Martrat et al., 2004, 2007, 2013; Dos Santos et al., 2013), as opposed to spring-SST recorded by *G. bulloides* (Elderfield and Ganssen, 2000; Ganssen and Kroon, 2000).

The $SST_{Mg/Ca}$ amplitude is similar for both glacial-interglacial transitions (7-8 ^{o}C) and smaller than the amplitude recorded by alkenones, which is higher for T2 (~12 ^{o}C) than for T1 (~9 ^{o}C). For MIS5e both proxies consistently reveal warmer-than-present SSTs. However, while alkenones record ~3^{o}C warmer thermal maximum (~23 ^{o}C) in the early MIS5e compared to the Holocene climatic optimum (~20^{o}C), $SST_{Mg/Ca}$ show very similar thermal maximum peaks during both interglacial periods around 21^{o}C. Evidently, the $SST_{Mg/Ca}$ record displays higher variability and lower glacial-interglacial amplitudes than the $SST_{Uk'37}$ profile with the most abrupt SST increase of 5-6°C occurring at ~14.9 ky marking the onset of the B/A, where SSTs reach interglacial levels or higher. By comparison, the $SST_{Uk'37}$ record shows the highest values of ~19-20°C at ~9-10 ky i.e., at the climatic optimum of the Holocene, and SST then steadily decreases to ~18°C during the late Holocene. Potential explanations for the different structure and variability among the two SST proxies, Mg/Ca and alkenones, will be further developed in Chapter "*Discussion, Chapter 1: ODP 976 and Alboran Sea palaeoclimatology during the last two deglaciations*".

The coherence of the ODP 976 $\delta^{18}O$ profile with those of other sites in the Alboran basin, ODP 977 and MD95-2043 (Cacho et al., 1999, 2002; Martrat et al., 2004, 2013; Sierro et al., 2005; Combourieu-Nebout et al., 2002, 2009) demonstrates the same signal is recorded at ODP Site 976, albeit at higher resolution. While previously published records from nearby core MD95-2043 (36^{o}9'N, 2^{o}37'W; Cacho et al., 1999, 2007) and ODP Site 977 (36^{o}1.9'N, 1^{o}57,3'W; Martrat et al., 2004) resolve the palaeoclimatic variability at a centennial time scale, an unprecedented multi-decadal temporal resolution is achieved with the new records at ODP 976. The overall excellent correlation between them confirms the reproducibility of palaeo-climatic signals in the Alboran Sea. A detail of the core-to-core comparison is that $\delta^{18}O$ levels at ODP 976 are more negative than the others and the record displays more prominently the multiple-step structure of T1. In this

regard, the climatic variability signal in the Alboran basin and its connection to North Atlantic climate is not based on one single core's results, but three different sites (ODP Sites 976, 977 and MD95-2043). The core-to-core comparison reveals a consistency and reproducibility of the climatic records at the three sites which at the same time are closely correlated with the Greenland ice core atmospheric temperature record (NGRIP, 2004), proving the suitability of this area to record North Atlantic climate variability at high resolution.

ODP 976 $\delta^{18}O$ records the onset of Termination 1 at ~17.5 ky (Fig. 16, grey stippled bar), followed by a multiple-step progressive $\delta^{18}O$ decrease until the onset of the Holocene (Fig. 16, red shading) at ~11.7 ky. From thereon $\delta^{18}O$ values keep progressively decreasing until reaching the climatic optimum at 9-10 ky from whereon they remain constant across the Holocene. The overall structure of the ODP 976 $\delta^{18}O$ profile over the past 25 ky correlates excellently with the glacial-interglacial transition and Holocene recorded in the NGRIP $\delta^{18}O$ record (NGRIP, 2004). This includes Heinrich event 1 (H1) from ~16.8 to 14.6 ky (Hemming, 2004) that was associated with massive North Atlantic iceberg melting and deposition of ice-rafted debris; this event is recorded in the ODP 976 $\delta^{18}O$ and SST records as a double-peak cold spell. A marked resumption of the AMOC after H1 (Gherardi et al., 2009) is represented by the abrupt transition to the subsequent Bölling/Allerod (B/A) warm interval which is likewise evident at ODP 976 by an $SST_{Mg/Ca}$ increase by ~5-6°C to full-interglacial levels, and a $SST_{Uk'37}$ increase by ~4°C.

The Bølling-Allerød warm interval is abruptly terminated by the Younger-Dryas (YD) when the Antarctic ice core records display the start of warming after the Antarctic Cold Reversal (ACR), which alludes to the interhemispheric thermal asymmetry connected with the so-called bipolar seesaw (Masson-Delmotte et al., 2010). The YD lasted from about ~12.8 to 11.5 ky in the NGRIP (2004) and the other Alboran sites (ODP 977 and MD95-2043), while, at ODP 976 $\delta^{18}O$ and SST records it appears as a much shorter event only lasting from ~12.6 to 12 ky, or as a two-stage event as will be later discussed. The YD in the ODP 976 oxygen isotope record is not as accentuated as for instance, in the NGRIP record, reaching intermediate $\delta^{18}O$ values between full-glacial and full-interglacial levels. The 8.2 ky cold event is identified in the early Holocene section of the Alboran basin $\delta^{18}O$ records with a transient increase reflecting the SST decrease that is often attributed to a meltwater outflow in the North Atlantic and an AMOC slowdown (Rohling and Pälike, 2005; Cheng et al., 2009).

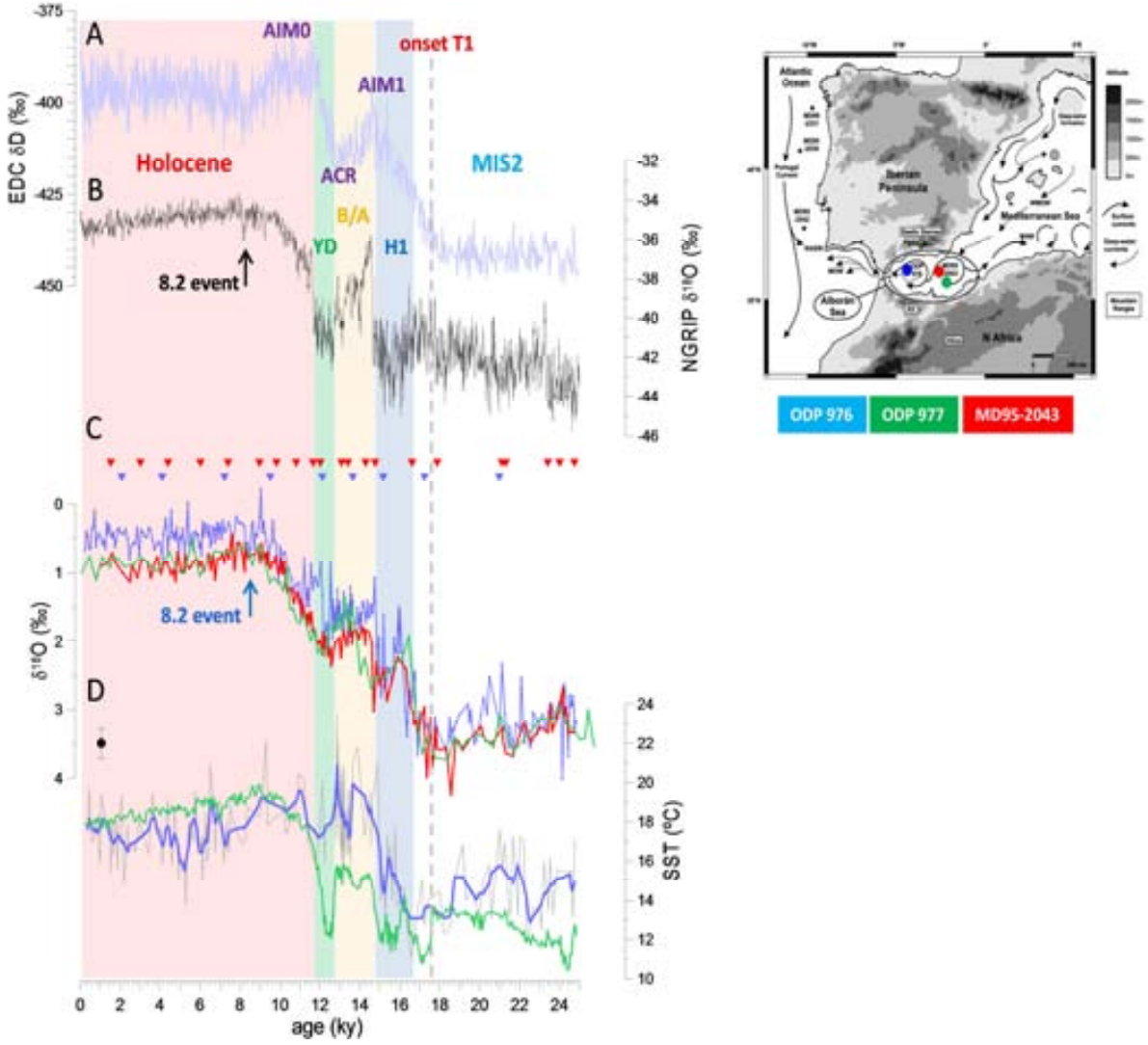

Figure 16. ODP 976 palaeo-records compared with reference records. Left panel. (A) Antarctic EDC δD profile (Loulergue et al., 2008) on the AICC2012 age scale (Bazin et al., 2013; Veres et al., 2013). Antarctic Isotopic Maxima 1 and 0 (AIM1, AIM0) and the Antarctic Cold reversal (ACR) are indicated. (B) North GRIP ice core $\delta^{18}O$ record (NGRIP members, 2004) on the AICC2012 age scale (Bazin et al., 2013; Veres et al., 2013). (C) *G. bulloides* $\delta^{18}O$ records in the Alboran basin: ODP 976 (blue, this thesis), ODP 977 (green, Martrat et al., 2004) and MD95-2043 (red, Cacho et al., 1999, 2002 and higher resolution: Cacho et al., 2013, unpublished). Triangles represent radiocarbon ages measured in ODP 976 (blue, Combourieu-Nebout et al., 2002) and MD95-2043 (red, Cacho et al., 1999, 2002). (D) ODP 976 SST records: $SST_{Mg/Ca}$ (grey= cleaned record, blue=5pt smoothed record, this thesis) and $SST_{Uk'37}$ (light green; Martrat et al., 2013, submitted). Grey stippled vertical line delimits the onset of Termination 1. The main features identified during the deglaciation in the NGRIP record are indicated by colour shadings: Heinrich 1 (H1), Bölling/Allerod (B/A) and Younger Dryas (YD). Right panel: Map showing locations of the different Alboran basin sites.

The MIS6-T2-LIG section (Fig. 17) likewise displays close correlation between the $\delta^{18}O$ records at Alboran Sea sites ODP976 and ODP977, confirming again the robustness of the higher-resolving ODP 976 record. The ODP 976 $SST_{Mg/Ca}$, as in the MIS2-T1-PIG section, displays higher variability than $SST_{Uk'37}$, while $SST_{Uk'37}$ during MIS5e is distinctly warmer than during the Holocene and also warmer than $SST_{Mg/Ca}$, and it displays a thermal maximum peak during MIS5e not observed at the onset of the Holocene.

Direct comparison with Greenland ice core-derived paleoclimate records is not possible as these records do not go back in time beyond ~129 ky (NEEM community members, 2013). The lack of Greenland ice core reference records for the MIS6-T2-MIS5e sequence adds value to the ODP 976 palaeoclimatic records that span this interval at a temporal resolution of 60-90yr (Fig. 17). The ODP 976 $\delta^{18}O$ record clearly depicts T2 as a multi-step transition, with some similarity to the structure of T1. The onset of MIS5e at 129 ky in the $\delta^{18}O$ record (Fig. 17C, red shading) coincides with maximum $SST_{Mg/Ca}$ coincident with the second warming recorded by $SST_{Uk'37}$, while maximum $SST_{Uk'37}$ is recorded ~2 ky later (Fig. 17D) coincident with minimum $\delta^{18}O$ values. $SST_{Mg/Ca}$ displays a semi-cyclical pattern during MIS5e into MIS5d that is not mimicked in the $SST_{Uk'37}$ record.

The timing of events recorded regionally in the North Atlantic during T2, such as Heinrich event 11 (H11), constitutes a marker event that can be used to improve the interpretation and synchronization of the ODP 976 $\delta^{18}O$ and SST records with other records. Multiproxy records, such as SST records (alkenones, Mg/Ca ratios), palynological records (pollen and dinocysts counts) and ice-rafted debris (IRD) records from key sites provide unambiguous palaeoclimatic information about the incursion and timing of H11.

The marine climatology at ODP 980 (McManus et al., 1999; Oppo et al., 2006, Govin et al., 2012) in the eastern subpolar North Atlantic (55°29′N, 14°42′W, 2179 m), is highly sensitive to regional climate change (McManus et al., 1994) and the site is well positioned to monitor the arrival of detritus-laden icebergs along their travel path across the northern North Atlantic (Ruddiman, 1977; Oppo et al., 2006). Therefore, the ODP 980 SST and IRD records serve as a reference to define the incursion of H11–related palaeoclimatic signals at ODP 976. SST at ODP980 is estimated using planktonic foraminiferal assemblage changes using the Modern Analog Technique (MAT; Prell, 1985) and the Brown University core-top database (Prell et al., 1999). This method likely produces SST estimates different from the Mg/Ca method used for ODP 976 but we

can expect that both methods structurally capture the SST decline during H11 as a clearly displayed SST minimum. Sharp decreases in the ODP 976 $SST_{Mg/Ca}$ and at ODP 980 SST_{MAT} (Fig. 17D) together with the maximum IRD abundance at ODP980 (Fig. 17G) clearly indicate the H11 event at about ~130-132 ky (Fig. 17, blue shading), together with a pronounced $\delta^{18}O$ minimum equivalent to about two thirds of the total glacial-interglacial $\delta^{18}O$ amplitude during T2 (Fig. 17C). This $\delta^{18}O$ feature reveals the meltwater effect of H11 that is further corroborated by palynological data showing maximum abundance of cysts of the *Bitectatodinium tepikiense* cold-water dinoflagellate (Fig. 17F, L. Londeix, pers. comm.) and of semi-desert pollen taxa at ODP 976 (Fig. 17E) (Combourieu-Nebout, unpublished). An exception to the SST and palynological pattern is seen in the ODP976 $SST_{Uk'37}$ profile that displays a 4°C warming during the H11 interval which seems inconsistent with the marine and terrestrial environmental conditions recorded by the other proxy records. Two further events (Fig. 17, yellow and green bars) are recorded with high semi-desert taxa and high *B. tepikiense* abundances and coincide with cold phases seen in the ODP 976 $SST_{Uk'37}$ and $SST_{Mg/Ca}$ profiles at ~132.5-134 ky and ~134.5-137 ky. These early cold phases either suggest the existence of pre-H11 events (yellow bar), or that H11 as a whole proceeded with two peak maxima (blue and yellow bars), not unlike the double structure of the H1 event during T1. Fitting with the bipolar see-saw concept, the H11 cold conditions coincide in Antarctic ice core temperature profiles with increased values that reach almost full-interglacial levels. Following H11, at about ~130 ky, $SST_{Mg/Ca}$ and $SST_{Uk'37}$ abruptly increase by 6.5°C and 5.5°C, as the Antarctic Isotopic Maximum (AIM) is reached after which Antarctic temperatures start to decrease (Masson-Delmotte et al., 2010).

Overall, we show that ODP 976 high resolution records reveal lighter $\delta^{18}O$ values and warmer $SST_{Mg/Ca}$ during MIS5e than the Holocene. The overall excellent correlation between this site and ODP 977 (Martrat et al., 2004) and MD95-2043 (Cacho et al., 1999, 2002) confirms the reproducibility of palaeo-climatic signals in the Alboran Sea, revealing consistency and reproducibility of the climatic records at the three sites which at the same time are closely correlated with the Greenland ice core atmospheric temperature record (NGRIP, 2004), proving the suitability of this area to record North Atlantic climate variability at high resolution. Importantly, beyond the present limit of Greenland ice core records (~129 ky, NEEM community

members, 2013), ODP 976 MIS-T2-MIS5e sequence provides with North Atlantic climate variability records at centennial to multi-decadal timescales.

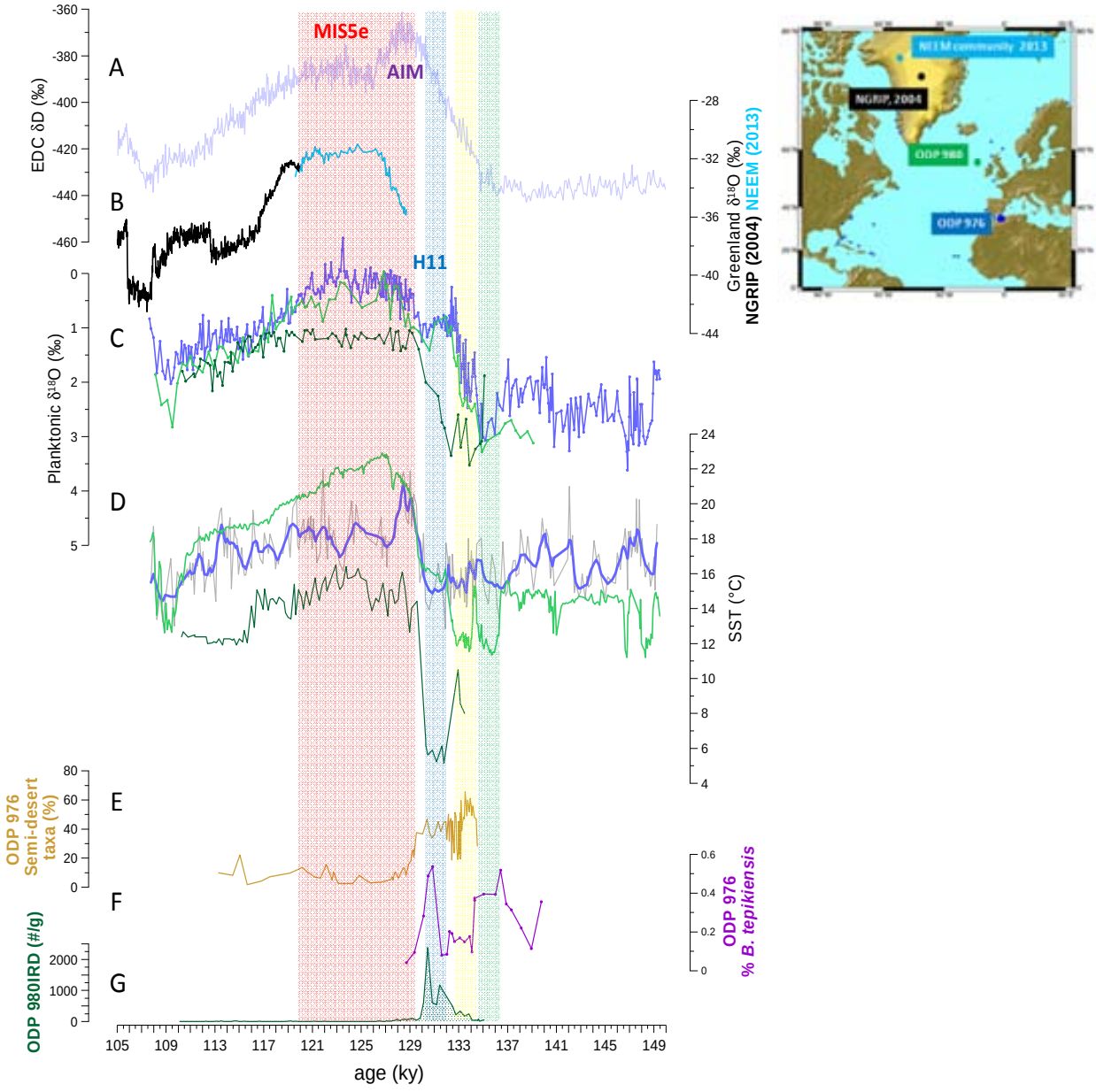

Figure 17. Left panel, palaeoclimatic records of the MIS6-T2-MIS5e sequence at ODP976 compared to reference records. (A) Antarctic EDC δD (Loulergue et al., 2008) on the AICC2012 age scale (Bazin et al., 2013; Veres et al., 2013). (B) Greenland ice core $\delta^{18}O$ records: NGRIP (black, NGRIP members, 2004) on AICC2012 age scale (Bazin et al., 2013; Veres et al., 2013) and NEEM (light blue, NEEM community members, 2013). (C) Planktonic $\delta^{18}O$ records: ODP 976 $\delta^{18}O$ record (blue, this study), ODP 977 (green, Martrat et al., 2004) and ODP 980 (dark green, Oppo et al., 2006 on age scale of Govin et al., 2012). (D) ODP 976 $SST_{Mg/Ca}$ (grey= unsmoothed record, blue=5 pt smoothed record, this study), ODP 976 $SST_{Uk'37}$ (light green, Martrat et al., 2013, submitted) and ODP 980 SST_{MAT} (dark green, McManus et al., 2002, Oppo et al., 2006 on age scale of Govin et al., 2012). (E) ODP 976 semi-desert pollen record (brown; N. Combourieu Nebout, pers. comm., unpublished data). (F) Abundance of cold-water dinoflagellate *B. tepikiensis* cysts (purple; L. Londeix, pers. comm.). (G) ODP 980 IRD record (dark green, Oppo et al., 2006 on the age scale of Govin et al., 2012). H11 is indicated by blue shading, pre-H11- events are highlighted with yellow and green shading, MIS5e by red shading and AIM=Antarctic Isotopic Maximum. Right panel: Map with the NGRIP and NEEM ice core locations, ODP 980 in the eastern subpolar North Atlantic and ODP 976.

References:

Bárcena, M. A., Flores, J. A., Sierro, F. J., Pérez-Folgado, M., Fabres, J., Calafat, A. and Canals, M. (2004) "Planktonic response to main ocenaographic changes in the Alboran Sea (Western Mediterranean) as documented in sediment traps and surface sediments." Marine Micropaleontology 53:423-445.

Boyle, E. A. (1983) "Manganese carbonate overgrowths on foraminifera tests." Geochimica et Cosmochimica Acta 47(19):1815-1819.

Cacho, I. (1999)."Dansgaard-Oeschger and Heinrich event imprints in the Alboran Sea paleotemperatures." Paleoceanography 14:698.

Combourieu-Nebout, N., Turon, J. L., Zahn, R., Capotondi, L., Londeix, L. and Pahnke, K. (2002) "Enhanced aridity and atmospheric high-pressure stability over the western Mediterranean during the North Atlantic cold events of the past 50 k.y." Geology 30(10):863-866.

Combourieu-Nebout, N., O. Peyron, et al. (2009) "Rapid climatic variability in the west Mediterranean during the last 25,000 years from high resolution pollen data." Climate of the Past 5(3):503.

Elderfield, H. and Ganssen, G., 2000. Past temperature and 18O of surface ocean waters inferred from foraminiferal Mg/Ca ratios. Nature. 405, 442-445.

Govin, A., Braconnot, P., Capron, Em., Cortijo, E., Duplessy, J. C., Jansen, E., Labeyrie, L., Landais, A., Marti, O., Michel, E., Mosquet, E., Risebrobakken, B., Swingedouw, D. and Waelbroeck, C. (2012) "Persistent influence of ice sheet melting on high northern latitude climate during the early Last Interglacial." Climate of the Past 8:483-507.

Hernández-Almeida, I., Bárcena, M. A., Flores, J. A., Sierro, F. J., Sanchez-Vidal, A. and Calafat, A. (2011) "Microplankton response to environmental conditions in the Alboran Sea (Western Mediterranean): one year sediment trap record." Marine Micropaleontology 78:14-24.

Martrat, B., J. O. Grimalt, et al. (2004). "Abrupt Temperature Changes in the Western Mediterranean over the past 250,000 years." Science 306 (5702):1762.

McManus, J. F., Bond, G. C., Broecker, W. S., Johnsen, S., Labeyrie, L. and Higgins, S. (1994) "High-resolution climate records from the North Atlantic during the last interglacial." Nature 371:326-329.

McManus, J. F., Oppo, D. W. and Cullen, J. L. (1999) "A 0.5-million-year record of millennial-scale climate variability in the North Atlantic." Science 283:971-975.

NEEM community members (2013) Eemian interglacial reconstructed from a Greenland folded ice core. Nature, vol. 493:489-494, doi:10.1038/nature11789.

North Greenland Ice Core Project (2004). Nature 431(7005):147-151.

Oppo, D. W., McManus, J. F. and Cullen, J. L. (2006) "Evolution and demise of the Last Interglacial warmth in the subpolar North Atlantic." Quaternary Science Reviews 25:3268-3277.

Prell, W.L., 1985. The stability of low-latitude sea surface temperatures: An evaluation of the CLIMAP reconstruction with emphasis on the positive SST anomalies. US Department of Energy, Washington, DC, (60p).

Prell, W., Martin, A., Cullen, J., Trend, M., 1999. The Brown University Foraminiferal Data Base, IGBP PAGES/World Data Center-A for Paleoclimatology Data Contribution Series #1999–027, NOAA/ NGDC Paleoclimatology Program. Boulder Co., USA.

Rigual-Hernández, A. S., Sierro, F. J., Bárcena, M. A., Flores, J. A. and Heussner, S. (2012) "Seasonal and interannual changes of planktic foraminiferal fluxes in the Gulf of Lions (NW Mediterranean) and their implications for paleoceanographic studies: two 12-year sediment trap records." Deep-Sea Research 66:26-40.

Ruddiman, W. F. (1977) "North Atlantic ice-Rafting: a major change at 75,000 years before the present." Science 196(4295):1208-1211.

Wit, J. C., Reichart, G. J.,, Jung, S. J. A. and Kroon, D. (2010) "Approaches to unravels seasonality in sea surface temperatures using paired single-specimen foraminiferal $d^{18}O$ and Mg/Ca analyses." Paleoceanography 25(4).

Chapter 1 - ODP 976 and Alboran Sea palaeoclimatology during the last two deglaciations.

Surface hydrology variability in the western Alboran Sea during the present and last interglacial and the preceding deglaciations is documented at an unprecedented time resolution in the ODP 976 oxygen isotope and SST records (Fig. 18 and 19). Robustness and reproducibility of these palaeo-signals is proved by comparing the records with similar data profiles from other Alboran Sea sites (ODP 976, 977 and MD95-2043; Fig. 18B and 19B; see also: chapter "*Results*", Figs. 16 and 17). Highest resolution is achieved at ODP 976 that displays a highly variable Mg/Ca derived SST signal (Fig. 18C and 19C, grey data points). This high variability can plausibly be attributed to the high temporal resolution of the data record, but it is to be noted that the structure of the smoothed record (Fig. 18C and 19C, dark blue record) coincides almost perfectly with that of Mg/Ca derived SST records from other Alboran Sea sites. Due to its position within the Atlantic inflow, ODP 976 displays the lightest $\delta^{18}O$ levels, and consequently the lowest $\delta^{18}O_{sw}$ levels (a proxy for palaeosalinity) among the sites compared. The heaviest values are documented at the easternmost site, MD99-2343 (Fig. 18C).

Secondary factors can impact the reconstruction of palaeo-SST such as post-depositional carbonate dissolution and variables independent of temperature, such as salinity, dissolution or nutrients concentration (Lea et al., 1999; Nürnberg et al., 1996; Huguet et al., 2011). Hence it is important to view and compare palaeoclimatic SST reconstructions from the perspective of multiple proxies. Here records of continental annual mean temperature and precipitation are compared with the marine proxy records in order to assess the robustness with which the marine and terrestrial palaeoclimatology in the westernmost Alboran Sea can be reconstructed. Previously, ODP 976 pollen records and pollen-based continental climate reconstructions have shown that changes in the western Mediterranean vegetation responded rapidly to the abrupt climatic fluctuations that punctuated the last climatic cycle in a manner suggesting a nearly instantaneous response to North Atlantic ocean and climate variability (Cacho et al., 1999, 2001; Combourieu-Nebout et al., 2002, 2009).

Regarding the marine SST proxies used in this study, some studies (González-Mora et al., 2008) suggested that the structure and levels of SST records derived from Mg/Ca profiles are similar to those derived from alkenones (r^2=0.41, n=171). The Mg/Ca and alkenone derived SST profiles generated for ODP976 are likewise correlated (r^2=0.20, n=371), although some differences between the proxy-specific SST records are evident. Differences between Mg/Ca and alkenones derived SST signals are not unknown and have been documented at a number of sites in the Atlantic, Pacific and Southern Oceans (Leduc et al., 2010). The ODP 976 $SST_{Mg/Ca}$ record displays much higher variability compared to the rather smooth structure of the $SST_{Uk'37}$ record. We mainly relate this proxy-specific difference to the ecology and environmental factors influencing the living habitats of the signal carriers. Previous studies (Leduc et al., 2010) have suggested that the regional palaeoceanography interacted with phytoplankton and zooplankton ecological behavior in a way that affected the proxy formation and SST recording by imposing, for instance, different seasonal imprints on the SST profiles. While *G. bulloides* is considered to record a spring-time SST signal (Elderfield and Ganssen, 2000; Ganssen and Kroon, 2000), alkenones plausibly depict an annually integrated SST (Martrat et al., 2004, 2007, 2013 submitted; Huguet et al., 2011; Dos Santos et al., 2013). Hence, $SST_{Uk'37}$ is more likely to display a smooth record when compared to the seasonal i.e., spring-time signal recorded by the $SST_{Mg/Ca}$ measured in foraminiferal shells. However, a recent calibration for the Iberian margin suggests that the maximum haptophyte (alkenone-producing algae) production takes place during the colder season, and therefore, $SST_{Uk'37}$ would be better reflecting winter SST rather than an annual average (Rodrigues et al., 2012).

The methodology used for each paleothermometry proxy is another factor possibly contributing to the proxy-specific difference between the SST records. This lies on the far higher abundance of alkenones in sediment samples compared to the much smaller foraminiferal shell availability, which varies in accordance with sediment volumes used to extract the shells and naturally occurring (seasonal, internannual, long-term climatic) variations during the course of sediment deposition. It has also been suggested that factors such as lateral transport through oceanic currents (Ohkuchi et al., 2002) or bioturbation (Bard, 2001) can contribute to modify the alkenone-derived SST signal regionally or down-core, respectively.

Drastic changes in the surface hydrography of the Alboran Sea have been demonstrated in association with H1 (Cacho et al., 1999, 2002; Martrat et al., 2013, submitted). Cool conditions and increased aridity (Fig. 18D) of the Alboran Sea borderlands are revealed by the large expansion of steppe or semi-desert pollen taxa (Fig. 18G, brown; Combourieu-Nebout et al., 2002, 2009 and unpublished data) and were linked with measurable SST decreases in the Mediterranean Sea at that time (Combourieu-Nebout et al., 2009). SST then increased during deglaciation well into the B/A warming interval (Fig. 18C, D and E, orange shading) and was accompanied by a significant increase of Mediterranean forest taxa presence (Fig. 18G, green; Combourieu-Nebout et al., 2002, 2009 and unpublished data). $SST_{Mg/Ca}$ at ODP976 reaches full-interglacial levels of ~21°C during the B/A (Fig. 18C), while $SST_{Uk'37}$ remained at ~16°C representing half of the glacial-interglacial $SST_{Uk'37}$ amplitude (Fig. 18E). This may indicate that a considerable degree of seasonality was established with the first resumption of the AMOC during the B/A with an enhanced northward transportation of marine heat favouring warmer conditions during the *G. bulloides* growth season.

During the subsequent YD episode (Fig. 18, green shading) all SST records ($SST_{Mg/Ca}$, $SST_{Uk'37}$, pollen-derived continental annual mean temperature) show a decrease in temperature of similar magnitude, around ~4-4.5°C relative to the B/A SST level with $SST_{Uk'37}$ falling to nearly full-glacial levels (~12°C). Continental proxy records likewise document this return to cold conditions, showing an increase of semi-desert taxa (Combourieu-Nebout et al., 2002, 2009 and unpublished data). The YD (~12.8-11.5 ky) has already been shown to consist of a two-phased cooling in this area (Combourieu-Nebout et al., 2009). Abrupt shifts to heavier oxygen isotopes, cold SST values and an increase in semi-desert taxa indicate a first dry and cold period (~12.5-12 ky) followed by a more humid interval (~12-11.5 ky), in which the oxygen isotopes shift rapidly to lighter values, together with increased precipitation as depicted in pollen records, notably the sudden decrease in semi-desert taxa. These synchronous events suggest that freshwater fluxes were enhanced as a result of enhanced humidity during the second phase of the YD. This two-phased YD is consistent with an intra-YD earlier Mediterranean warming at ~12.2 ky observed in previous studies (Goslar et al., 1993; Brauer et al., 2000; Cacho et al., 2002) that has been suggested to be a response to warming transmitted from the European continent, potentially related to a northward migration of the North Atlantic polar front (Cacho et al., 2001). An explanation to this climatic change was suggested by Brauer et al. (2000) and relies on the fact that strong westerlies during the YD drove

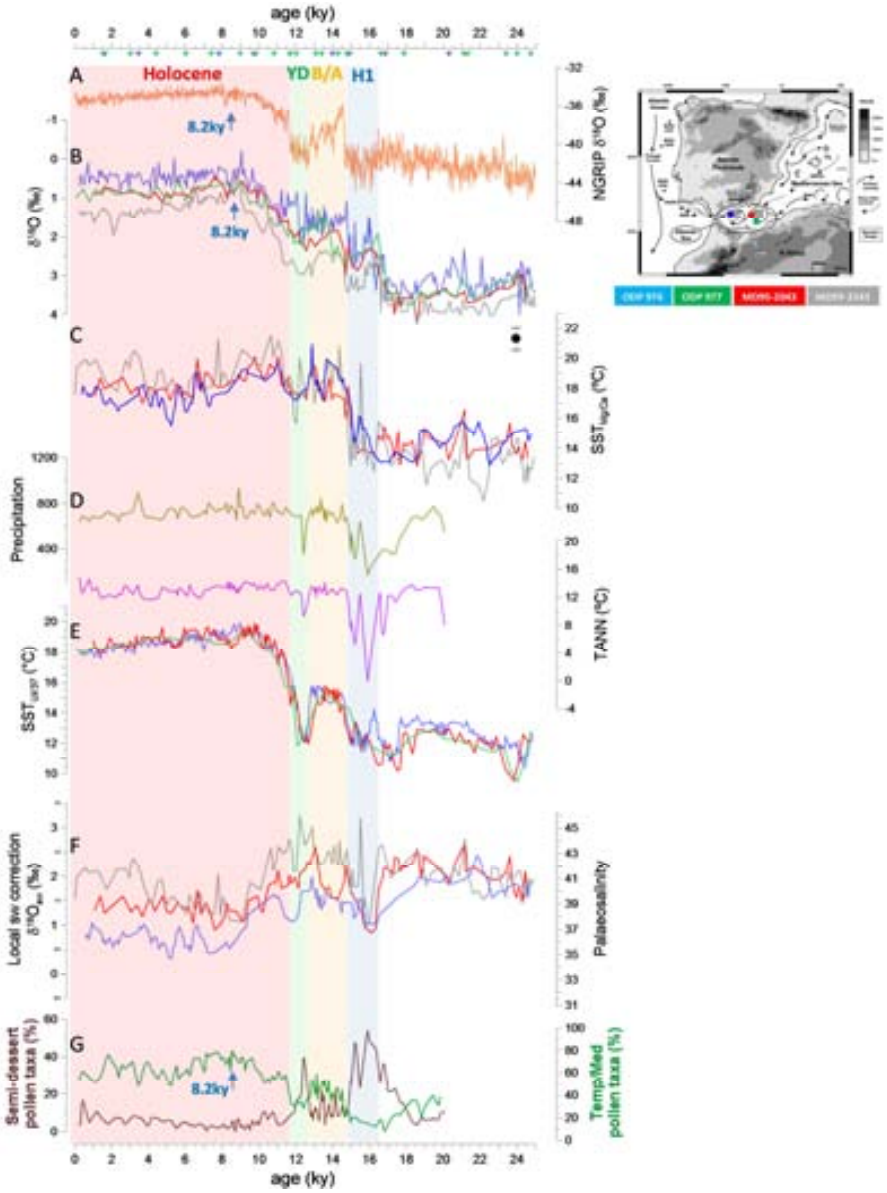

Figure 18. ODP 976 marine and terrestrial palaeoclimatology during the MIS2-T1-Holocene period. Triangles along the upper x-axis represent radiocarbon measurements from ODP 976 (blue, Combourieu-Nebout et al., 2002) and MD95-2043 (green, Cacho et al., 2001). (A) NGRIP $\delta^{18}O$ ice core record (orange, NGRIP members, 2004) on the AICC2012 age scale (Bazin et al., 2013; Veres et al., 2013). (B) *G. bulloides* $\delta^{18}O$ records: ODP 976 (dark blue, this study), MD95-2043 (red, Cacho et al., 1999 and 2002; high resolution data from Cacho et al., 2013, unpublished), ODP 977 (green, Martrat et al., 2004) and MD99-2343 (grey, Frigola et al., 2007). (C) SST derived from Mg/Ca ratios ($SST_{Mg/Ca}$) measured in *G. bulloides.* ODP 976 (dark blue= smoothed record, this study), MD95-2043 (red, Cacho, unpublished data) and MD99-2343 (grey, Cacho, unpublished data). (D) Continental annual mean precipitation (olive green) and temperature (TANN, purple) derived from pollen associations (Combourieu-Nebout, et al., 2009, unpublished data). (E) SST derived from alkenones ($SST_{Uk'37}$): ODP 976 (blue, Martrat et al., 2013, submitted), ODP 977 (green, Martrat et al., 2004) and MD95-2043 (green, Cacho et al., 1999, 2002). (F) $\delta^{18}O_{sw}$ derived from $\delta^{18}O_{cc}$ and $SST_{Mg/Ca}$: ODP 976 (dark blue= smoothed, this study), MD95-2043 (red, Cacho, unpublished data) and MD99-2343 (grey, Frigola and Cacho, unpublished data). (G) Fossil pollen records: semi-desert taxa (brown), temperate and Mediterranean forest taxa (green) (Combourieu-Nebout, et al., 2002, 2009, and unpublished data). Main features identified during the deglaciation are indicated by colour shadings: Heinrich event 1 (blue, H1), Bölling/Allerod (orange, B/A), Younger Dryas (green, YD) and the 8.2 ky event (blue arrows). MIS=Marine Isotope Stage; T=Termination. Top right panel: map showing locations of the different Alboran basin sites.

the northward shift of the sea ice boundary during the second part of the YD, leading to a change from relatively dry air (originating over sea ice) to relatively humid air (originating over open sea water), resulting in increasing precipitation over northern Europe. A coeval marked decrease in $\delta^{18}O_{sw}$ is evident at the YD (Fig. 18F).

While $SST_{Mg/Ca}$ have reached maximum SST levels at the onset of the Holocene (11.7 ky), it is not until 9.5-10 ky that $SST_{Uk'37}$ reach maximum interglacial values. The forest expansion (Fig. 18G, green) is delayed by up to 3 millennia since the onset of the Holocene (11.7 ky). It is not until ~9.5-10 ky that the temperate and Mediterranean interglacial vegetation are fully established, which coincides with the "climatic optimum" of the Holocene. This progressive expansion of the Mediterranean forest is synchronous to the increasing $SST_{Uk'37}$ and the planktonic $\delta^{18}O$ shift towards the minimum interglacial values, reflecting the climate improvement in the marine environments in this region at the beginning of the Holocene (Cacho et al., 2001; Combourieu-Nebout et al., 1998, 1999, 2002). The climatic optimum at the beginning of the Holocene was interrupted by a globally revealed temperature anomaly, the 8.2 ky event which is often attributed to a meltwater outflow in the North Atlantic and a consequent AMOC slowdown (Röhling and Pälike, 2005; Cheng et al., 2009). The ODP 976 records also capture this event as a decrease in forest expansion (Fig. 18G, green), pollen-derived continental temperatures (Fig. 18D), both SST records (Fig. 18C, E) and the $\delta^{18}O$ record (Fig. 18B). Holocene SST stabilizes around 17.5°C ($SST_{Mg/Ca}$) and 18°C ($SST_{Uk'37}$) closely matching today's Alboran Sea region modern spring and annual average SST, respectively (MEDATLAS II, Medar Group, 2002).

The penultimate deglaciation (T2) also shows multiple-step features albeit at different magnitudes and relative timings, alluding to offsets in dynamics between T2 and T1 (Fig. 19). In principle, the main difference observed between the last two glacial terminations is the lack of a pronounced YD-type cooling event during T2. Previous studies Carlson, 2008; Oppo et al., 2001) have explained the lack of such a cold episode based on the rapidity of greater Northern Hemisphere ice sheet retreat under a greater boreal summer insolation, suppressing the resumption of the AMOC until the near end of the T2, while during T1 it strengthened relatively earlier with the B/A warm interval. Therefore, during T2, the increased freshwater input to the North Atlantic took place prior to the resumption of the AMOC, having little effect on the AMOC. A

"climatic pause" during the T2 warming trend has been seen as a distinctive feature in several benthic $\delta^{18}O$ marine records from the North Atlantic by previous studies (Lototskaya and Ganssen, 1998, 1999; Gouzy et al., 2004; Shackleton et al., 2000, 2003), which was mainly attributed to a pause in the melting of polar ice sheets. This "pause" is also identified in our ODP976 $\delta^{18}O$ record at 130-132 ky (Fig. 19, dark blue shading), although no "pause" is observed in the $SST_{Mg/Ca}$ record. T2 shows several $\delta^{18}O$ steps to lighter values but compared to T1 these steps are embedded in what appears a single large and prominent excursion to lighter oxygen isotope values, interrupted by a plateau (~132-130 ky), and a final decrease to minimum interglacial $\delta^{18}O$ levels in a ~1 ky interval (~130-129 ky). The plateau of depleted $\delta^{18}O$ during T2 is recorded synchronously with cold full-glacial $SST_{Mg/Ca}$ that in combination indicate the incursion of the H11 meltwater event. The combined structure of the $SST_{Mg/Ca}$ and planktonic $\delta^{18}O$ records hence suggests that T2 was almost entirely controlled by the single massive meltwater surge of H11 or that this massive meltwater surge embedded the main H11 event in it. The palaeo-salinity proxy $\delta^{18}O_{sw}$ shows a pronounced decrease supporting the massive dimension of the H11 event (Fig. 19F).

Following H11, $SST_{Mg/Ca}$ steeply and uninterruptedly increased by ~5°C (~15-20°C) in 1 millennium (130-129 ky), reaching full interglacial conditions at ~129 ky (onset of MIS5e), and showing a second and maximum SST peak at 128 ky which coincides with the maximum temperate and Mediterranean forest expansion (Fig. 19G). During the pre-H11 event (134-132 ky, Fig. 19, light blue shading), $SST_{Mg/Ca}$ and $SST_{Uk'37}$ cold spells are recorded synchronously with indications of cold and dry continental conditions as revealed by pollen-based terrestrial temperature and precipitation, high semi-dessert taxa abundances, low temperate forests abundances and enhanced abundance of the cysts of the cold-water dinoflagellate *B. tepikiensis*.

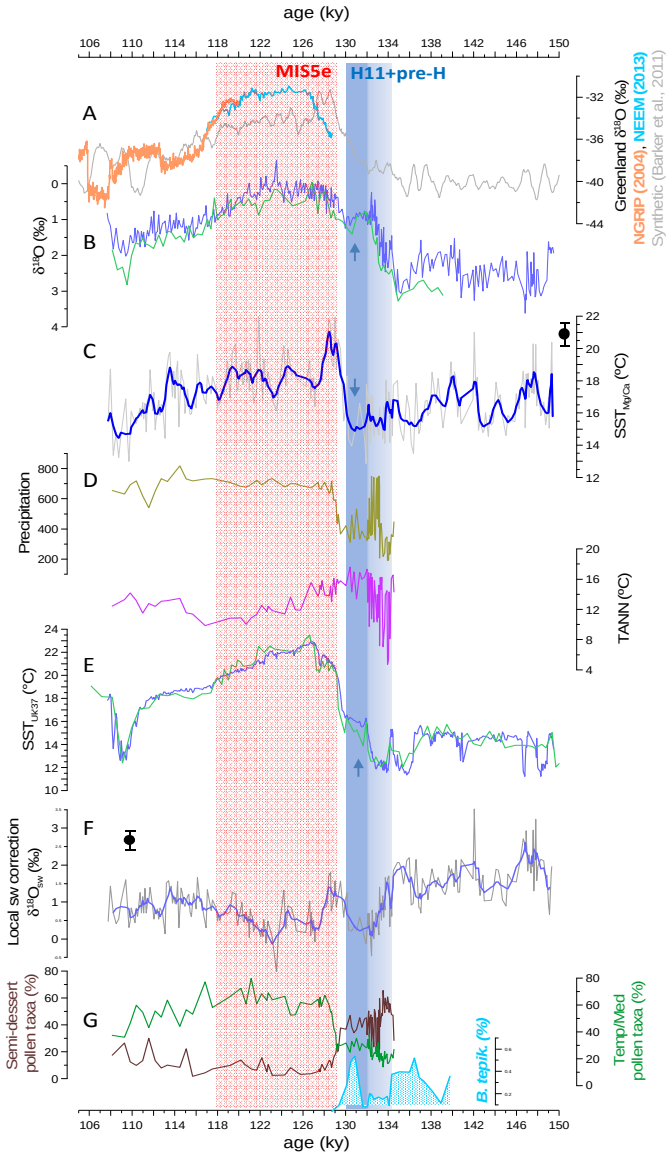

Figure 19. ODP 976 marine and terrestrial palaeoclimatology during the MIS6-T2-MIS5e period. (A) Greenland $\delta^{18}O$ ice core records: NGRIP (orange, NGRIP members, 2004) on the AICC2012 age scale (Bazin et al., 2013; Veres et al., 2013), NEEM (light blue, NEEM community members, 2013) and the synthetic record Greenland climate variability (grey, Barker et al., 2011). (B) *G. bulloides* $\delta^{18}O$ records: ODP 976 (dark blue, this study) and ODP 977 (green, Martrat et al., 2004). (C) ODP 976 SST derived from Mg/Ca ratios ($SST_{Mg/Ca}$) measured in *G. bulloides* (grey=unsmoothed record, dark blue= smoothed record, this study). (D) Continental annual mean precipitation (olive green) and temperature (TANN, purple) derived from pollen associations (Combourieu-Nebout and Peyron, unpublished data). (E) SST derived from alkenones ($SST_{Uk'37}$): ODP 976 (blue, Martrat et al., 2013, submitted) and ODP 977 (green, Martrat et al., 2004). (F) ODP 976 $\delta^{18}O_{sw}$ derived from $\delta^{18}O$ and $SST_{Mg/Ca}$ (grey=unsmoothed record, blue= smoothed record, this study). (G) Fossil pollen records: semi-desert taxa (brown), temperate and Mediterranean forest taxa (green) (Masson-Delmotte et al., 2005; Combourieu-Nebout, unpublished data) and ODP 976 abundances (%) of cysts of the cold-water dinoflagellate *Bitectatodinium tepikiense* (L. Londeix, pers. comm.). The main features identified during the deglaciation are indicated by colour shadings: Heinrich event 11 (dark blue, H11) and pre-Heinrich 11 events (light blue). MIS=Marine Isotope Stage.

At 132.5 ky, the intermittent $\delta^{18}O$ minimum coincides with an increase in the pollen-based precipitation and terrestrial annual temperature conditions and with both $SST_{Uk'37}$ and $SST_{Mg/Ca}$ records, in response to the meltwater perturbation. This event immediately precedes the main H11 event. While $SST_{Mg/Ca}$ reveals cold H11 temperatures at the full-glacial level (Fig. 19C, blue arrow), $SST_{Uk'37}$ warms by ~4°C to an intermittent plateau that interrupts the T2 warming trend and they do not display a reversal to colder temperatures. This interval has been considered a potential B/A-analogue event by previous studies (Martrat et al., 2013; Gouzy et al., 2004), largely based on the structural similarity of the $\delta^{18}O$ and $SST_{Uk'37}$ records with the B/A event during T1 (Fig. 18, orange shading). However, in addition to the persistence of full-glacial cold temperatures recorded during this event in the $SST_{Mg/Ca}$ record, a coeval decrease in precipitation and a second abundance maximum of semi-dessert taxa (Fig. 19D, G) reflect arid conditions during this stage. Combined with a well-defined abundance peak of *B. tepikiensis* (L. Londeix, pers. comm; Fig. 19G) this evidence strongly suggests the presence of cold-water conditions at that time. Taking this new evidence at face value then indicates that the structural B/A type feature seen in planktonic $\delta^{18}O$ and $SST_{Uk'37}$ records carries features that much rather are connected with type H-event environmental changes (meltwater-induced negative $\delta^{18}O$ anomaly, full-scale SST drop, presence of cold-water conditions) that are consistent with the incursion of H11. It is not until the influence of this massive Heinrich event disappears that $SST_{Mg/Ca}$ initiates its steep increase directly into MIS5e at ~129 ky.

In all, the last two glacial terminations in ODP976 show multiple-step features albeit at different magnitudes and relative timings, alluding to offsets in dynamics between T2 and T1. The combined structure of ODP 976 $SST_{Mg/Ca}$ and planktonic $\delta^{18}O$ records, together with additional ODP 976 multi-proxy climatic records suggests that T2 was almost entirely controlled by the single massive meltwater surge, H11, or embedding the main H11 event in it. It is not until the influence of this massive Heinrich event disappears that $SST_{Mg/Ca}$ initiates its steep increase directly into full interglacial conditions at ~129 ky, the onset of MIS5e.

References:

Bard, E., 2001. Palaeoceanographic implications of the difference in deep-sea sediment mixing between large and fine particles. Paleoceanography 16 (3):235–239.

Barker, S., G. Knorr et al. (2011). "800,000 years of abrupt climate variability." Science 334(6054):347.

Brauer, A., Günter, C., Johnsen, S. J. and Negendack, J. F. W. (2000) "Land-ice teleconnections of cold climatic periods during the last glacial/interglacial transition." Climate Dynamics 16:229-239.

Bazin, L., Landais, A., Lemieux-Dudon, B., Toy«e Mahamadou Kele, H., Veres, D., Parrenin, F., Martinerie, P., Ritz, C., Capron, E., Lipenkov, V., Loutre, M.-F., Raynaud, D., Vinther, B., Svensson, A., Rasmussen, S., Severi, M., Blunier, T., Leuenberger, M., Fischer, H., Masson-Delmotte, V., Chappellaz, J., and Wolff, E. (2013) "An optimized multi-proxies, multi-site Antarctic ice and gas orbital chronology (AICC2012): 120-800 ka." Climate of the Past 9(4):1715-1731.

Cacho, I. (1999)."Dansgaard-Oeschger and Heinrich event imprints in the Alboran Sea paleotemperatures." Paleoceanography 14:698.

Cacho, I., J. O. Grimalt, et al. (2001) "Variability of the western Mediterranean Sea surface temeprature during the last 25,000 years and its connection with the Northern Hemisphere Climatic changes." Paleoceanography 16(1):40.

Cacho, I., J. O. Grimalt, et al. (2002). "Response of the Western Mediterranean Sea to rapid Climatic variability during the last 50,000 years: a molecular biomarker approach." Journal of Marine Systems 33-34(0):253.

Cheng, H., Edwards, R. L. et al. (2009) "Ice age Terminations." Science 326(5950):248.

Combourieu-Nebout, N., Paterne, M., Turon, J. L. and Siani, G. (1998) "A high-resolution record of the last deglaciation in the central Mediterranean Sea: palaeovegetation and palaeohydrological evolution." Quaternary Science Reviews 17(4-5):303-317.

Combourieu-Nebout, N., Turon, J. L., Zahn, R., Capotondi, L., Londeix, L. and Pahnke, K. (2002) "Enhanced aridity and atmospheric high-pressure stability over the western Mediterranean during the North Atlantic cold events of the past 50 k.y." Geology 30(10):863-866.

Combourieu-Nebout, N., O. Peyron, et al. (2009) "Rapid climatic variability in the west Mediterranean during the last 25,000 years from high resolution pollen data." Climate of the Past 5(3):503.

Dos Santos, R. A., Spooner, M. I. et al. (2013) "Comparison of organic (Uk'37, TEXH86, LDI) and faunal proxies (foraminiferal assemblages) for reconstruction of late Quaternary sea surface temperature variability from offshore southeastern Australia." Paleoceanograpgy 28(3):377.

Elderfield, H. and Ganssen, G., 2000. Past temperature and 18O of surface ocean waters inferred from foraminiferal Mg/Ca ratios. Nature. 405, 442-445.

Frigola, J., Moreno, A., Cacho, I., Canals, M., Sierro, F. J., Flores, J. A., Grimalt, J. O., Hodell, D. A., and Curtis, J. H. (2007)Holocene climate variability in the Western Mediterranean region from a deepwater sediment record." Paleooceanography, 22 .

Ganssen, G.M. and Kroon, D. (2000) "The isotopic signature of planktonic foraminifera from NE Atlantic surface sediments implications for the reconstruction of past oceanic conditions." Journal of the Geological Society, 157 (2000), pp. 693–699.

González-Mora, B., Sierro, F. J., Schönfeld, J. (2008) "Temperature and stable isotope variations in different wáter masses from the Alboran Sea (Western Mediterranean) between 250 and 150 ka." Geochemistry, Geophysics, Geosystems 9(10):1525-2027.

Goslar, T., Kuc, T., Ralska-Jasiewiczowa, M., Rózánski, K., Arnold, M., Bard, E., van Geel, B., Pazdur, M. F., Szeroczynske, K., Wicik, B., Wieckowski, K. and Walanus, A. (1993) "High-resolution lacustrine record of the late glacial/Holocene transition in central Europe." Quaternary Science Reviews 12:187-294.

Gouzy, A. Malaizé, B., Pujol, C. and Charlier, K. (2004) "Climatic "pause" during Termination II identified in shallow and intermediate waters off the Iberian margin." Quaternary Science Reviews 23:1523-1528.

Huguet, C., Martrat, B., Grimalt, J.O., Sinninghe Damsté, J.S., Schouten, S. (2011) "Coherent millennial.scale patterns in Uk'37 and TEX H86 temperature records during the penultimate interglacial-to-glacial cycle in the western Mediterranean." Paleoceanography 26.

Lea, D. W., Mashiotta, T. A., Spero, H. J., 1999. Controls on magnesium and strontium uptake in planktonic

foraminifera determined by live culturing. Geochimica Et Cosmochimica Acta. 63, 2369-2379.

Leduc, G., Schneider, R., Kim, J. H. and Lohmann, G. (2010) "Holocene and Eemian sea surface temperature trends as revealed by alkenone and Mg/Ca paleothermometry." Quaternary Science Reviwes 29:989-1004.

Lototskaya, A., Ziveri, P., Ganssen, G., & van Hinte, J. E. (1998). Calcareous nannoflora response to Termination II at 45° N, 25° W(northeast Atlantic). *Marine Micropaleontology*, *34*, 47}70.

Lototskaya, A. and Ganssen, G. M. (1999) "The structure of Termination II (penultimate deglaciation and Eemian) in the North Atlantic." Quaternary Science Reviews 18:1641-1654.

Martrat, B., J. O. Grimalt, et al. (2004). "Abrupt Temperature Changes in the Western Mediterranean over the past 250,000 years." Science 306 (5702):1762.

Martrat, B., Grimalt, J. O., Shackleton, N. J., de Abreu, L., Hutterli, M. A. and Stocker, T. F. (2007) Four climate cycles of recurring deep and surface water destabilizations on the Iberian Margin. Science, vol. 317 (502), doi: 10.1126/science.1139994.

Masson-Delmotte, V., Landais, A., Combourieu-Nebout, N., von Grafenstein, U., Jouzel, J., Caillon, N., Chappellaz, J., Dahl-Jensen, D., Johnsen, S. J. and Stenni, B. (2005) "Rapid climate variability during warm and cold periods in polar regions and Europe." Geoscience 337:935-946.

NEEM community members (2013) Eemian interglacial reconstructed from a Greenland folded ice core. Nature, vol. 493:489-494, doi:10.1038/nature11789.

North Greenland Ice Core Project (2004). Nature 431(7005):147-151.

Nürnberg, D., Bijma, J., Hemleben, C., 1996. Assessing the reliability of magnesium in foraminiferal calcite as a proxy for water mass temperatures. Geochimica Et Cosmochimica Acta. 60, 803-814.

Ohkouchi, N., Eglinton, T.I., Keigwin, L.D., Hayes, J.M., 2002. Spatial and temporal offsets between proxy records in a sediment drift. Science 298, 1224–1227.

Rohling, E. and Pälike, H. (2005) "Centennial-scale climate cooling with a sudden cold event around 8,200 years ago." Nature 434:975-979.

Rodrigues, T., Rufino, M., Santos, C., Salgueiro, E., Abrantes, F. and Oliveira, P. (2012) "Iberian Sea Surface Temperature calibration based in alkenones paleotemperature index Uk37." 7º Simpósio sobre a Margem Ibérica Atlantica, MIS 2012.

Sánchez Goñi, M. F., Bakker, P., Desprat, S., Carlson, A. E., van Meerbeeck, C. J., Peyron, O., Naughton, F., Fletcher, W. J., Eynaud, F., Rossignol, L. and Renssen, H. (2012) European climate optimum and enhanced Greenland melt during the Last Interglacial. Geology, vol. 40(7):627-630.

Shackleton, N. J. and Hall, M. A., Vincent, E. (2000) "Phase relationships between millennial-scale events 64,000-24,000 years ago. Paleoceanography, vol. 15(6):565-569.

Shackleton, N. J., Sánchez Goñi, M. F., Pailler, D. and Lancelot, Y. (2003) "Marine Isotope Substage 5e and the Eemian Interglacial." Global and Planetary Change (36):151-155.

Shackleton, N. J., Fairbanks, R. G., Chiu, T. and Parrenin, F. (2004) "Absolute calibration of the Greenland time scale: implications for Antarctic time scales and for Δ^{14}C." Quaternary Science Reviews 23:1513-1522.

Schönfeld, J., Zahn, R. and Abreu, L. (2003) "Surface and deep water response to rapid climate changes at the Western Iberian Margin." Global and Planetary Change 36(4):237-264.

Skinner, L. (2003) "Millennial climate change in the northeast Atlantic: The role of surface and deep hydrographic change determined by stable isotope geochemistry and Mg/Ca palaeothermometry." Doctoral Thesis, University of Cambridge, 142pp.

Veres, D., Bazin, L., Landais, A., Lemieux-Dudon, B., Parrenin, F., Martinerie, P., Toy«e Mahamadou Kele, H., Capron, E., Chappellaz, J., Rasmussen, S., Severi, M., Svensson, A., Vinther, B., and Wolff, E.: The Antarctic ice core chronology (AICC2012): an optimized multi-parameter and multi-site dating approach for the last 120 thousand years, Climate of the Past.9(4).

Voelker, A. H. L., Lebreiro, S. M., Schönfeld, J., Cacho, I., Erlenkeuser, H. and Abrantes, F. (2006) "Mediterranean outflow strengthening during northern hemisphere coolings: A salt source fr the glacial Atlantic?." Earth and Planetary Science Letters 245:39-55.

Chapter 2 – ODP976 as a palaeo-monitoring station of North Atlantic Ocean and climate variability.

In order to assess the influence of North Atlantic surface waters on the climatology at the Iberian margin and its propagation into the western Mediterranean we compare our ODP 976 records with reference records of Iberian Margin cores MD 95-2042 (Shackleton et al., 2000, 2003, 2004), MD 99-2334K (Skinner et al., 2003), MD95-2040 (Schönfeld et al., 2003) and MD99-2339 (Voelker et al., 2006) (Table 1.).

	Latitude	Longitude	Depth (m)	References
MD95-2040	40°34.91′N,	9°51.67′W	2465	*Schönfeld et al., 2003*
MD95-2042	37°48′N	10°10′W	3146	*Shakleton et al., 2000, 2002, 2004.*
MD99-2334K	37°48′N	10°10′W	3146	*Skinner et al., 2003*
MD99-2339	35°88′N	7°53′W	1170	*Voelker et al., 2006*

Table 1. List of cores in the Iberian margin used for comparison with ODP 976.

The Iberian Margin hydrography is dominated by the southward branch of the North Atlantic Drift (Sánchez Goñi et al., 2008) and is a focal point for studies of past climate variability during the late Pleistocene. Sedimentation rates are high allowing high resolution palaeoclimatic reconstructions and, due to its latitudinal position, the region is influenced by both high- and low-latitude processes; this makes it a climatically very sensitive region. Latitudinal migrations of the ocean polar front in the past across the northern North Atlantic produced large swings of the ocean climatology in the eastern North Atlantic such as, for instance, advances and retreats of polar conditions (Hodell et al., 2013) that affected the Iberian Margin most prominently during the Heinrich stadials of the last glacial cycle (Ruddiman and McIntyre, 1981; Cacho et al., 1999; Shackleton et al., 2000; Eynaud et al., 2009; Naughton et al., 2009; Voelker and de Abreu, 2011). High-resolution marine sediment cores from the Iberian margin record a range of water mass

signals coming from the northern North Atlantic and Antarctic regions. The $\delta^{18}O$ of planktonic foraminifera in this region has been unambiguously correlated to the structure of Greenland ice core $\delta^{18}O$ records (Shackleton et al., 2000; Martrat et al., 2007; Skinner et al., 2007), while the $\delta^{18}O$ of benthic foraminifera was found to resemble the structure of air temperature signals contained in Antarctic ice cores (Shackleton et al., 2000; Martrat et al., 2007). The alkenone derived SST records ($SST_{UK'37}$) of cores MD01-2444 and MD95-2042 have been documented to be in very close agreement with a similar record from ODP 977 in the westernmost Alboran basin (Martrat et al., 2007). In the Discussion Chapter 1 of this thesis, we have proved the nearly perfect reproducibility of climatic variability at three Alboran Sea sites (ODP Sites 976, 977; MD95-2043) (see "Results" chapter, Fig. 16 and Discussion Chapter 1: "*ODP 976 and Alboran Sea palaeoclimatology during the last two deglaciations*", Fig. 18). In this Chapter we confirm and reinforce the strong connection between the marine palaeoclimatology in the Alboran Sea and the Iberian margin, through water transports through the Strait of Gibraltar, which ultimately highlights the affinity of the Alboran Sea palaeoceanography to North Atlantic climate variability (Fig. 20).

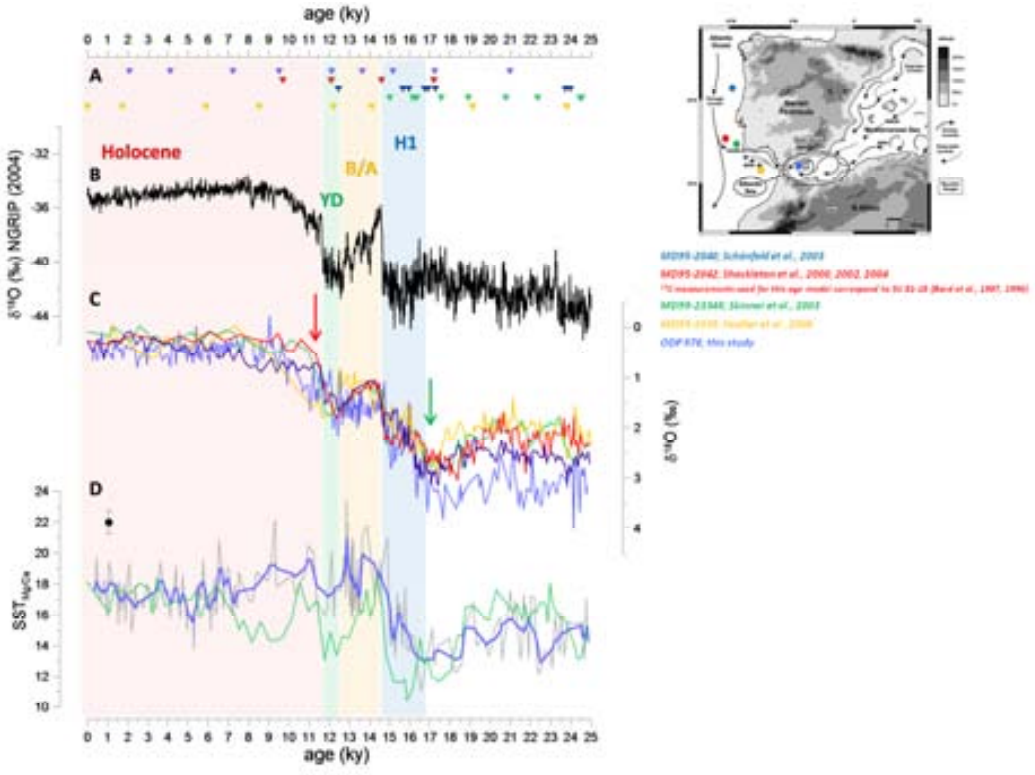

Figure 20. ODP 976 planktonic $\delta^{18}O$ and SST records compared with similar records from Iberian Margin cores: MD95-2042 (red, Shackleton et al., 2000, 2002, 2004); MD99-2334K (green, Skinner et al., 2003); MD95-2040 (dark blue, Schönfeld et al., 2003) and MD99-2339 (yellow, Voelker et al., 2006). (A) Coloured triangles along the top x-axis represent radiocarbon dates used in each sediment core. (B) NGRIP ice core $\delta^{18}O$ record (black, NGRIP members, 2004) on the AICC2012 age model (Bazin et al., 2013; Veres et al., 2013). (C) Planktonic foraminiferal $\delta^{18}O$ records from each sediment core. (D) Mg/Ca derived SST from MD99-2334K (green, Skinner et al., 2003) and ODP 976 (grey=individual data points, blue= smoothed record, this study). Vertical SST error bar indicated in black on the left. Vertical coloured bars indicate Heinrich event (blue, H1), Bölling/Allerod (orange, B/A) warm interval and Younger Dryas (green, YD). Arrows indicate convergence (green) or divergence (red) between the records.

The very close agreement among the different $\delta^{18}O$ records (Fig. 20C) confirms that the climatic signal recorded at the Iberian margin is transmitted directly and unaltered to ODP 976. During MIS2, the ODP 976 $\delta^{18}O$ record displays heavier values than the Iberian margin $\delta^{18}O$ records, potentially indicating colder SST and/or higher salinity at the core site during the growth season of the planktonic foraminifera used to generate the records (*G. bulloides*). At ~17 ky, with the onset of H1 event, the $\delta^{18}O$ offset disappears and the records converge on a common $\delta^{18}O$ level (Fig. 20, green arrow), which is maintained during the deglaciation. At ~11 ky, the Iberian margin sites (MD95-2040, MD95-2042 and MD99-2334K) (Fig. 20, red arrow), display a rapid decrease towards full interglacial $\delta^{18}O$ levels that mimics a similar development seen in the Greenland $\delta^{18}O$ record, while ODP 976 $\delta^{18}O$ continues to decrease more gradually to interglacial values that are reached at 9 ky, ~2 ky after the onset of the Holocene that is established in the Greenland ice core records at 11.7 ky. We have no radiocarbon measurements in this core interval and therefore, the ODP976 chronology of this particular section is floating so that it is not possible to robustly confirm a late onset of interglacial conditions at this location.

The $SST_{Mg/Ca}$ records in ODP 976 and MD99-2334 reveal a very close structure agreement although an offset is observed between these records. Higher $SST_{Mg/Ca}$ are recorded in ODP 976 than in MD99-2334 throughout the deglaciation and during the early Holocene, until 6.5 ky, when they converge on a very close SST range, around 18°C (Fig. 20D). Foraminiferal Mg/Ca values in the Mediterranean Sea have been previously observed to be higher than those obtained in the open sea (Bousetta et al., 2011, 2012; van Raden et al., 2011). To assess the possible source of this high Mg/Ca derived SST we checked other factors than temperature (diagenetic secondary overgrowths, salinity and dissolution) that are known to potentially influence the Mg/Ca ratio on the calcite shell, biasing consequently the temperature estimation derived from this proxy (Arbuszewski et al., 2010; van Raden et al., 2011; Boussetta et al., 2011, 2012). Bousetta et al. (2011) suggested that Mg-rich calcite peaks in the foraminiferal shells were compatible with inorganic calcite precipitated directly from the seawater. However, XRD analyses showed that the presence of these high-Mg calcite overgrowths reached up to 21% in the Eastern Mediterranean basin, but only up to 5% in the Western basin, where ODP Site 976 is located. Regarding a possible influence of salinity, particularly high foraminiferal Mg/Ca ratios have been found in the Eastern Mediterranean where salinity is unusually high, up to 40 psu (Ferguson et al., 2008). However,

ODP 976 is considered to be located in a "safe" salinity area (~36 psu). Additionally, according to van Raden et al. (2011), the supersaturated state with respect to calcite of Mediterranean intermediate and deep water masses has been suggested to be causing secondary calcite overgrowths increasing Mg/Ca values in foraminiferal tests. They observed that the calcite saturation state trend increases from west to east in the Mediterranean, so the diagenetic overprint in increased Mg/Ca observed in their study was mainly present in foraminifera from eastern locations (van Raden et al., 2011). Hence, the Mg/Ca derived SST records in ODP 976 can be considered to reveal indeed warmer SSTs than in the Iberian margin.

Moreover, the $SST_{Mg/Ca}$ warming in ODP 976 during the B/A interval is mimicked by a likewise large warming of 6-7°C warming in MD99-2334, suggesting that this high-amplitude warming is a robust feature of the Mg/Ca derived SST records, both in the Alboran Sea (ODP 977 and MD95-2043, Cacho, unpublished; for details, Discussion Chapter 1 *"ODP 976 and Alboran Sea palaeoclimatology during the last two deglaciations*", Fig. 18C) and the Iberian margin, where colder SST values are recorded. ^{14}C measurements are available for this period in core MD95-2043 (see Discussion Chapter 1: "*ODP 976 and Alboran Sea palaeoclimatology during the last two deglaciations*", Fig. 18; Cacho et al., 2001) that provide an absolute dating of this interval. The MD95-2043 SST record is closely correlated with that of ODP977 (Martrat et al., 2004, 2013 submitted) and based on the almost perfect correlation between ODP 976 and 977 (see Chapter "*Results"*, Fig. 16), we can tentatively conclude that the Alboran Sea profiles record a temporal SST and $\delta^{18}O$ evolution at the onset of the Holocene that is different from and delayed after that at the Iberian Margin.

No benthic records have been generated in ODP 976 as the signal recorded by the benthic foraminifera at this site does not reflect North Atlantic deep circulation. Therefore, in order to compare our surface records with MD95-2042 benthic records and, considering the close correlation of $\delta^{18}O$ between ODP 976 and MD95-2042 in the MIS2-T1-Holocene section (Fig. 20), we now correlate the MIS6-T2-MIS5e sections of these records by using the higher resolved ODP 976 as a reference (Fig. 21).

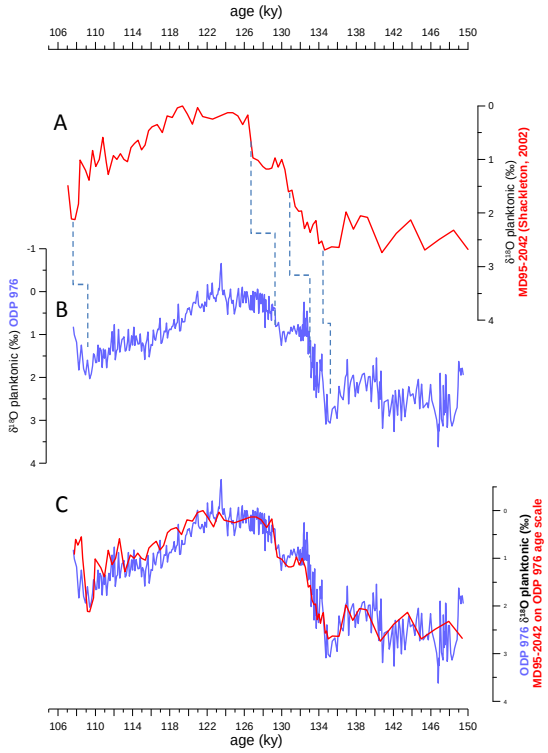

Figure 21. Synchronizing ODP 976 (B) and Iberian Margin site MD95-2042 (A) $\delta^{18}O$ profiles (Shackleton et al., 2000, 2002) across the MIS6-T2-MIS5e sequence. Stippled lines represent tie points used for the age model synchronization. (C) Resulting new age model for MD95-2042 planktonic $\delta^{18}O$ record (this study).

The synchronized timescale of core MD95-2042 now allows comparing the benthic isotopes record of this core with the ODP976 palaeo-profiles. The MD95-2042 benthic $\delta^{13}C$ record has been shown to be consistent with similar profiles from other North Atlantic sites in that it reveals a measurably reduced ventilation of North Atlantic Deep Water (NADW) during North Atlantic cold events (Shackleton et al., 2000, 2003). Inspection of longer benthic $\delta^{13}C$ profiles shows that the AMOC strength evolved differently during the last two deglaciations (Fig. 22). In the MIS2-T1-Holocene sequence, a close coupling exists between the development of North Atlantic surface ocean climatology and the AMOC as expressed by NADW ventilation. A period of marked strengthening of enhanced NADW production is revealed by rapidly increasing benthic $\delta^{13}C$ values (Fig. 22D, left panel) reflecting the resumption of the AMOC, which is associated with the incursion of the Bölling/Allerod (B/A) warm interval, as shown by ODP 976 $\delta^{18}O$ and both $SST_{Mg/Ca}$ and $SST_{Uk'37}$ records (Fig. 22B, E, orange shading). Earlier investigations indeed considered this time,

the B/A interval, the first establishment after the last glacial of a modern-type AMOC with full-strength NADW production (Weaver et al., 2003).

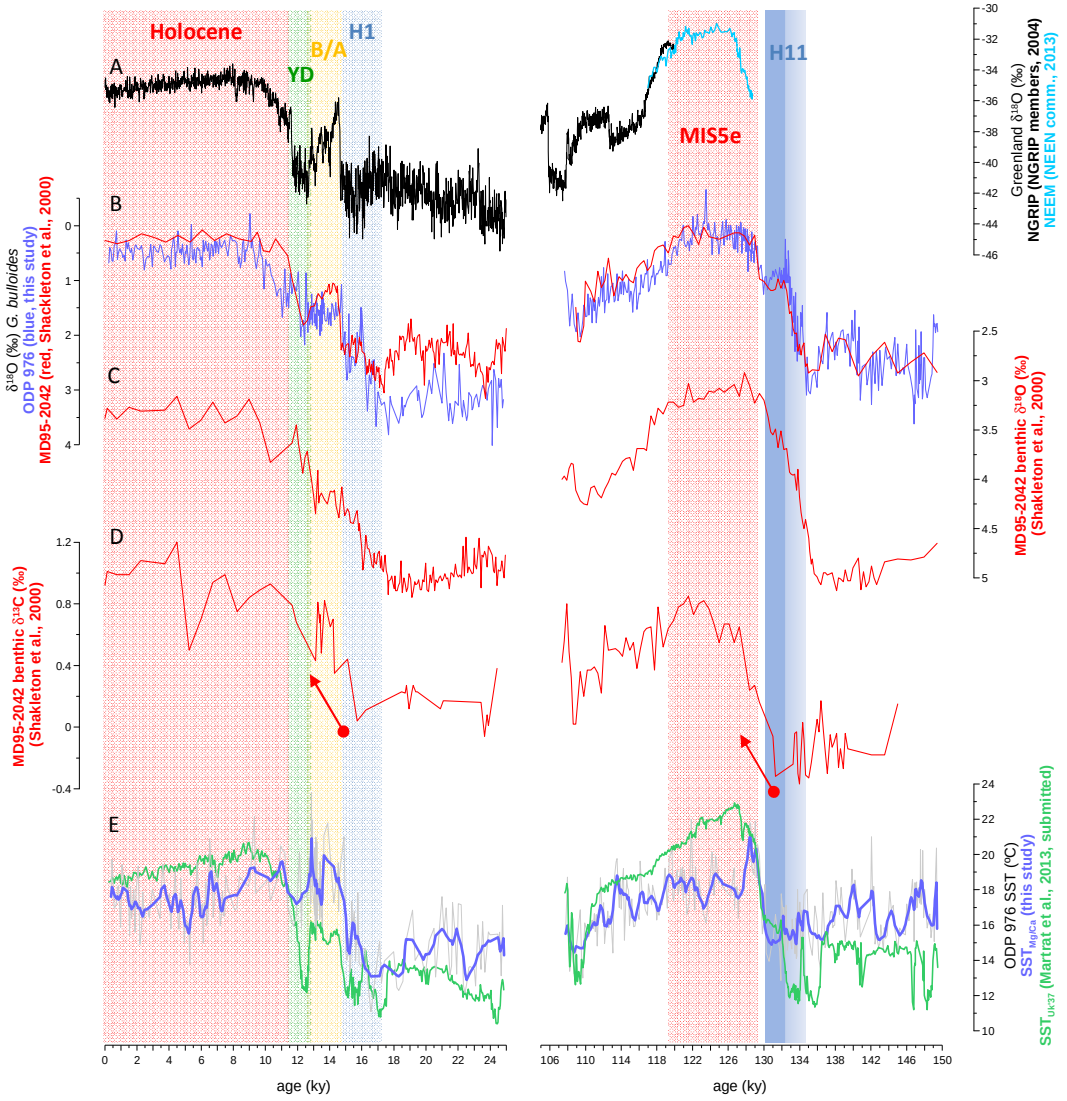

Figure 22. ODP 976 and MD95-2042 (Shackleton, 2000, 2002, 2004). Left panel: MIS2-T1-Holocene section. MD95-2042 records shown on their original age scale (Shackleton et al., 2000). Right panel: MIS6-T2-MIS5e section. MD95-2042 records synchronized to the ODP 976 age model (this study) (A) Greenland ice core records: NGRIP (black, NGRIP members, 2004) on the AICC2012 age scale (Bazin et al., 2013; Veres et al., 2013) and NEEM (light blue, NEEM community, 2013). (B) *G. bulloides* $\delta^{18}O$ records: ODP 976 (blue, this study), MD95-2042 (red, Shackleton et al., 2000, 2002, 2003). (C) Benthic $\delta^{18}O$ and (D) benthic $\delta^{13}C$ of core MD95-2042 (red, Shackleton et al., 2000, 2002, 2003). (D) ODP 976 SST records: $SST_{Mg/Ca}$ (grey=unsmoothed record, dark blue= smoothed record, this study) and $SST_{Uk'37}$ (Martrat et al., 2013, submitted). Vertical coloured bars indicate Heinrich events (left panel: blue, H1; right panel: darker blue, H11 and lighter blue, pre-H11 events), Bölling/Allerod (orange, B/A) warm interval, Younger Dryas (green, YD) and both interglacials, Holocene and MIS5e (red).

During T2, the MD95-2042 $\delta^{13}C$ benthic record reveals NADW production remained consistently low during the glacial-interglacial transition, indicating a continually weak AMOC at the end of MIS6. The precise timing of AMOC strengthening and NADW ventilation increase is not directly depicted in the benthic $\delta^{13}C$ record because of data gaps related to low abundances of epibenthic foraminifera in the H11 sediment section. However, measurably increased $\delta^{13}C$ is not recorded until the onset of MIS5e. Such an AMOC development is consistent with our planktonic $\delta^{18}O$ and $SST_{Mg/Ca}$ records from ODP 976 that indicate T2 was prominently dominated by the presence in the northern North Atlantic of glacial-level SST and elevated levels of meltwater that were associated with the northern hemisphere H11 ice sheet collapse. Only once the H11 polar conditions ceased did NADW production rapidly increase but did not reach its full strength until well into MIS5e (Fig. 22D). This is different from the AMOC development during T1 that follows the two-step evolution of surface hydrology. The main difference between both terminations is that H1 was abruptly terminated by the B/A warm interval while the H11 event and associated meltwater flux spanned nearly the entire T2 without a clearly visible interruption.

Dating of marine sediment cores sections and determining the timing of climatic events beyond 50 ky or so is challenging because this is beyond the range of radiocarbon dating. Moreover, palaeoclimatic profiles from Greenland ice cores that are dated independently from ice layer counting and ice flow modelling are presently limited to the last 129 ky (NEEM community members, 2013) and are not available for age model transfer to marine profiles. This leaves us with orbital tuning and using H11 as a characteristic marker event in the North Atlantic for the synchronization of North Atlantic palaeoclimatic records (see Chapter "*Results*", Fig. 17) during the MIS6-T2-MIS5e period. The latitudinal migration of the polar front reached as far south as 40°N during Heinrich events (Bard et al., 1987, Abrantes et al., 1998; Eynaud et al., 2009; Naughton et al., 2009), imprinting substantial changes in sea surface hydrology on the Iberian Margin sites. The existence of ice-rafted debris (IRD) at the Iberian Margin provides unambiguous evidence of the incursion of polar conditions during episodes of major ice sheet melting (Eynaud et al., 2009). IRD presence from 127-133 ky in Iberian Margin core MD95-2039 (Fig. 23, Schönfeld et al., 2003) confirms prolonged Heinrich-like conditions across the full glacial-interglacial transition, further corroborating our interpretation of the ODP 976 planktonic $\delta^{18}O$ and $SST_{Mg/Ca}$ profiles. The lack of a distinct negative $\delta^{18}O$ meltwater signal in MD95-2039 alludes to the cold SST conditions as a mechanism to compensate the low- $\delta^{18}O$ freshwater imprint.

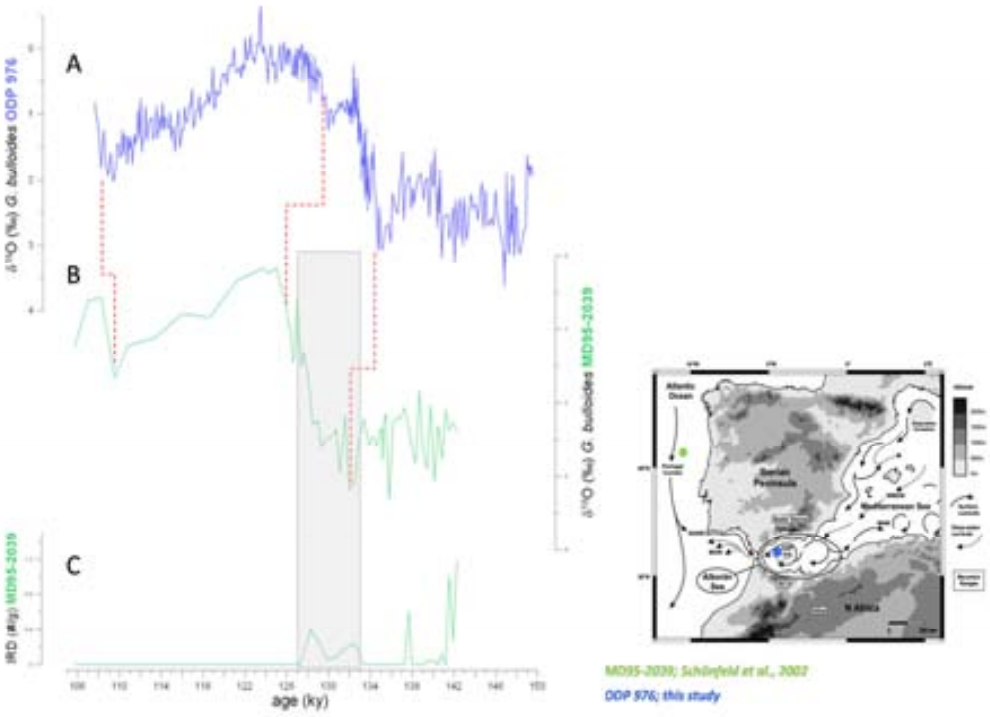

Figure 23. H11 at the Iberian Margin. (A) ODP 976 $\delta^{18}O$ *G. bulloides* (blue, this study). (B) MD95-2039 $\delta^{18}O$ *G. bulloides* (Schönfeld et al., 2003). (C) IRD concentration in MD95-2039 (Schönfeld et al., 2002). Grey shading highlights the H11 IRD event in MD95-2039. Red stippled lines indicate synchronization tie-points.

In the open North Atlantic, Hodell et al. (2008) observed a large IRD event centered at ~129 ky (Fig. 24) that was characterized by a coeval peak in Si/Sr and low bulk $\delta^{18}O$, coinciding with H11, described at other sites in the North Atlantic (Heinrich, 1988; McManus et al., 1994; Oppo et al., 2001, 2006). These characteristics are different from H1 sedimentology and geochemistry, alluding to different origins for H1 and H11. H1 was sourced in Hudson Strait (HS), was rich in detrital carbonate and characterized by a concomitant increase in Ca/Sr and a decrease in bulk $\delta^{18}O$; H11 was poor in biogenic carbonate but rich in silicate minerals, as revealed by coeval peaks of high Si/Sr, low Ca/Sr and bulk $\delta^{18}O$ (Hodell et al., 2008). Accordingly, H11 plausibly involved multiple ice sheets and contained substantial contributions from European ice sheets (Hodell et al., 2008).

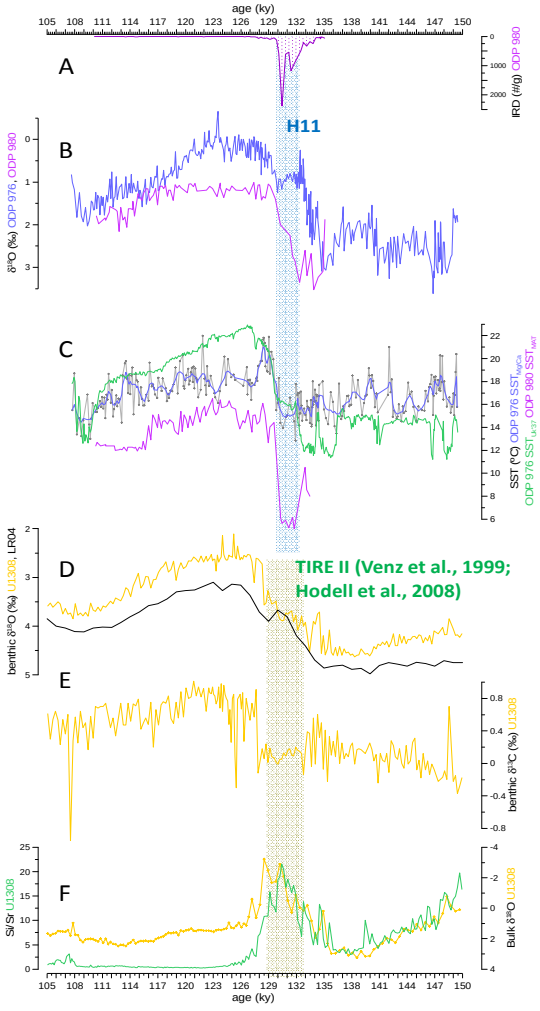

Figure 24. H11 at ODP 976 and North Atlantic reference records. (A) ODP 980 Ice Rafted Debris (IRD, lithics/g; McManus et al., 1999, 2002; Oppo et al., 2001, 2003, 2006). (B) Marine $\delta^{18}O$ records: ODP 976 (dark blue, this study); ODP 980 $\delta^{18}O$ *N. pachyderma (d)* (purple, McManus et al., 1999; Oppo et al., 2006; age model by Govin et al., 2012). (C) SST records. ODP 976 $SST_{Mg/Ca}$ (grey=unsmoothed, blue= smoothed); ODP 976 $SST_{UK'37}$ (green, Martrat et al., 2013, submitted); ODP 980 SST_{MAT} (purple, McManus et al., 1999; Oppo et al., 2006; age model by Govin et al., 2012). (D) Benthic $\delta^{18}O$ and (E) benthic $\delta^{13}C$ records: U1308 (yellow, Hodell et al., 2008); Global benthic $\delta^{18}O$ LR04 (black, Liesicki and Raymo, 2005). (F) U1308 bulk carbonate $\delta^{18}O$ (yellow) and Si/Sr (green), proxies for IRD: Si/Sr reflects layers poor in biogenic carbonate and rich in detrital silicate minerals. Bulk carbonate $\delta^{18}O$ reflects the relative proportion of biogenic and detrital carbonate (lithic-to-foraminifera ratio) (Hodell et al., 2008). The main features identified are indicated by colour shadings: Heinrich event 11 (blue, H11), which coincides with the Terminal Ice Rafted Event during T2 (TIRE II, yellow shading) (Venz et al., 1999; Hodell et al., 2008). Bottom: locations of North Atlantic sites.

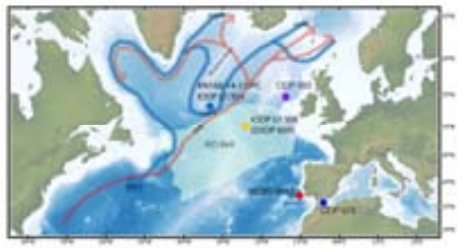

Evidence for a slowed AMOC at that time (Bauch et al., 2012; Hodell et al., 2008) confirms the same tight correlation between iceberg discharge and benthic $\delta^{13}C$ variability that is observed for the H events of the last glacial period, further corroborating the immediate coupling between freshwater fluxes to the North Atlantic from iceberg melting, lowered salinity and a weakening of the AMOC. As H11 comes to an end and meltwater fluxes cease the ODP 976 $SST_{Mg/Ca}$ record displays a rapid large-amplitude warming of 5-6°C to full interglacial levels that are reached immediately after 130 ky. Coeval with this dramatic change in surface ocean climatology incurs an abrupt increase of benthic $\delta^{13}C$ at Atlantic site U1308 (Fig. 24E) signifying the abrupt strengthening of the AMOC as H11 comes to an end. The delay between the abrupt warming and the abrupt benthic d13C increase is possibly an artifact of time scaling due to the lack of absolute dating in

this interval and therefore, the uncertainty in each of the own age scales in which the records are represented.

Heinrich events were also significant components of the low-latitude climates, suggesting they constituted large-scale perturbations that interacted with high and low latitude climatic regimes alike (Schulz et al., 1998; Kelly et al., 2006). Absolute dated speleothem records from Hulu and Dongge caves in China of Asian palaeo-monsoon activity highlight the impact of North Atlantic H events on the weakening of summer monsoons (Wang et al., 2001; Yuan et al., 2004; Kelly et al., 2006; Cheng et al., 2006). A ~6 ky period of prolonged monsoon failure is documented in the Dongge Cave speleothem record, the so-called Weak Monsoon Interval (WMI) during T2 (135.5 and 129 ky) (Fig. 25F, right panel). Based on correlations with both marine ice-rafted debris and atmospheric CH_4 records, Cheng et al. (2006) demonstrated that most of the WMI coincided with T2. According to our ODP976 palaeo-records this was a period when the northern North Atlantic experienced severe cold conditions in conjunction with the terminal MIS6 ice sheet collapse, as is independently confirm by the close correlation of the anomalous $\delta^{18}O$ and $SST_{Mg/Ca}$ structure during T2 in the ODP976 records with the timing and extent of H11 at core sites in the open North Atlantic (Kelly et al., 2006; Cheng et al., 2006) (Fig. 25, blue shading).

Oxygen isotope stratigraphy (Shackleton, 1969, Sánchez Goñi et al., 1999; Shackleton et al., 2002, 2003) defines the MIS6/5 stage boundary as the mid-point of the benthic $\delta^{18}O$ transition of T2. H11 in the ODP 976 $\delta^{18}O$ record spans across the T2 mid-point suggesting that the main ice sheet melting and concomitant fresh water surging persisted across the MIS6/5 boundary without interruption. During T1 instead, the MIS2/1 boundary coincides with the sharp onset of the B/A warm interval that terminated H1 and coincided with substantial AMOC strengthening (Fig. 22). The planktonic $\delta^{18}O$ profile displays a similar structure during T1 and T2, albeit at different magnitudes and relative timing, suggesting a similar sequence of events and a similar dynamics of both terminations (Fig. 25). Following the massive H11 meltwater interval that is indicated in the negative $\delta^{18}O$ "hump" during T2 (Fig. 25C, blue shading), $SST_{Mg/Ca}$ increase steeply reaching a thermal maximum at 129 ky (Fig. 25D, orange arrow and shading) before decreasing again at 128 ky (Fig. 25D, green arrow and stippled shading). This sequence resembles that occurring during T1: following H11, a warming interval event takes place (B/A warm interval in T1), later interrupted by

a cold reversal (YD event in T1) before climate finally reaches full-interglacial conditions. Two alternative scenarios are suggested.

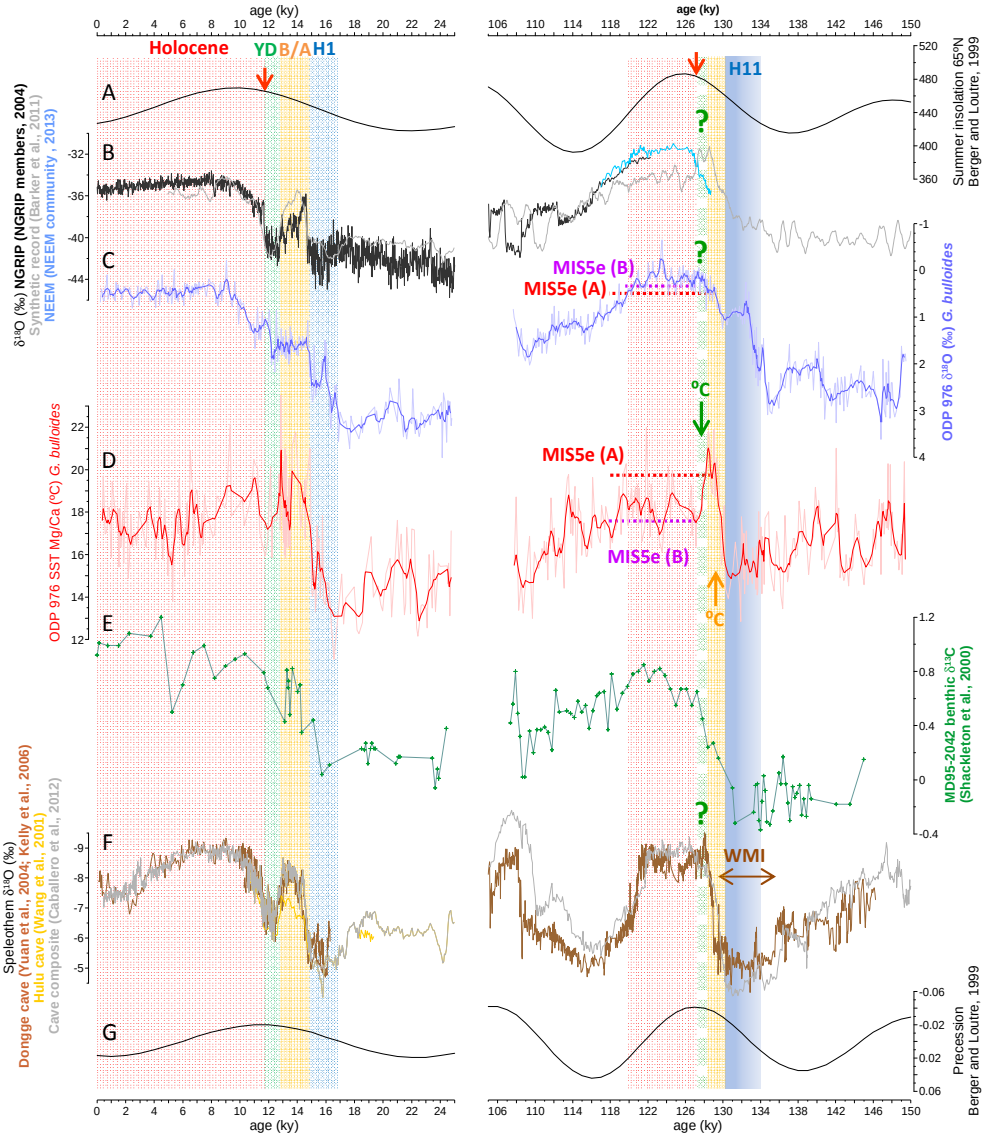

Figure 25. Left panel: MIS2-T1-Holocene period. Right panel: MIS6-T2-MIS5e period. (A) Summer insolation at 65ºN (Berger and Loutre, 1999). (B) Greenland ice core $\delta^{18}O$ records: NGRIP (black, NGRIP members, 2004) on the AICC2012 age model (Bazin et al., 2013; Veres et al., 2013), synthetic record (light grey, Barker et al., 2011) and NEEM (dark blue, NEEM community, 2013). (C) ODP 976 $\delta^{18}O$ *G. bulloides* record (blue, this study). (E) ODP 976 $SST_{Mg/Ca}$ record (pink=individual datapoints, red=5pt-smoothed record, this study). (E) MD95-2042 benthic $\delta^{13}C$ record (Shackleton et al., 2000). For the MIS2-T1-Holocene period, MD95-2042 age model is the original by Shackleton et al. (2000). For the MIS6-T2-MIS5e period, MD95-2042 age model is synchronized to the ODP 976 age model (Fig. 22). (F) Asian monsoon records: Dongge Cave $\delta^{18}O$ record (brown, Yuan et al., 2004; Kelly et al., 2006); Hulu cave (yellow, Wang et al., 2001); Cave composite record (grey, Caballero-Gill et al., 2012). (G) Precession parameter (Berger and Loutre, 1999). Left panel: vertical coloured bars indicate Heinrich event (blue, H1), Bölling/Allerod (orange, B/A) warm interval, Younger Dryas (green, YD) and the Holocene (red). Right panel: vertical coloured bars indicate H11 and precursor previous H-events (dark to light blue bar, H11), the warming overshoot interval (orange), the following SST decrease (green stippled bar), the onset of MIS5e in scenario A (red stippled horizontal line) and scenario B (purple stippled horizontal line) and the Weak Monsoon Interval (brown, WMI).

In a first scenario A, T2 (135-129 ky) mostly consists of a massive multiple Heinrich event, containing the main H11 event and ending with the abrupt warming to peak SST (Fig. 25C, D, red stippled line "MIS5e (A)") at 129 ky. In this first scenario, the warming "overshoot" at the end of T2 and the subsequent SST decrease occur during early MIS5e. However, if we place the onset of the MIS5e in the summer insolation record at a position similar to that at the onset of the Holocene (Fig. 25A, red arrow), an alternative scenario B emerges. MIS5e in this scenario starts at 127 ky (Fig. 25C, D, purple stippled line "MIS5e (B)"), and the SST maximum at 129 ky is part of T2; in this scenario the sequence of events during T2 closely resembles that of T1 in that the SST maximum at 129 ky would be the T2 analogue of the B/A interval during T1. However, it must be noticed that the B/A $\delta^{18}O$ levels remain at intermediate levels of the full glacial-interglacial transition, while during T2 the $\delta^{18}O$ values that are associated with the SST maximum are near full-interglacial values. The subsequent SST decrease (Fig. 25, green stippled shading) may then be viewed as a T2-analogue of the YD, but there is no imprint of the cold event in the ODP 976 $\delta^{18}O$ record or in the Asian monsoon $\delta^{18}O$ record.

Viewed in combination, the onset of the meltwater-induced $\delta^{18}O$ decrease at 135 ky at ODP 976 and the late cessation of H11 immediately before the end of T2 indicates that the penultimate glacial-interglacial transition was almost entirely controlled by a single massive meltwater surge that was coincident with H11 or that embedded the main H11 event in it. Following H11, an uninterrupted rapid warming reaches the full interglacial conditions at 129 ky, synchronously to the establishment of interglacial flora, as shown by ODP976 (see Discussion Chapter 1: "*ODP 976 and Alboran Sea palaeoclimatology during the last two deglaciations*"**,** Fig. 18F, Combourieu-Nebout et al., in prep.), MD95-2042 (Shackleton et al., 2003; Sánchez Goñi et al., 2012) and MD01-2444 (Tzedakis, 2013, pers. comm.), suggesting an in-phase onset of the interglacial period regarding both terrestrial and marine environments, suggesting that both terrestrial and marine environments entered interglacial conditions synchronously at 129 ky (Fig. 26).

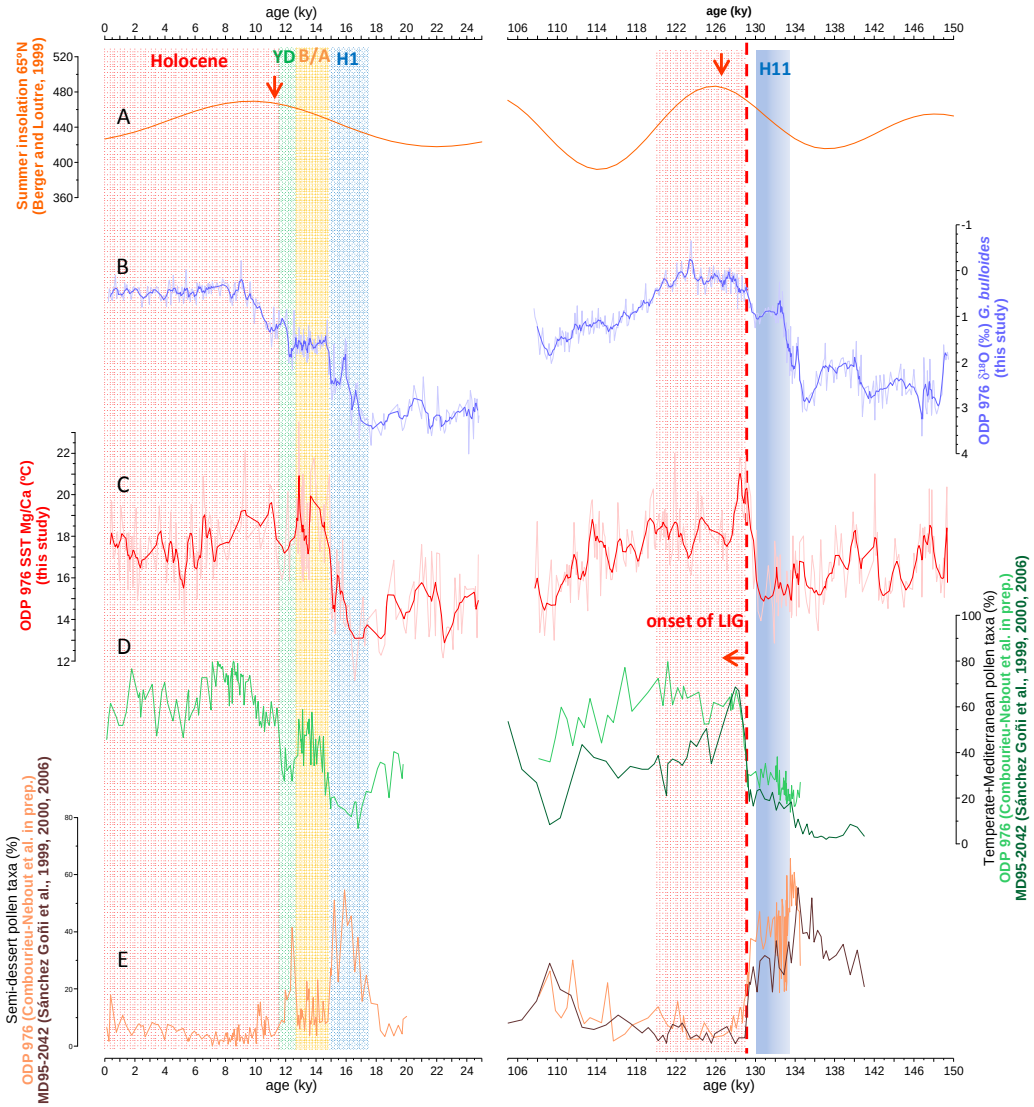

Figure 26. Left panel: MIS2-T1-Holocene sequence. Right panel: MIS6-T2-MIS5e sequence. (A) Summer insolation at 65ºN (orange; Berger and Loutre, 1999). (B) ODP 976 $\delta^{18}O$ *G. bulloides* record (blue, this study). (C) ODP 976 $SST_{Mg/Ca}$ record (pink=unsmoothed, red=5pt-smoothed, this study). (D) Temperate and Mediterranean forest and (D) semi-desert taxa: ODP 976 (light green (D) and light brown (E), Combourieu-Nebout, et al., 2002, 2009 and unpublished data; Masson-Delmotte et al., 2005) and MD95-2042 (dark green (D) and dark brown (E), Sánchez Goñi et al., 1999, 2000, 2006) on the age scale of Sánchez Goñi et al., 2012. Vertical coloured bars indicate (left panel) Heinrich event (blue, H1), Bölling/Allerod (orange, B/A) warm interval, Younger Dryas (green, YD) and the Holocene (red); (right panel) H11 and precursor previous H-events (dark to light blue bar, H11) and the onset of full interglacial conditions (red shading) based on the establishment of interglacial flora. Red arrows indicate the summer insolation state at the onset of the Holocene, and during the MIS6-T2-MIS5e period. This analogy was used to define the onset of MIS5e.

A weak AMOC until the end of H11 coupled to the massive iceberg discharge events in the North Atlantic (Fig. 22, 24) is consistent with a reduced intensity of Atlantic Ocean heat transfer towards the Arctic characterizing MIS5e (Bauch et al., 2012, 2013), therefore accumulating heat at mid-northern latitudes instead, explaining the warmer-than Holocene air-sea temperatures reconstructed for the NE Atlantic sector and Western Europe (Bauch et al., 2011). Recent modeling results incorporating proxy-based reconstructions show maximum Greenland Ice Sheet (GIS) melting and a weaker AMOC during strongest warming in Western Europe of MIS5e (Sánchez Goñi et al., 2012). This contrasts with the view of European cooling being associated with increased freshwater input to the North Atlantic that caused the AMOC to slow down (Swingedou, 2007; Stouffer et al., 2006). The model simulations indeed suggest that the GIS meltwater runoff inhibited deep water convection off the southern coast of Greenland and led to a cooling at a local scale in response to 24% reduction of the AMOC. However, deep water convection in the Nordic Seas was not perturbed which left the poleward marine heat transport and temperatures in Europe unperturbed (Sánchez Goñi et al., 2012). Switches in the North Atlantic subpolar gyre (SPG) extent and circulation may explain some of the spatial heterogeneity in this region, given its importance as a primary control of surface inflow into the Nordic Seas and influencing the state of the AMOC (Irvali et al., 2012; Chapman et al., pers. comm., 2013). An enhanced freshwater flux into the SPG through the East Greenland current (EGC) weakens the SPG circulation and therefore, decreases the westward transportation of warm and saline waters in the Irminger Current (IC), hence acting as a positive feedback driving further cooling and freshening in the region (Born et al., 2011; Irvali et al., 2012). But also, a weakened SPG would allow warmer subtropical water to enter the Nordic Seas (Hátún et al., 2005) thereby warming the eastern Nordic Seas while cooling the region off South Greenland. A recent study by Chapman et al. (2013) uses $SST_{Mg/Ca}$ and $\delta^{18}O$ records of cores U1305 (57°29'N, 48°32'W, Labrador Sea) and MD99-2253 (56°22'N, 27°49'W, at the eastern edge of the North Atlantic SPG) and shows a contracted SPG almost exclusively restricted to the west of the Mid-Atlantic Ridge during MIS5e suggesting enhanced melting of the Greenland ice sheet due to the advection of saline and warm subtropical waters into the Irminger Basin, the northern Labrador Sea and Baffin Bay, which lead to a warming of the northwestern sub-arctic seas.

The $SST_{Mg/Ca}$ and $\delta^{18}O$ records of cores U1305 and MD99-2253 are similar in structure during T2 and MIS5e to our records from ODP976. This agreement supports ODP 976 records closely

reconstructing North Atlantic climate variability at centennial to multi-decadal timescales, not only beyond the Alboran Sea and the Iberian margin, but also reflecting surface hydrology signals also recorded in northern North Atlantic.

References:

Abrantes, F., Baas, J., Haflidason, H., Rasmussen, T., Klitgaard, D., Loncaric, N., and Gaspar, L. (1998) "Sediment fluxes along the northeastern European Margin: inferring hydrological changes between 20 and 8 kyr." Marine geology, 152(1), 7-23.

Arbuszawski, J., deMenocal, P., Kaplan, A. and Farmer, E. C. (2010) "On the fidelity of shell-derived $\delta^{18}O_{seawater}$ estimates." Earth and Planetary Sciences 200:185-196.

Bard, E., Arnold, M., Maurice, P., Duprat, J., Moyes, J., and Duplessy, J. C. (1987) "Retreat velocity of the North Atlantic polar front during the last deglaciation determined by 14 C accelerator mass spectrometry." Nature,328(6133), 791-794.

Barker, S., G. Knorr et al. (2011). "800,000 years of abrupt climate variability." Science 334(6054):347.

Bazin, L., Landais, A., Lemieux-Dudon, B., Toy«e Mahamadou Kele, H., Veres, D., Parrenin, F., Martinerie, P., Ritz, C., Capron, E., Lipenkov, V., Loutre, M.-F., Raynaud, D., Vinther, B., Svensson, A., Rasmussen, S., Severi, M., Blunier, T., Leuenberger, M., Fischer, H., Masson-Delmotte, V., Chappellaz, J., and Wolff, E. (2013) "An optimized multi-proxies, multi-site Antarctic ice and gas orbital chronology (AICC2012): 120-800 ka." Climate of the Past 9(4):1715-1731.

Bauch, H. A., Kandiano, E. S., Helmke, J., Andersen, N., Rosell-Mele, A., and Erlenkeuser, H. (2011) "Climatic bisection of the last interglacial warm period in the Polar North Atlantic." Quaternary Science Reviews, 30(15), 1813-1818.

Bauch, H. A., Kandiano, E. S. and Helmke, J. P. (2012) "Contrasting ocean changes between the subpolar and polar North Atlantic during the past 135 ka." Geophysical Research Letters 39.

Bauch, H. A. (2013) "Interglacial climates and the Atlantic meridional overturning circulation: is there an Arctic controversy?" Quaternary Science Reviews, 63, 1-22.

Born, A., Nisancioglu, K. H., and Risebrobakken, B. (2011) "Late Eemian warming in the Nordic Seas as seen in proxy data and climate models." Paleoceanography, 26(2).

Boussetta, S., Bassinot, F., Sabbatini, A., Caillon, N., Nouet, J., Kallel, N., Rebaubier, H., Klinkhammer, G. and Labeyrie, L., (2011) "Diagenetic Mg-rich calcite in Mediterranean sediments: Quantification and impact on foraminiferal Mg/Ca thermometry." Marine Geology. 280, 195-204.

Caballero-Gill, R. P., Clemens, S. C., and Prell, W. L. (2012) "Direct correlation of Chinese speleothem $\delta^{18}O$ and South China Sea planktonic $\delta^{18}O$: Transferring a speleothem chronology to the benthic marine chronology." Paleoceanography,27(2).

Cacho, I. (1999)."Dansgaard-Oeschger and Heinrich event imprints in the Alboran Sea paleotemperatures." Paleoceanography 14:698.

Cacho, I., J. O. Grimalt, et al. (2001) "Variability of the western Mediterranean Sea surface temeprature during the last 25,000 years and its connection with the Northern Hemisphere Climatic changes." Paleoceanography 16(1):40.

Chapman, M., Middle, L., Farmer, E. and Hillaire-Marcel, C. (2013) "Reduced Subpolar Gyre Circulation in the North Atlantic during the Last Interglacial." 11th International Conference on Paleoceanography.

Cheng, H., Edwards, R. L., Wang, Y., Kong, X., Ming, Y., Kelly, M. J. and Liu, W. (2006) "A penultimate glacial monsoon record from Hulu Cave and two-phase glacial terminations." Geology, 34(3), 217-220.

Eynaud, F., de Abreu, L., Voelker, A., Schönfeld, J., Salgueiro, E., Turon, J. L. Penaud, A., Toucanne, S, Naughton, F. (2009) "Position of the polar front along the western Iberian marign during key cold episodes of the last 45 ky." Geochemistry, Geophysics, Geosystems 10(7):1525-2027.

Ferguson, J.E., Henderson, G.M., Kucera, M. and Rickaby, R.E.M., (2008) "Systematic change of foraminiferal Mg/Ca ratios across a strong salinity gradient." Earth and Planetary Science Letters 265, 153–166,

Govin, A., Braconnot, P., Capron, Em., Cortijo, E., Duplessy, J. C., Jansen, E., Labeyrie, L., Landais, A., Marti, O., Michel, E., Mosquet, E., Risebrobakken, B., Swingedouw, D. and Waelbroeck, C. (2012) "Persistent influence of ice sheet melting on high northern latitude climate during the early Last Interglacial." Climate of the Past 8:483-507.

Hátún, H., Sandø, A. B., Drange, H., Hansen, B. and Valdimarsson, H. (2005) "Influence of the Atlantic subpolar gyre on the thermohaline circulation." Science,309(5742), 1841-1844.

Heinrich, H. (1988) "Origin and consequences of cyclic ice rafting in the Northeast Atlantic Ocean during the past 130,000 years." Quaternary Research 29:142-152.

Hodell, D. A., Channell, J. E., Curtis, J. H., Romero, O. E., and Röhl, U. (2008) "Onset of "Hudson Strait" Heinrich events in the eastern North Atlantic at the end of the middle Pleistocene transition (~ 640 ka)?." Paleoceanography, 23(4).

Hodell, D., Crowhurst, S., Skinner, L., Tzedakis, P. C., Margari, V., Channell, J. E. T., Kamenov, G., Maclachlan, S. and Rothwell, G. (2013) "Response of the Iberian Margin sediments to orbital and suborbital forcing over the past 420 ka." Paleoceanography 28:185-199.

Irvali, N., Ninnemann, U. S., Galaasen, E. V., Rosenthal, Y., Kroon, D., Oppo, D. W., Kleiven, H. F., Darling, K. F. and Kissel, C. (2012) "Rapid switches in subpolar North Atlantic hydrography and climate during the Last Interglacial (MIS5e)." Paleoceanography 27.

Kelly, M. J., Lawrence Edwards, R., Cheng, H., Yuan, D., Cai, Y., Zhang, M., Lin, Y. and An, Z. "High resolution characterization of the Asian Monsoon between 146,000 and 99,000 years B.P. from Dongge Cave, China and global correlation of events surrounding Termination II." Paleaeogeography, Palaeoclimatology, Palaeoecology 236:20-38.

Lisiecki, L. E., and Raymo, M. E. (2005) "A Pliocene-Pleistocene stack of 57 globally distributed benthic δ18O records." Paleoceanography, 20(1).

Martrat, B., J. O. Grimalt, et al. (2004) "Abrupt Temperature Changes in the Western Mediterranean over the past 250,000 years." Science 306 (5702):1762.

Martrat, B., Grimalt, J. O., Shackleton, N. J., de Abreu, L., Hutterli, M. A. and Stocker, T. F. (2007) "Four climate cycles of recurring deep and surface water destabilizations on the Iberian Margin." Science, vol. 317 (502), doi: 10.1126/science.1139994.

McManus, J. F., Bond, G. C., Broecker, W. S., Johnsen, S., Labeyrie, L. and Higgins, S. (1994) "High-resolution climate records from the North Atlantic during the last interglacial." Nature 371:326-329.

McManus, J. F., Oppo, D. W. and Cullen, J. L. (1999) "A 0.5-million-year record of millennial-scale climate variability in the North Atlantic." Science 283:971-975.

McManus, J. F., Oppo, D. W., Keigwin, L. D., Cullen, J. L., & Bond, G. C. (2002) "Thermohaline circulation and prolonged interglacial warmth in the North Atlantic." Quaternary Research, 58(1), 17-21.

Masson-Delmotte, V., Landais, A., Combourieu-Nebout, N., von Grafenstein, U., Jouzel, J., Caillon, N., Chappellaz, J., Dahl-Jensen, D., Johnsen, S. J. and Stenni, B. (2005) "Rapid climate variability during warm and cold periods in polar regions and Europe." Geoscience 337:935-946.

Naughton, F., Sánchez Goñi, M. F., Kageyama, M., Bard, E., Duprat, J., Cortijo, E., Desprat, S., Malaizé, B., Joly, C., Rostek, F. and Turon, J. L. (2009) "Wet to dry trend in north-western Iberia within Heinrich events." Earth and Planetary Science Letters 284:329-342.

NEEM community members (2013) "Eemian interglacial reconstructed from a Greenland folded ice core." Nature, vol. 493:489-494, doi:10.1038/nature11789.

North Greenland Ice Core Project (2004). Nature 431(7005):147-151.

Oppo, D. W., Keigwin, L. D., McManus, J. F., and Cullen, J. L. (2001) "Persistent suborbital climate variability in marine isotope stage 5 and Termination II.Paleoceanography," 16(3), 280-292.

Oppo, D. W., McManus, J. F., and Cullen, J. L. (2003) "Palaeo-oceanography: Deepwater variability in the Holocene epoch." Nature, 422(6929), 277-277.

Oppo, D. W., McManus, J. F. and Cullen, J. L. (2006) "Evolution and demise of the Last Interglacial warmth in the subpolar North Atlantic." Quaternary Science Reviews 25:3268-3277.

Ruddiman, W. F. and McIntyre, A. (1981) "The North Atlantic Ocean during the last deglaciation." Palaeogeography, Palaeoclimatoogy, Palaeoecology 35:145-214.

Sánchez Goñi, M. F., Eynaud, F., Turon, J. L. and Shackleton, N. J. (1999) "High resolution palynological record off the Iberian margin: direct land-sea correlation for the Last Interglacial complex." Earth and Planetary Science Letters 171:123-137.

Sánchez Goñi, M. F., Landais, A., Fletcher, W. J., Naughton, F., Desprat, S. and Duprat, J. (2008) "Contrasting impacts of Dansgaard-Oeschger events over a western European latitudinal transect modulated by orbital parameters." Quaternary Science Reviews 27:1136-1151.

Sánchez Goñi, M. F., Bakker, P., Desprat, S., Carlson, A. E., van Meerbeeck, C. J., Peyron, O., Naughton, F., Fletcher, W. J., Eynaud, F., Rossignol, L. and Renssen, H. (2012) "European climate optimum and enhanced Greenland melt during the Last Interglacial." Geology, vol. 40(7):627-630.

Shackleton, N. J. and Hall, M. A. and Vincent, E. (2000) "Phase relationships between millennial-scale events 64,000-24,000 years ago. Paleoceanography, vol. 15(6):565-569.

Shackleton, N. J., Sánchez Goñi, M. F., Pailler, D. and Lancelot, Y. (2003) "Marine Isotope Substage 5e and the Eemian Interglacial." Global and Planetary Change (36):151-155.

Shackleton, N. J., Fairbanks, R. G., Chiu, T. and Parrenin, F. (2004) "Absolute calibration of the Greenland time scale: implications for Antarctic time scales and for Δ^{14}C." Quaternary Science Reviews 23:1513-1522.

Schönfeld, J., Zahn, R. and Abreu, L. (2003) "Surface and deep water response to rapid climate changes at the Western Iberian Margin." Global and Planetary Change 36(4):237-264.

Schulz, H., von Rad, U. and Erlenkeuser, H. (1998) "Correlation between Arabian Sea and Greenland climate oscillations of the past 110,000 years." Nature 393:54-57.

Skinner, L. (2003) "Millennial climate change in the northeast Atlantic: The role of surface and deep hydrographic change determined by stable isotope geochemistry and Mg/Ca palaeothermometry." Doctoral Thesis, University of Cambridge, 142pp.

Skinner, L. C. and Elderfield, H. (2007) "Rapid fluctuations in the deep North Atlantic heat budget during the last deglaciation." Paleoceanography 22.

Stouffer, R. J., Yin, J., Gregory, J. M., Dixon, K. W., Spelman, M. J., Hurlin, W., and Weber, S. L. (2006) "Investigating the causes of the response of the thermohaline circulation to past and future climate changes." Journal of Climate,19(8), 1365-1387.

Swingedouw, D. (2007). "Decrease in the Atlantic overturning does not significantly impact oceanic CO 2 uptake over century timescales." In Geophysical Research Abstracts (Vol. 9, p. 01632).

Tzedakis, P. C. (2007) "Seven ambiguities in the Mediterranean palaeoenvironmental narrative." Quaternary Science Reviews 26:2042-2066.

Tzedakis, P. C. (September, 2013) "A stratigraphical 'Rosetta Stone' from the Portuguese Margin." Oral presentation, ICP11, International Conference on Paleoceanograpgy.

van Raden, U. J., Groeneveld, J., Raitzsch, M., Kucera, M., (2011) "Mg/Ca in the planktonic foraminifera Globorotalia inflata and Globigerinoides bulloides from Western Mediterranean plankton tow and core top samples." Marine Micropaleontology. 78, 101-112.

Venz, K. A., Hodell, D. A., Stanton, C., and Warnke, D. A. (1999) "A 1.0 Myr record of Glacial North Atlantic Intermediate Water variability from ODP site 982 in the northeast Atlantic." Paleoceanography, 14(1), 42-52.

Veres, D., Bazin, L., Landais, A., Lemieux-Dudon, B., Parrenin, F., Martinerie, P., Toy«e Mahamadou Kele, H., Capron, E., Chappellaz, J., Rasmussen, S., Severi, M., Svensson, A., Vinther, B., and Wolff, E. "The Antarctic ice core chronology (AICC2012): an optimized multi-parameter and multi-site dating approach for the last 120 thousand years." Climate of the Past.9(4).

Voelker, A. H. L., Lebreiro, S. M., Schönfeld, J., Cacho, I., Erlenkeuser, H. and Abrantes, F. (2006) "Mediterranean outflow strengthening during northern hemisphere coolings: A salt source fr the glacial Atlantic?." Earth and Planetary Science Letters 245:39-55.

Voelker, A. H. L. and de Abreu, L. (2011) "A review of abrupt climate change events in the Northeastern Atlantic Ocean (Iberian margin): latitudinal, longitudinal and vertical gradients." Geophysical Monograph Series 193:15-37.

Wang, Y.J., Cheng, H., Edwards, R.L., An, Z.S.,Wu, J.Y., Shen, C.-C. and Dorale, J.A., (2001) "A high-resolution absolute-dated Late Pleistocene monsoon record from Hulu Cave, China." Science 294, 2345–2348.

Yuan, D., Cheng, H., Edwards, R.L., Dykoski, C.A., Kelly, M.J., Zhang, M., Qing, J., Lin, Y.,Wang, Y.,Wu, J., Dorale, J.A., An, Z., Cai, and Y., (2004) "Timing, duration, and transitions of the Last Interglacial Asian Monsoon." Science 304, 575–578.

Chapter 3 - ODP 976 Mg/Ca record and speleothem $\delta^{18}O$ records.

The difficulty to absolutely date marine sediment records beyond the limits of radiocarbon methods complicates precise determination of the timing of climatic events during the MIS6-T2-MIS5e sequence, including the correlation of continental, marine and ice core records (Tzedakis et al., 1997; Sánchez Goñi et al., 1999; Shackleton et al., 2003). Speleothems (crystalline $CaCO_3$ deposits formed in caves) offer an indirect solution of this problem because of the following two main reasons: firstly, if collected in the right settings they are highly sensitive to climate and record climate signals at very fine detail (McDermott, 2004) and secondly, they can be absolutely dated by ^{230}Th-^{234}U analysis using multi-collector inductively coupled plasma mass spectrometry (Hellstrom, 2003). Recent studies improved considerably the understanding of the processes forming the isotopic signals recorded in speleothems and provided a suite of absolute dated palaeo-climatic records across Europe and the Mediterranean borderlands (Bard et al., 2002; Bar-Matthews et al., 2003; Genty et al., 2003; Couchoud et al., 2009; Drysdale et al., 2004, 2005, 2007, 2009).

Stable oxygen isotope records of stalagmites recovered from the Antro del Corchia Cave in Tuscany, Italy, and the Bourgeois-Delaunay Cave at La Chaise de Vouthon (BD-La Chaise), France, provide reference records of palaeo-climate and notably, palaeo-rainfall patterns in those regions (Fig. 27) (Couchoud et al., 2009; Drysdale et al., 2004, 2005, 2007; McDermott, 2004; Zanchetta et al., 2007). Importantly, the timing along both speleothems of $\delta^{18}O$ changes closely agrees, and these changes directly co-vary with SST changes in the western Mediterranean Sea and the Northeast Atlantic (Couchoud et al., 2009; Drysdale et al., 2009). The remarkable correspondence between the rainfall amount (inferred from stalagmite $\delta^{18}O$) and regional sea surface temperatures suggested by Drysdale et al. (2009) was highlighted using an "Iberian-margin stack" of benthic $\delta^{18}O$ and $SST_{Uk'37}$ records that were put on a common time scale by tuning the palaeo-records (core MD01-2444, Skinner and Shackleton (2006); core MD95-2042, Sánchez Goñi et al. (1999); Shackleton et al., 2003; Pailler and Bard (2002)) to the ODP 977 chronology of Martrat et al. (2004, 2007). Three humid phases, indicated by low $\delta^{18}O$ values in the last interglacial sections of the speleothems, were shown to be synchronous to western Mediterranean Sea warm

intervals. Comparing the structure of the two speleothem $\delta^{18}O$ records with the $SST_{Mg/Ca}$ record of ODP976 confirms the coupling of rainfall in southern Europe and higher SST in the western Mediterranean. This marine-atmosphere coupling allows us to use the speleothem records as reference for correlation with the ODP976 $SST_{Mg/Ca}$ record and to transfer the U/Th dated speleothem age scale to the ODP976 marine record (Fig. 27).

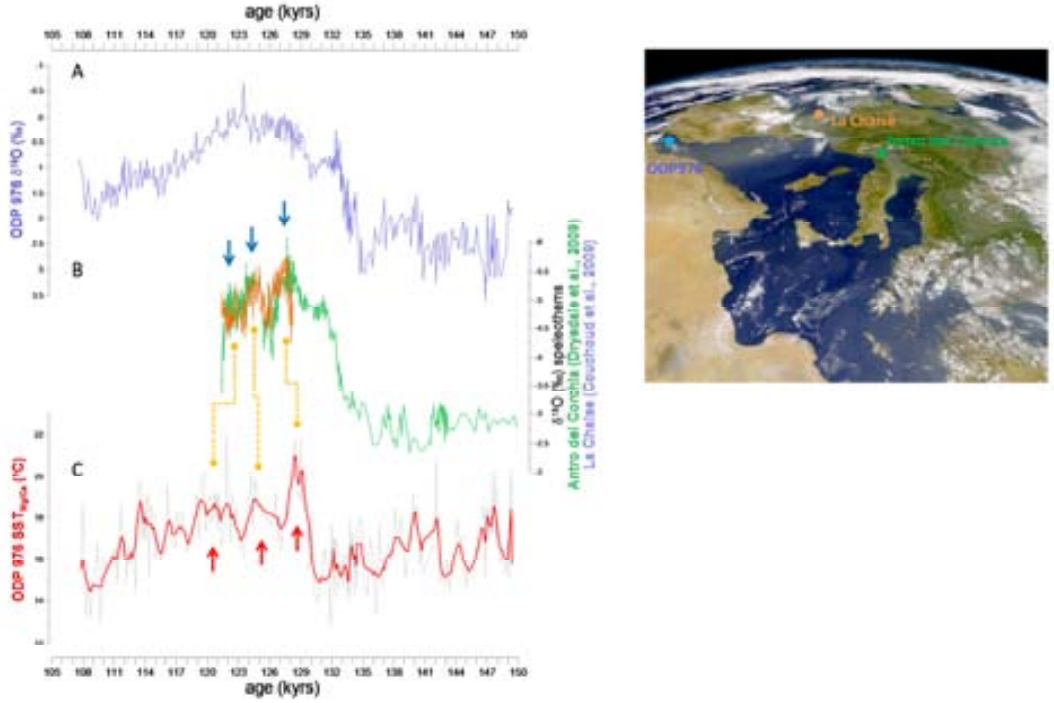

Figure 27. ODP 976 and correlation with European speleothems (A) ODP 976 $\delta^{18}O$ record (blue, this study). (B) European speleothem $\delta^{18}O$ profiles: Antro del Corchia, Italy (green, Drysdale et al., 2009) and BD-La Chaise, France (orange, Couchoud et al., 2009). (C) ODP 976 $SST_{Mg/Ca}$ (grey=unsmoothed; red=5pt smoothed, this study). Three humid phases, indicated by low $\delta^{18}O$ values (blue arrows) in the last interglacial sections of the speleothems are suggested to be synchronous with warm $SST_{Mg/Ca}$ intervals at ODP976 (red arrows). Yellow stippled lines indicate tie-points suggested for synchronization of these features. Right panel: location of ODP976 and speleothem sites. For a detailed discussion see text and Figure 29.

The ODP976 $SST_{Mg/Ca}$ record reflects the temperature of North Atlantic surface water entering the Alboran Sea and therefore, the profile documents the evolution of North Atlantic climatology. The close correspondence of $\delta^{18}O$ variation along the stalagmite profiles with SST demonstrates the impact of variable warm-water transport to the North Atlantic from the tropics, driven by the AMOC, and its subsequent advection to the Mediterranean Sea that stimulates atmospheric

convection and moist air transport with the prevailing westerly winds which ultimately drives the rainfall patterns over the Mediterranean borderlands (Drysdale et al., 2004, 2005, 2009). An atmospheric connection between the North Atlantic and the western Mediterranean is provided by the North Atlantic Oscillation (NAO) (Hurrell, 1995; Trigo et al., 2002; Krichak and Alpert, 2005; Giorgi and Lionello, 2008): A negative NAO phase results in a more zonal trajectory of North Atlantic low pressure systems that predominantly enter the Mediterranean region and cause above-normal rainfall and humidity there. This condition favours higher rainfall amounts in the region of the Antro del Corchia and BD-La Chaise caves, resulting in lower $\delta^{18}O$ values in the speleothem record. Antro del Corchia receives most of its recharge rainfall via westerly air masses crossing the North Atlantic (Drysdale et al., 2004) and the amplitude of $\delta^{18}O$ change in the speleothem record is thought to directly reflect the degree of $\delta^{18}O$ depletion of North Atlantic-sourced vapour in comparison to vapour from the western Mediterranean (Celle-Jeanton et al., 2001). Under glacial climatic conditions when a weaker AMOC results in a southward shift of the North Atlantic polar front, mid-latitude air temperatures are low, as are evaporation and moisture transport, hence causing the amount of rainfall to be low reaching the two cave sites in southern France and northern Italy which ultimately results in positive $\delta^{18}O$ signals in the speleothem records.

The ocean-atmosphere teleconnection reaches beyond the North Atlantic–Mediterranean climatic coupling. Several climatological studies demonstrate that Mediterranean climates and the Asian monsoon regime are tightly linked (Rodwell and Hoskins, 2001; Eshel, 2002; Alpert et al., 2006). The Asian monsoon regime transports heat and moisture from the warmest part of the tropical ocean namely, the West Pacific Warm Pool, to northern mid-latitudes. This meridional feature is modulated by high northern latitude climate variability, as is demonstrated by the direct correlation between weak (strong) summer monsoon with cold (warm) North Atlantic climatology (Schulz et al., 1999; Gupta et al., 2003). The structure of oxygen isotope records from Hulu Cave (China) closely resembles that of oxygen isotope records from Greenland ice cores. Wang et al. (2001) demonstrated a connection between millennial-scale weak (strong) Asian monsoon events and Greenland Stadials (Interstadials) in the GISP2 ice core record, suggesting that the intensity of the Asian monsoons varied synchronously with the palaeo-temperature record of Greenland, hence North Atlantic climate (Wang et al., 2001; Yuan et al., 2004) (Fig. 28). This coupling

demonstrates that the linking of North Atlantic climate with the Asian monsoon system is a robust feature of global climate (Gupta et al., 2003). A connection with North Atlantic climatology is underscored by recent studies that demonstrate a temporal coincidence between past intensification of the Indian summer monsoon (ISM, part of the Asian monsoon) and the onset of the B/A warming period that was driven by AMOC-induced warming of the North Atlantic area (Sinha et al., 2005; Kessarkar et al., 2013). Sánchez Goñi et al. (2008) likewise observed similarities between Mediterranean palaeoclimatic and Asian monsoon records during the last glacial period, suggesting an atmospheric teleconnection between the two regions comparable to the one existing today.

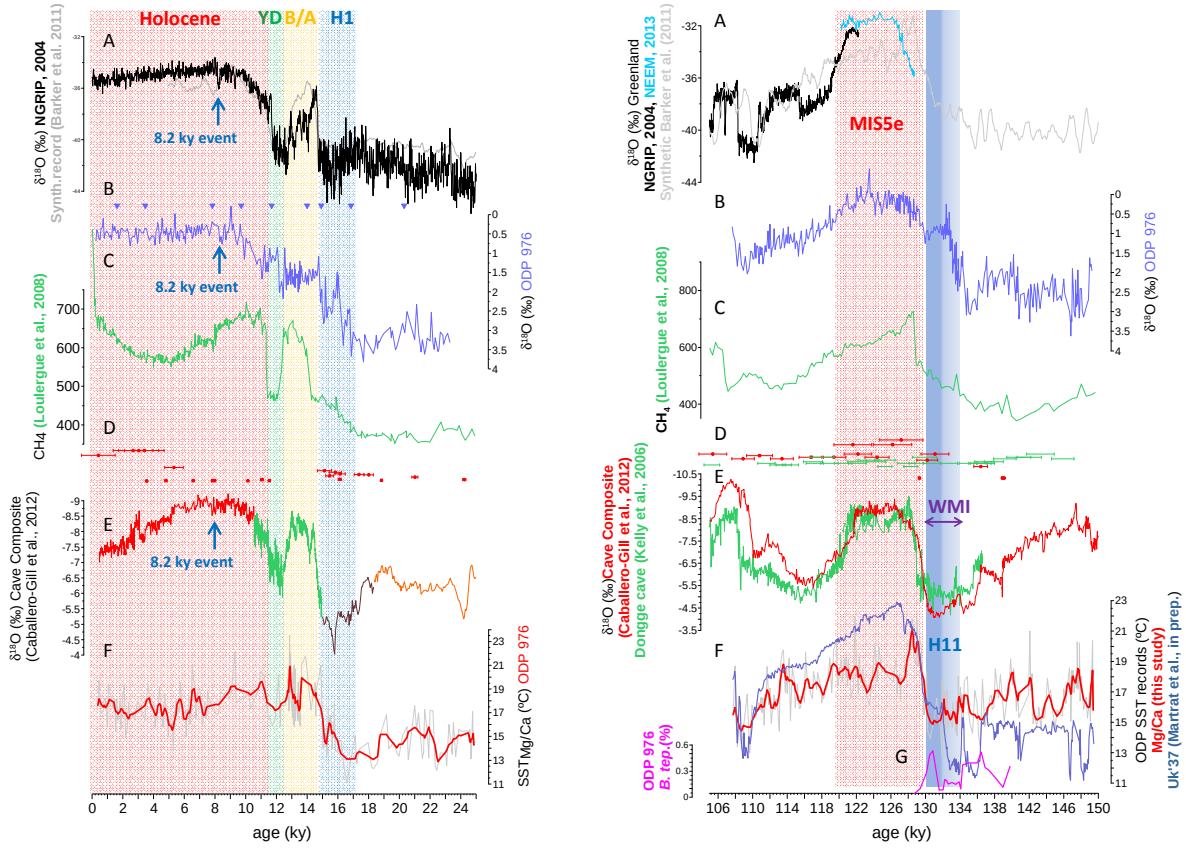

Figure 28. Comparison of Greenland temperatures, atmospheric CH_4 and Asian monsoon palaeo-records with ODP 976 profiles for the MIS2-T1-Holocene sequence (left panel) and the MIS6-T2-MIS5e sequence (right panel). (A) Greenland $\delta^{18}O$ records: NGRIP (black, NGRIP members, 2004), Synthetic record (grey, Barker et al., 2011) and NEEM (light blue, NEEM community, 2013). (B) ODP 976 $\delta^{18}O$ record (blue, this study). Radiocarbon ages are indicated with blue triangles above the $\delta^{18}O$ profile in the MIS2-T1-Holocene (left) panel. (C) Antarctic atmospheric CH_4 record (green, Loulergue et al., 2008). (D) Cave composite radiometric ages with 95% error bars (red, Caballero-Gill et al., 2012) and Dongge speleothem radiometric ages (green, Kelly et al., 2006). (E) Speleothem $\delta^{18}O$ records. MIS2-T1-Holocene (left): Cave composite record (Caballero-Gill et al. (2012): Sanbao (red), Dongge (green), Hulu (brown and orange). MIS6-T2-MIS5e (right): Sanbao section of cave composite record (red, Caballero-Gill et al., 2012) and Dongge cave (green, Kelly et al., 2006). (F) ODP 976 SST records: $SST_{Uk'37}$ (dark blue, Martrat et al., 2013, submitted) and $SST_{Mg/Ca}$ (grey=unsmoothed; red=5pt smoothed, this study). (G) ODP 976 abundance of cold-water dinoflagellate *B. tepikiensis* cysts (L. Londeix, 2013, pers. comm.). Colour shading highlights Marine Isotope Stage (MIS) 2, Younger Dryas (YD), Bölling-Allerod (B/A), Heinrich event 1 (H1), MIS5e, Weak Monsoon Interval (WMI), Heinrich 11 (H11), and pre-H11 events (light blue).

An overarching, common driver of the synchronous development of Mediterranean climate and the Asian summer monsoon regime is orbital precession that determines the amount of solar radiation received at mid-to-high northern latitudes. Precession minima, indicative of maximum northern hemisphere insolation, stimulate warming in the North Atlantic region and at the same time they drive the monsoons to maximum strength (Rohling et al., 1991; Tzedakis, 2007). On the other hand, atmospheric CH_4 is impacted by monsoon strength and the CH_4 changes are essentially globally synchronous due to the rapid mixing time of the atmosphere (Blunier et al., 1998; Masson-Delmotte et al., 2004). Coeval changes in atmospheric CH_4, Mediterranean SST and speleothem $\delta^{18}O$ therefore support the contention that Mediterranean and North Atlantic climate and atmospheric CH_4 levels responded to Asian monsoon variability (Kelly et al., 2006; Sánchez Goñi et al., 2008) (Fig. 28). This relationship was established for the series of climatic events during MIS2-T1-Holocene sequence, and a similar relationship is suggested for the MIS6-T2-MIS5e sequence (Cheng et al., 2006; Kelly et al., 2006; Yuan et al., 2004). Accordingly, a slow initial CH_4 increase during T2 was associated with a strong Antarctic temperature warming, preceding the Asian monsoon increase at 129 ky but coeval with North Atlantic warming, and a sharp methane rise and CO_2 overshoot coinciding with the end of the Antarctic thermal optimum. The phasing of climatic signals recorded in the North Atlantic, Asian monsoon and Antarctic regions suggests an involvement of the "bipolar seesaw" mechanism during T2 in determining the interhemispheric timing and direction of climatic signals (Kelly et al., 2006; Yuan et al., 2004; Cheng et al., 2006; Masson-Delmotte et al., 2010).

The tight correlation of North Atlantic and Mediterranean temperature with the Asian monsoons and Mediterranean rainfall patterns suggests the possibility to establish an alternative age model for the MIS6-T2-MIS5e period by synchronizing the ODP 976 $SST_{Mg/Ca}$ record with absolutely dated Asian and European speleothem records. For the Asian monsoon we chose the Dongge cave record (Kelly et al., 2006) over the Hulu and Sanbao records (Wang et al., 2001, 2008; Cheng et al., 2009) because of its tighter age control from closely spaced ^{230}Th datums. As an initial synchronization, the ODP 976 $SST_{Mg/Ca}$ record was graphically tuned to the Dongge $\delta^{18}O$ record using tie-points that were centred on the mid-points of $\delta^{18}O$ changes in both profiles, including the most prominent events: onset of the Weak Monsoon Interval (WMI), the abrupt onset of Asian Monsoon during T2 and the end of the interglacial monsoon maximum (Fig. 29).

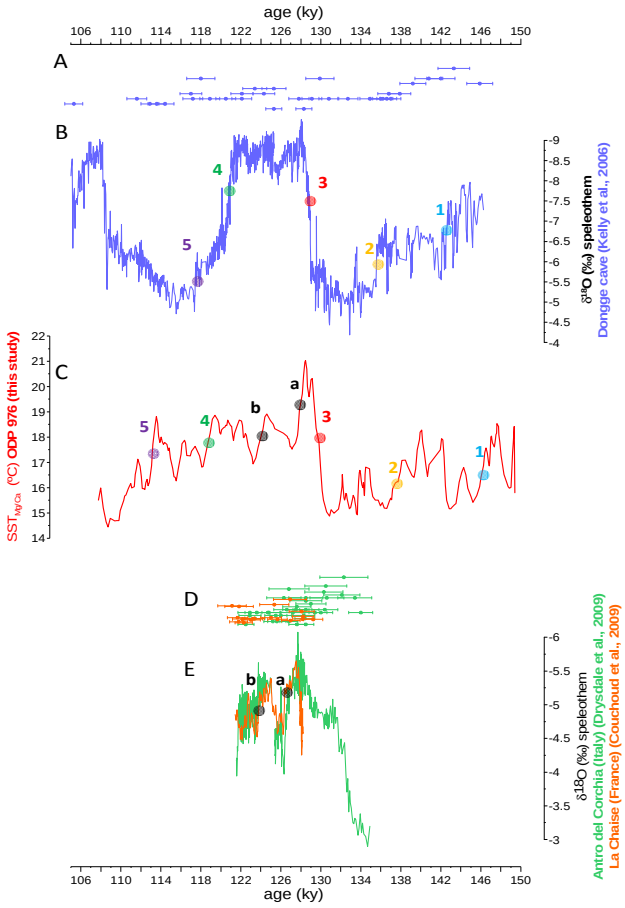

Figure 29. Synchronization of ODP976 and speleothem $\delta^{18}O$ profiles (A) Dongge cave speleothem radiometric ages with 95% error bars. (B) Dongge speleothem $\delta^{18}O$ profiles (blue, Kelly et al., 2006). (C) ODP 976 $SST_{Mg/Ca}$ (grey=unsmoothed; red=5pt smoothed, this study). (D) Speleothem radiometric ages with 95% error bars: Corchia (green, Drysdale et al., 2009) and BD-La Chaise (orange, Couchoud et al., 2009). (E) European speleothem $\delta^{18}O$ profiles: Corchia (green, Drysdale et al., 2009) and BD-La Chaise (orange, Couchoud et al., 2009). Coloured dots and labels represent tie-points used for synchronization with Dongge; black dots (labelled a, b) represent tie-points used for synchronization with Corchia and BD-La Chaise.

As a second step, we tuned the MIS5e section of the ODP 976 $SST_{Mg/Ca}$ profile to the Antro del Corchia $\delta^{18}O$ record. This particular speleothem profile was used previously (Drysdale et al., 2009; Couchoud et al., 2009) to demonstrate a close correspondence between speleothem $\delta^{18}O$ and western Mediterranean SST (Figs. 27, 29). The resulting age model (Fig. 30) was then used to compare ODP976 $SST_{Mg/Ca}$ with Antarctic atmospheric CH_4 which revealed that both profiles are closely correlated, hence confirming the validity of the synchronization exercise.

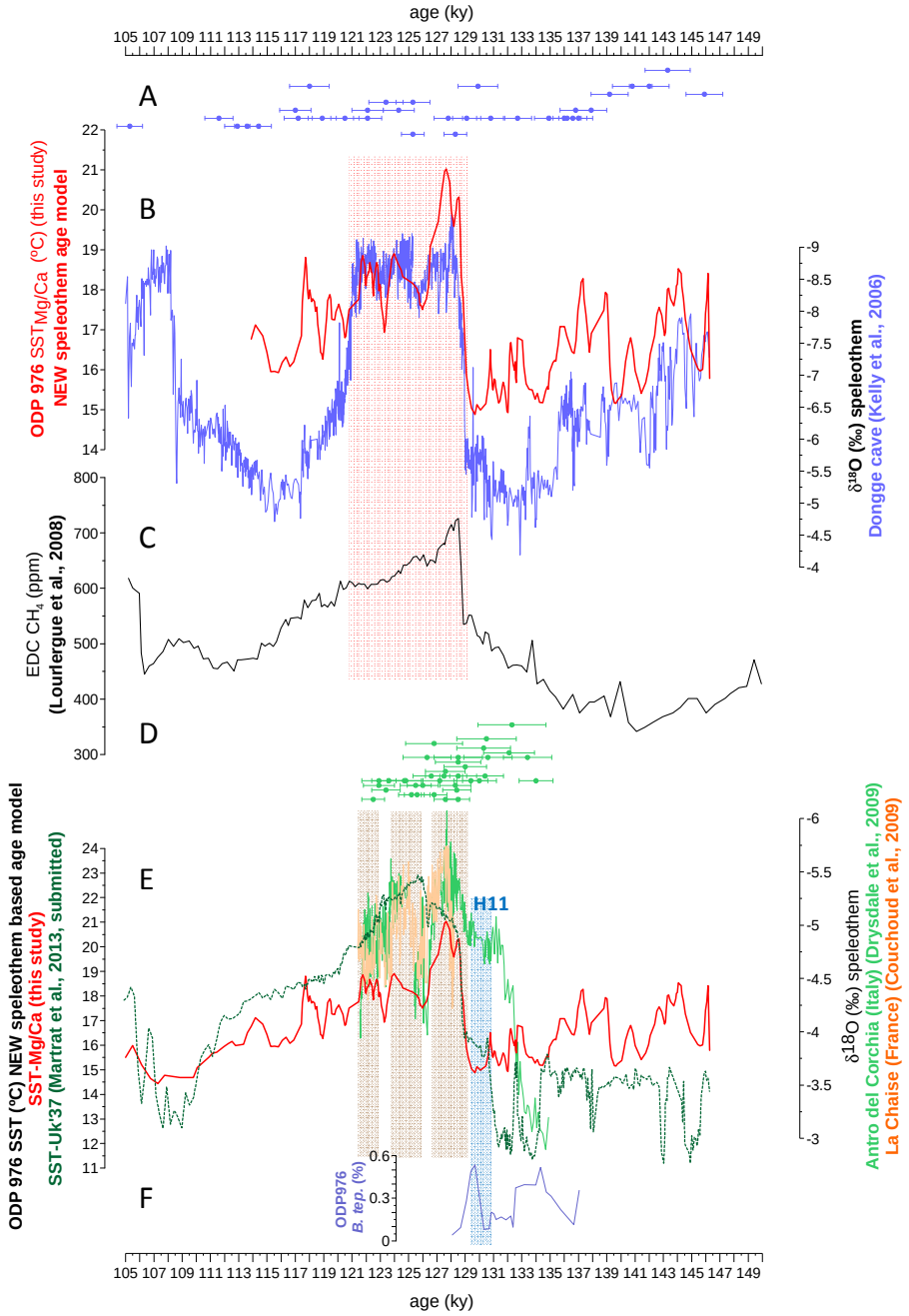

Figure 30. ODP 976 age scale synchronized with Dongge and Corchia ^{230}Th dated age scales. (A) Dongge speleothem radiometric ages (blue, Kelly et al., 2006). (B) ODP 976 $SST_{Mg/Ca}$ on the synchronized age scale (red=5pt smoothed, this study) and Dongge $\delta^{18}O$ record (blue, Kelly et al., 2006). (C) Antarctic atmospheric CH_4 record (black, Loulergue et al., 2008). (D) Corchia speleothem radiometric ages with 95% error bars (green, Drysdale et al., 2009). (E) European speleothem $\delta^{18}O$ profiles: Corchia (green, Drysdale et al., 2009) and La Chaise (orange, Couchoud et al., 2009) and ODP 976 SST records on the synchronized age scale: $SST_{Mg/Ca}$ (red=5pt smoothed, this study) and $SST_{Uk'37}$ (stippled dark green, Martrat et al., 2013, submitted). (F) ODP 976 abundance of the cysts of the cold-water dinoflagellate *B. tepikiensis* (L. Londeix, 2013, pers. comm.). Brown shading indicates the three warm ODP 976 $SST_{Mg/Ca}$ intervals synchronized with the three humid intervals indicated by Corchia and BD-La Chaise speleothem $\delta^{18}O$ minima

Similar synchronizations were developed previously for T2 by correlating the ODP 977 $SST_{Uk'37}$ record with the Corchia $\delta^{18}O$ record (Drysdale et al., 2009). However, those synchronizations differ from the one presented here because Drysdale et al. (2009) relied on the ODP976 SST_{Uk37} record that shows a warming step during T2 not seen in our ODP976 $SST_{Mg/Ca}$ record (Fig. 28F, right panel and see also: Chapter "*Results*", Fig. 17D). This warming feature in the SST_{Uk37} was aligned with the "hump" in the $\delta^{18}O$ transition during T2 in the Corchia speleothem profile which results in T2 ages that are a ~3 ky older than in our synchronized age model where the steep increase in $SST_{Mg/Ca}$ is correlated with the likewise steep $\delta^{18}O$ change in the Dongge $\delta^{18}O$ record. Comparing the $SST_{Mg/Ca}$ and SST_{Uk37} profiles of ODP976 shows that the initial warming step seen in SST_{Uk37} coincides with H11 as reflected by the high presence of the cysts of the cold-water dinoflagellate *B. tepikiensis* at Site 976 (L. Londeix, personal communication; Fig. 28G, right panel and Fig. 30F; see also Discussion Chapter 1: "*ODP 976 and Alboran Sea palaeoclimatology during the last two deglaciations*", Fig. 19) and by cold $SST_{Mg/Ca}$. An early warming step as suggested by the SST_{Uk37} profile during T2 would be confirmed by the incurrence of the "hump" seen in the Corchia $\delta^{18}O$ profile. However, such a two-step development is not indicated in the Asian monsoon records even though those records are thought to be directly linked with North Atlantic SST. This leaves the possibility that ambient environmental conditions were differently recorded during H11 in the records, for instance in the case of SST_{Uk37} and $SST_{Mg/Ca}$, because of different ecologic responses of the algae and foraminiferal communities to the anomalous conditions during H11. Lorenz et al. (2006) suggested that a shift in the season of maximum insolation during the Holocene may have accounted for changes in the seasonal timing of phytoplankton production of alkenones from which the SST signal is derived (Lorenz et al., 2006). Hence, coccolithophore production may have shifted to the warmer summer season during H11, hence recording a warmer seasonal SST_{Uk37}. However, while it is generally accepted that $SST_{Uk'37}$ represent annual average SST (Martrat et al., 2004, 2007), some studies suggest a maximum haptophyte production during the colder season, hence, suggesting that alkenones would be better reflecting winter seasonal temperatures more than a annual average temperature (Rodrigues et al., 2012).

The two-step change in the Corchia $\delta^{18}O$ profile, on the other hand, could reflect $\delta^{18}O$ changes of the vapour source, either due to a different trajectory of moisture transports during H11 or related to the meltwater-induced negative $\delta^{18}O$ budget of the North Atlantic and (western)

Mediterranean surface waters. Additional evidence is provided by the timing of growth of speleothem in the hyper-arid Negev Desert (Israel, Vaks et al., 2010), which shows a peak in growth rates coeval to this "hump" seen in Corchia, so coeval to North Atlantic H11 event. For speleothems to grow in such arid conditions, a source of water and therefore rainfall is required. So, if speleothems in the Negev Desert show increasing growth rates during North Atlantic cold conditions and therefore reduced eastward atmospheric moisture transports, then vapour transport from southern sources (i.e. the Indian Ocean) due to changes in air mass trajectories could explain this discrepancy between these signals. If this were the case, the $\delta^{18}O$ signals in the Corchia profile would be decoupled from North Atlantic SST in that the initial $\delta^{18}O$ decrease would correlate with cold SST. Such a connection, however, is not supported by the Corchia speleothem $\delta^{13}C$ data, speleothem growth rates and Mg and U concentrations; these complementary data, in conjunction with speleothem $\delta^{18}O$, all are consistent with ambient warming and increased rainfall (Drysdale et al., 2009). Hence at this point the apparent discrepancy between the fine structure of the speleothem and marine profiles during T2 cannot be resolved.

Yet, the overall correlation of the ODP976 SST profiles with the speleothem records and supports the dynamical connection between North Atlantic and western Mediterranean SST and atmospheric moisture transport to and rainfall patterns over the Mediterranean borderlands on orbital and suborbital timescales. Beyond its environmental significance this correlation and notably, the similarity of fine-structure during MIS5e of ODP976 $SST_{Mg/Ca}$ with the Corchia and BD-La Chaise $\delta^{18}O$ profiles, allows to develop an age model for the MIS6-T2-MIS5e sequence by transferring the uranium-series dated age model of the speleothem profiles to the ODP976 marine profiles.

References:

Alpert, P., M. Baldi, et al. (2006). Chapter 2 Relations between climate variability in the Mediterranean region and the tropics: ENSO, South Asian and African monsoons, hurricanes and Saharan dust. Developments in Earth and Environmental Sciences, Elsevier. Volume 4: 149-177.

Bar-Matthews, M., Ayalon, A., Gilmour, M., Matthews, A., and Hawkesworth, C. J. (2003) "Sea–land oxygen isotopic relationships from planktonic foraminifera and speleothems in the Eastern Mediterranean region and their implication for paleorainfall during interglacial intervals." Geochimica et Cosmochimica Acta,67(17), 3181-3199.

Bard, E., Delaygue, G., Rostek, F., Antonioli, F., Silenzi, S., and Schrag, D. P. (2002) "Hydrological conditions over the western Mediterranean basin during the deposition of the cold Sapropel 6 (ca. 175 kyr BP)." Earth and Planetary Science Letters, 202(2), 481-494.

Barker, S., G. Knorr et al. (2011). "800,000 years of abrupt climate variability." Science 334(6054):347.

Blunier, T., Chappellaz, J., Schwander, J., Dällenbach, A., Stauffer, B., Stocker, T. F.,and Johnsen, S. J. (1998) "Asynchrony of Antarctic and Greenland climate change during the last glacial period." Nature, 394(6695), 739-743.

Caballero-Gill, R. P., Clemens, S. C., and Prell, W. L. (2012) "Direct correlation of Chinese speleothem $d^{18}O$ and South China Sea planktonic $d^{18}O$: Transferring a speleothem chronology to the benthic marine chronology." Paleoceanography,27(2).

Celle-Jeanton, H., Travi, Y., and Blavoux, B. (2001) "Isotopic typology of the precipitation in the Western Mediterranean region at three different time scales." Geophysical Research Letters, 28(7), 1215-1218.

Cheng, H., Edwards, R. L., Wang, Y., Kong, X., Ming, Y., Kelly, M. J. and Liu, W. (2006) "A penultimate glacial monsoon record from Hulu Cave and two-phase glacial terminations." Geology, 34(3), 217-220.

Couchoud, I., Genty, D., Hoffmann, D., Drysdale, R., and Blamart, D. (2009) "Millennial-scale climate variability during the Last Interglacial recorded in a speleothem from south-western France." Quaternary Science Reviews, 28(27), 3263-3274.

Drysdale, R. N., Zanchetta, G., Hellstrom, J. C., Fallick, A. E., Zhao, J., Isola, I. and Bruschi, G. (2004) "Palaeoclimatic implicatins of the growth history and stable isotope (d18O and d13C) geochemistry of a Middle to Late Pleistocene stalagmite from central-western Italy (2004). Earth and Planetary Science Letter 227(3-4):215-229.

Drysdale, R. N., Zanchetta, G., Hellstrom, G., Fallick, A. E. and Zhao, J. (2005) "Stalagmite evidence for the onset of the Last Interglacial in southern Europe at 129±1 ka." Geophysical Research letters 32.

Drysdale, R. N., Zanchetta, G., Hellstrom, J. C., Fallick, A. E., McDonald, J., and Cartwright, I. (2007) "Stalagmite evidence for the precise timing of North Atlantic cold events during the early last glacial." Geology, 35(1), 77-80.

Drysdale, R. N., J. C. Hellstrom, et al., (2009) "Evidence for obliquity forcing of Glacial Termination II." Science 325 (5947):1527.

Eshel, G. (2002). Mediterranean climates. Israel Journal of Earth Sciences,51(3), 157-168.

Genty, D., Blamart, D., Ouahdi, R., Gilmour, M., Baker, A., Jouzel, J., and Van-Exter, S. (2003) "Precise dating of Dansgaard–Oeschger climate oscillations in western Europe from stalagmite data." Nature, 421(6925), 833-837.

Giorgi, F. and P. Lionello (2008). "Climate change projections for the Mediterranean region." Global and Planetary Change 63(2-3): 90-104.

Gupta, A. K., Anderson, D. M., and Overpeck, J. T. (2003) "Abrupt changes in the Asian southwest monsoon during the Holocene and their links to the North Atlantic Ocean." Nature, 421(6921), 354-357.

Hurrell, J. W. (1995). NAO index data provided by the climate analysis section.NCAR, Boulder, USA.

Kelly, M. J., Lawrence Edwards, R., Cheng, H., Yuan, D., Cai, Y., Zhang, M., Lin, Y. and An, Z. "High resolution characterization of the Asian Monsoon between 146,000 and 99,000 years B.P. from Dongge Cave, China and global correlation of events surrounding Termination II." Paleaeogeography, Palaeoclimatology, Palaeoecology 236:20-38.

Kessarkar, P. M., Purnachadra Rao, V., Naqvi, S. W. A., and Karapurkar, S. G. (2013) "Variation in the Indian summer monsoon intensity during the Bølling-Ållerød and Holocene." Paleoceanography, 28(3), 413-425.

Krichak, S., Alpert, P., Bassat, K., and Dayan, M. An RCM Evaluation of Climate Change Trends and Uncertainties over the Eastern Mediterranean Region for GLOWA Jordan River Project.

Lorenz, S.J., Kim, J.-H., Rimbu, N., Schneider, R.R. and Lohmann, G., (2006) "Orbitally driven insolation forcing on Holocene climate trends: evidence from alkenone data and climate modeling." Paleoceanography 21, PA1002. doi:10.1029/2005PA001152.

Loulergue, L., Schilt, A., Spahni, R., Masson-Delmotte, V., Blunier, T., Lemieux, B. and Chappellaz, J. (2008) "Orbital and millennial-scale features of atmospheric CH4 over the past 800,000 years." Nature, 453(7193), 383-386.

Martrat, B., J. O. Grimalt, et al. (2004). "Abrupt Temperature Changes in the Western Mediterranean over the past 250,000 years." Science 306 (5702):1762.

Martrat, B., Grimalt, J. O., Shackleton, N. J., de Abreu, L., Hutterli, M. A. and Stocker, T. F. (2007) Four climate cycles of recurring deep and surface water destabilizations on the Iberian Margin. Science, vol. 317 (502), doi: 10.1126/science.1139994.

Masson-Delmotte, V., Stenni, B., and Jouzel, J. (2004) "Common millennial-scale variability of Antarctic and Southern Ocean temperatures during the past 5000 years reconstructed from the EPICA Dome C ice core." The Holocene, 14(2), 145-151.

Masson-Delmotte, V., Stenni, B., Pol, K., Braconnot, P., Cattani, O., Falourd, S., and Otto-Bliesner, B. (2010) "EPICA Dome C record of glacial and interglacial intensities." Quaternary Science Reviews, 29(1), 113-128.

McDermott, F. (2004) "Palaeo-climate reconstruction from stable isotope variations in speleothems: a review." Quaternary Science Reviews, 23(7), 901-918.

NEEM community members (2013) "Eemian interglacial reconstructed from a Greenland folded ice core." Nature, vol. 493:489-494, doi:10.1038/nature11789.

North Greenland Ice Core Project (2004). Nature 431(7005):147-151.

Pailler, D., and Bard, E. (2002) "High frequency palaeoceanographic changes during the past 140 000 yr recorded by the organic matter in sediments of the Iberian Margin." Palaeogeography, Palaeoclimatology, Palaeoecology, 181(4), 431-452.

Rodrigues, T., Rufino, M., Santos, C., Salgueiro, E., Abrantes, F. and Oliveira, P. (2012) "Iberian Sea Surface Temperature calibration based in alkenones paleotemperature index Uk37." 7º Simpósio sobre a Margem Ibérica Atlantica, MIS 2012.

Rodwell, M. J., and Hoskins, B. J. (2001) "Subtropical anticyclones and summer monsoons." Journal of Climate, 14(15), 3192-3211.

Rohling, E. J., & Hilgen, F. J. (1991). The eastern Mediterranean climate at times of sapropel formation: a review. Geol. Mijnbouw, 70, 253-264.

Sánchez Goñi, M. F., Eynaud, F., Turon, J. L. and Shackleton, N. J. (1999) "High resolution palynological record off the Iberian margin: direct land-sea correlation for the Last Interglacial complex." Earth and Planetary Science Letters 171:123-137.

Sánchez Goñi, M. F., Landais, A., Fletcher, W. J., Naughton, F., Desprat, S. and Duprat, J. (2008) "Contrasting impacts of Dansgaard-Oeschger events over a western European latitudinal transect modulated by orbital parameters." Quaternary Science Reviews 27:1136-1151.

Schulz, M., and Paul, A. (2002) "Holocene climate variability on centennial-to-millennial time scales: 1. Climate records from the North-Atlantic realm." In Climate development and history of the North Atlantic realm (pp. 41-54). Springer Berlin Heidelberg.

Shackleton, N. J., Sánchez Goñi, M. F., Pailler, D. and Lancelot, Y. (2003) "Marine Isotope Substage 5e and the Eemian Interglacial." Global and Planetary Change (36):151-155.

Sinha, A., Cannariato, K. G., Stott, L. D., Li, H. C., You, C. F., Cheng, H., and Singh, I. B. (2005) "Variability of southwest Indian summer monsoon precipitation during the Bølling-Ållerød." Geology, 33(10), 813-816.

Skinner, L. and Shackleton, N.J. (2006) "Deconstructing Terminations I and II: revisiting the glacioeustatic paradigm based on deep-water temperature estimates." Quaternary Science Reviews 25, 3312-3321

Trigo, R. M., Osborn, T. J., and Corte-Real, J. M. (2002). The North Atlantic Oscillation influence on Europe: climate impacts and associated physical mechanisms. Climate Research, 20(1), 9-17.

Tzedakis, P. C., Andrieu, V., De Beaulieu, J. L., Crowhurst, S. D., Follieri, M., Hooghiemstra, H., ... and Wijmstra, T. A. (1997) "Comparison of terrestrial and marine records of changing climate of the last 500,000 years." Earth and Planetary Science Letters, 150(1), 171-176.

Tzedakis, P. C. (2007) "Seven ambiguities in the Mediterranean palaeoenvironmental narrative." Quaternary Science Reviews 26:2042-2066.

Vaks, A., Bar-Matthews, M., Matthews, A., Ayalon, A., and Frumkin, A. (2010) "Middle-Late Quaternary paleoclimate of northern margins of the Saharan-Arabian Desert: reconstruction from speleothems of Negev Desert," Israel.Quaternary Science Reviews, 29(19), 2647-2662.

Wang, Y.J., Cheng, H., Edwards, R.L., An, Z.S.,Wu, J.Y., Shen, C.-C. and Dorale, J.A., (2001) "A high-resolution absolute-dated Late Pleistocene monsoon record from Hulu Cave, China." Science 294, 2345–2348.

Wang, Y., Cheng, H., Edwards, R. L., Kong, X., Shao, X., Chen, S. and An, Z. (2008) "Millennial-and orbital-scale changes in the East Asian monsoon over the past 224,000 years." Nature, 451(7182), 1090-1093.

Yuan, D., Cheng, H., Edwards, R.L., Dykoski, C.A., Kelly, M.J., Zhang, M., Qing, J., Lin, Y.,Wang, Y.,Wu, J., Dorale, J.A., An, Z., Cai, and Y., (2004) "Timing, duration, and transitions of the Last Interglacial Asian Monsoon." Science 304, 575–578.

Zanchetta, G., Drysdale, R. N., Hellstrom, J. C., Fallick, A. E., Isola, I., Gagan, M. K., and Pareschi, M. T. (2007) "Enhanced rainfall in the Western Mediterranean during deposition of sapropel S1: stalagmite evidence from Corchia cave (Central Italy)." Quaternary Science Reviews, 26(3), 279-286.

Conclusions

This thesis presents high-resolution data from ODP Site 976 in the Alboran Sea, westernmost Mediterranean. The data profiles encompass $\delta^{18}O$ and $SST_{Mg/Ca}$ records measured in the planktonic foraminifera *Globigerina bulloides* spanning the present (Holocene) and last (Marine Isotope Stage, MIS5e) interglacial periods and their preceding deglaciations: the MIS6-T2-MIS5e (150-105 ky) and MIS2-T1-Holocene (25-0 ky) periods. Due to its position in the advection path of North Atlantic surface water entering the Mediterranean, ODP Site 976 receives and records North Atlantic climate variability signals. Surface hydrology variability in the western Alboran basin in the two stratigraphic sequences is documented at an unprecedented time resolution in the ODP 976 oxygen isotope and SST records at multi-decadal (60-90 yr, $\delta^{18}O$) to centennial (110-150 yr, $SST_{Mg/Ca}$) time scales. To achieve such highly resolved profiles is the main goal of working in the Alboran basin that provides a depositional regime in which sedimentation rates are exceptionally high, up to 23 cm/ky. Robustness and reproducibility of the ODP 976 palaeo-signals is proved by comparing the multi-proxy records generated ($\delta^{18}O$, $SST_{Mg/Ca}$) with similar proxy profiles from other Alboran Sea sites, ODP 977 and MD95-2043.

Due to the short instrumental record of direct observations, palaeoclimatic records provide the only opportunity to obtain information on the longer-term North Atlantic climate variability. The Greenland ice core records best resolve North Atlantic atmospheric climate variability but they do not go beyond 129 ky (NEEM community members, 2013). The high correlation of the fine-scale ODP 976 $\delta^{18}O$ profile with the ice-core $\delta^{18}O$ record from Greenland (NGRIP, 2004) confirms the quality of ODP 976 as representing North Atlantic climate evolution, which remarkably adds value to the ODP 976 palaeoclimatic records that go beyond the limits of Greenland ice core records at multi-decadal to centennial resolution.

This thesis underscores the strong connection between the marine palaeoclimatology in the Alboran Sea and the Iberian margin (MD95-2040, MD95-2042, MD99-2334), by means of surface water transports through the Strait of Gibraltar, which ultimately highlights the affinity of the Alboran Sea palaeoceanography to North Atlantic climate variability.

Comparison between $SST_{Mg/Ca}$ and $SST_{UK'37}$ records reveals higher variability of the SST signal derived from planktonic foraminifera Mg/Ca ratios. The proxy-specific difference plausibly results from differences in ecology and environmental factors influencing the living habitats of signal carriers i.e., planktonic foraminifera vs. coccolithophores. While *G. bulloides* is considered to record spring-time SST (Elderfield and Ganssen, 2000; Ganssen and Kroon, 2000), alkenones are plausibly depicting a mean annual integration of SST (Martrat et al., 2004, 2007, 2013, submitted; Huguet et al., 2011; Dos Santos et al., 2013). Additionally, the specific methodology used for each paleothermometry proxy can also influence the proxy-specific signals due to the higher abundance of alkenones in comparison with the smaller foraminiferal shell abundance in the sediment samples.

During the MIS2-T1-Holocene sequence the multi-proxy data profiles from the Alboran Sea and the Iberian margin are tightly correlated with ODP976 consistently displaying highest temporal resolution hence confirming the quality of this site as representing the North Atlantic climate evolution. Multiple-step features connected with the incursion of accelerated ice-sheet disintegration are captured by the ODP 976 palaeo-climatic records. The penultimate deglaciation (T2) shows multiple-step features similar to T1, albeit at different magnitudes and relative timings, alluding to offsets in dynamics between T2 and T1. Viewing the multiproxy data base in combination, T2 was almost entirely controlled by a single massive meltwater surge that was coincident with Heinrich event 11 (H11, 132-130 ky) or that embedded the main H11 event in it. The $\delta^{13}C$ benthic record of Iberian margin core MD95-2042 reveals consistently low NADW production during T2, indicating a continually weak AMOC at the end of MIS6 until the onset of MIS5e. Such an AMOC development is consistent with our planktonic $\delta^{18}O$ and $SST_{Mg/Ca}$ records from ODP 976 that indicate T2 was prominently dominated by the presence in the northern North Atlantic of glacial-level SST and elevated levels of meltwater that were associated with the H11 ice sheet collapse. Only once polar conditions ceased did NADW production rapidly increase but did not reach its full strength until well into MIS5e. Following H11, an abrupt ~5^{o}C warming is recorded in the Mg/Ca ratios that reaches full interglacial SST at 129 ky, synchronously with the establishment of interglacial flora on the bordering continent, as shown by the pollen records of ODP 976 (Combourieu-Nebout et al., in prep.), MD95-2042 (Sánchez Goñi et al., 1999, 2012) and MD01-2444 (Tzedakis, 2013, pers. comm.); this suggests an in-phase onset of the interglacial conditions in the regional terrestrial and marine environments.

During MIS5e we observe a close correspondence of the Antro del Corchia (Italy) and BD-La Chaise (France) speleothem $\delta^{18}O$ records with the ODP 976 $SST_{Mg/Ca}$ record. Those speleothem $\delta^{18}O$ records are thought to reflect regional rainfall patterns at the cave sites, and the close correlation with 976 $SST_{Mg/Ca}$ confirms the coupling of rainfall in southern Europe with higher SST in the western Mediterranean. This link demonstrates the significance of variable warm-water transport to the North Atlantic from the tropics, driven by the AMOC, and its subsequent advection to the Mediterranean Sea in driving atmospheric convection and moist air transport with the prevailing westerly winds which ultimately determines the rainfall patterns over the Mediterranean borderlands (Drysdale et al., 2004, 2005, 2009). Beyond the Mediterranean-North Atlantic connection, several climatological studies demonstrate that Mediterranean climates and the Asian monsoon regime are very closely linked (Rodwell and Hoskins, 2001; Eshel, 2002; Alpert et al., 2006). The tight correlation of North Atlantic and Mediterranean temperature with the Asian monsoons is reflected in the close correspondence between the structure of oxygen isotope records from Asian monsoon speleothems (i.e. Hulu and Dongge caves) and Greenland ice cores (Wang et al., 2001) suggesting that the intensity of the Asian monsoons varied synchronously with the palaeo-temperature record of Greenland, hence North Atlantic climate (Wang et al., 2001; Yuan et al., 2004). This offers the possibility to establish an alternative age model for the MIS6-T2-MIS5e period by synchronizing the ODP 976 $SST_{Mg/Ca}$ record with absolutely dated Asian and European speleothem $\delta^{18}O$ records. Comparison of ODP976 $SST_{Mg/Ca}$ on the speleothem-based age model with Antarctic atmospheric CH_4 reveals that both profiles are closely correlated. Such a correlation is expected because orbital modulation determines northern hemisphere insolation that impacts temperatures of the North Atlantic region and modifies the strength of the Asian monsoon (Rohling et al., 1991; Tzedakis, 2007) that, in turn, controls CH_4 emission from wetlands (Kelly et al., 2006; Sánchez Goñi et al., 2008). With the new absolutely dated age model the timing and phasing of palaeo-environmental changes in the marine and terrestrial domains can be constrained more firmly.

The ODP 976 multi-decadal to centennial scale records of North Atlantic variability presented in this thesis aid our knowledge of the sensitivity with which the ocean-atmosphere system are coupled with climate. The data provide the basis for the climate modeling community to test their models and the quality with which they simulate climate and ocean circulation under the boundary conditions of the past. Notably the MIS6-T2-MIS5e data sequence presented here shall tell if the models adequately respond to the climate forcing extant during this time period, namely

the higher radiative forcing brought about by increased incoming solar radiation that serves as an analogue of increasing greenhouse gas forcing expected for the coming century.

References:

Alpert, P., Baldi, M., Ilani, R., Krichak, S., Price, C., Rodo´ , X., Saaroni, H., Ziv, B., Kishcha, P., Barkan, J., Mariotti, A., Xoplaki, E., (2006) Relations between climate variability in the Mediterranean region and the tropics: ENSO, South Asian and African Monsoons, Hurricanes and Saharan dust. In: Lionello, P., Malanotte-Rizzoli, P., Boscolo, R. (Eds.), The Mediterranean Climate: An Overview of the Main Characteristics and Issues. Elsevier, Amsterdam, The Netherlands.pp. 149–177.

Elderfield, H. and Ganssen, G., 2000. Past temperature and 18O of surface ocean waters inferred from foraminiferal Mg/Ca ratios. Nature. 405, 442-445.

Dos Santos, R. A., Spooner, M. I. et al. (2013) "Comparison of organic (Uk'37, TEXH86, LDI) and faunal proxies (foraminiferal assemblages) for reconstruction of late Quaternary sea surface temperature variability from offshore southeastern Australia." Paleoceanograpgy 28(3):377.

Drysdale, R. N., Zanchetta, G., Hellstrom, J. C., Fallick, A. E., Zhao, J., Isola, I. and Bruschi, G. (2004) "Palaeoclimatic implicatins of the growth history and stable isotope (d18O and d13C) geochemistry of a Middle to Late Pleistocene stalagmite from central-western Italy (2004). Earth and Planetary Science Letter 227(3-4):215-229.

Drysdale, R. N., Zanchetta, G., Hellstrom, G., Fallick, A. E. and Zhao, J. (2005) "Stalagmite evidence for the onset of the Last Interglacial in southern Europe at 129±1 ka." Geophysical Research letters 32.

Drysdale, R. N., J. C. Hellstrom, et al., (2009) "Evidence for obliquity forcing of Glacial Termination II." Science 325 (5947):1527.

Eshel, G., 2002. Mediterranean climates. Israel Journal of Earth Sciences 51, 157–168.

Huguet, C., Martrat, B., Grimalt, J.O., Sinninghe Damsté, J.S., Schouten, S. (2011) "Coherent millennial.scale patterns in Uk'37 and TEX H86 temperature records during the penultimate interglacial-to-glacial cycle in the western Mediterranean." Paleoceanography 26.

Kelly, M. J., Lawrence Edwards, R., Cheng, H., Yuan, D., Cai, Y., Zhang, M., Lin, Y. and An, Z. "High resolution characterization of the Asian Monsoon between 146,000 and 99,000 years B.P. from Dongge Cave, China and global correlation of events surrounding Termination II." Paleaeogeography, Palaeoclimatology, Palaeoecology 236:20-38.

Martrat, B., J. O. Grimalt, et al. (2004). "Abrupt Temperature Changes in the Western Mediterranean over the past 250,000 years." Science 306 (5702):1762.

Martrat, B., Grimalt, J. O., Shackleton, N. J., de Abreu, L., Hutterli, M. A. and Stocker, T. F. (2007) Four climate cycles of recurring deep and surface water destabilizations on the Iberian Margin. Science, vol. 317 (502), doi: 10.1126/science.1139994.

NEEM community members (2013) Eemian interglacial reconstructed from a Greenland folded ice core. Nature, vol. 493:489-494, doi:10.1038/nature11789.

North Greenland Ice Core Project (2004). Nature 431(7005):147-151.

Rodwell, M. J. and Hoskins, B. J. (2001) "Subtropical anticyclones and summer monsoons." Journal of Climate 14:3192-3211.

Rohling, E. J. (1991) "Shoaling of the Eastern Mediterranean pycnocline due to the reduction of excess evaporation: implications for sapropel formation." Paleoceanography 6(6):747-753.

Sánchez Goñi, M. F., Eynaud, F., Turon, J. L. and Shackleton, N. J. (1999) "High resolution palynological record off the Iberian margin: direct land-sea correlation for the Last Interglacial complex." Earth and Planetary Science Letters 171:123-137.

Sánchez Goñi, M. F., Landais, A., Fletcher, W. J., Naughton, F., Desprat, S. and Duprat, J. (2008) "Contrsting impacts of Dansgaard-Oeschger events over a western European latitudinal transect modulated by orbital parameters." Quaternary Science Reviews 27:1136-1151.

Sánchez Goñi, M. F., Bakker, P., Desprat, S., Carlson, A. E., van Meerbeeck, C. J., Peyron, O., Naughton, F., Fletcher, W. J., Eynaud, F., Rossignol, L. and Renssen, H. (2012) European climate optimum and enhanced Greenland melt during the Last Interglacial. Geology, vol. 40(7):627-630.

Tzedakis, P. C. (2007) "Seven ambiguities in the Mediterranean palaeoenvironmental narrative." Quaternary Science Reviews 26:2042-2066.

Wang, Y.J., Cheng, H., Edwards, R.L., An, Z.S.,Wu, J.Y., Shen, C.-C., Dorale, J.A., 2001. A high-resolution absolute-dated Late Pleistocene monsoon record from Hulu Cave, China. Science 294, 2345–2348.

Yuan, D., Cheng, H., Edwards, R.L., Dykoski, C.A., Kelly, M.J., Zhang, M., Qing, J., Lin, Y.,Wang, Y.,Wu, J., Dorale, J.A., An, Z., Cai, Y., (2004) Timing, duration, and transitions of the Last Interglacial Asian Monsoon. Science 304, 575–578.